Assessment of the impact of widespread integration of compressed natural gas filling stations and biomethane injection on the gas network

Niamh Keogh B.E. (honours)

Supervisors: Dr Rory Monaghan

A thesis submitted to the National University of Ireland Galway as fulfilment of the requirements for the Degree of Doctor of Philosophy, in the College of Science and Engineering.

Mechanical Engineering,
National University of Ireland Galway

July 2022

Abstract

The research in this thesis has explored, investigated and analysed the integration of biomethane production and injection facilities and compressed natural gas (CNG) filling stations in to gas distribution networks, through technical, economic and environmental modelling. First, a simulation of a gas distribution (Dx) network was built to investigate the impacts of technical limits imposed by gas network operation and safety standards on the quantity of biomethane which can be injected. The Dx network simulation also incorporates annual consumer demand profiles based SCADA data, taking into consideration the seasonal variations in the gas demand. Scenarios of maximum, minimum and no demand at a grid-connected compressed natural gas (CNG) filling station were computed, to determine the impact of the addition a CNG filling station to the gas network. The location of the biomethane production and injection facility is also analysed. The results calculated the grid capacity to accept biomethane on an hourly basis over the course of a year. This data was used to determine a range of possible plant sizes for each potential facility location and CNG demand scenario. Next, a spatially explicit geographical information systems model was created to map the distribution of feedstocks suitable for biomethane production in the surrounding area and determine the transport distances. These two submodels fed into a techno-economic assessment that calculated the levelised cost of energy and net present value for each configuration, and techno-econo-environmental models that calculated the total cost of carbon abatement for each configuration. Key parameters for both of these models include the capital and operating cost of the anaerobic digester, upgrader, injection facility and CNG station, the feedstock transportation cost, and the potential incentives for biomethane and bioCNG. The techno-econo-environmental model also incorporates a life cycle assessment for the production and use of biomethane as either a fuel for residential heating or a fuel for CNG heavy goods vehicles, to determine the overall environmental costs and benefits. This work contributes to gas grid, biomethane and bioCNG research, by presenting a novel method of modelling the integration of biomethane

injection facilities and CNG filling stations into gas Dx networks, to assess the overall technical, economic and environmental impacts.

Dissemination of Research

1.1 Journal Articles

- Keogh.N, Corr.D, Monaghan.RFD "Biogenic Renewable Gas Injection into Natural Gas Grids: A Review of Technical and Economic Modelling Studies", Journal Renewable and Sustainable Energy Reviews, 2022; DOI: 10.1016/J.RSER.2022.112818

- Keogh.N, Corr.D, O'Shea.R, Monaghan.RFD "The Gas Grid as a Vector for Regional Decarbonisation - A Techno Economic Case Study for Biomethane Injection and Natural Gas Heavy Goods Vehicles". Applied Energy, 2022; DOI: 10.1016/J.APENERGY.2022.119590

- Keogh.N, Corr.D, Monaghan.RFD "An Environment and Economic Assessment for Biomethane Injection and Natural Gas Heavy Goods Vehicles", in preparation.

1.2 Conference Articles

- Paper entitled "Technical Feasibility of Biomethane and CNG in a Gas Distribution Network" at the European Biomass Conference and Exhibition (EUBCE), 28th April 2021.

Acknowledgements

Firstly, I would like to sincerely thank my supervisor Dr. Rory Monaghan, for his knowledge, expertise and his constant support, guidance and assistance throughout the duration of this project. I am eternally grateful to Rory for the numerous opportunities that have been offered to me before, during and after my PhD, for keeping my work interesting and enjoyable, and his mentorship in shaping the direction of my research, introductions to key people in related topics and guidance on writing journal papers, proposals, and this thesis.

I would like to express my gratitude to the following individuals for their generosity in sharing their knowledge, expertise, and data, and without whom this work would not have been possible; Damien Corr, Maurice Power, Greta Cussen, Dr, Richard O'Shea, Dr. Tubagus Aryandi Gunawan, Dr, Alessandro Singlitico, and Ashutosh Rai. I would also like to thank Prof. Seán Leen, Dr. Noel Harrison, and Dr. Mingming Tong for their contribution as my graduate research committee.

I am grateful to the funding institution who have supported an funded this research, including CINEA in partnership with Gas Networks Ireland and NUI Galway under the Causeway project, and Science Foundation Ireland (SFI) through the Sustainable Energy and Fuel Efficiency (SEFE) Spoke of MaREI, the Research Centre for Energy, Climate and Marine under grant numbers 12/RC/2302 and 16/SP/3829.

Thank you to all my colleagues and friends who I have met through my PhD research at NUI Galway, for making my time there a thoroughly enjoyable experience.

I would also like to express my infinite gratitude to my family and friends for their love, support, and inspiration in particular to my parents Catherine and Dara, my sisters Laura, Caoimhe, Éilis and Maebh, my grandparents Mary, John, Moira and Colm, my boyfriend Seán and my friends Helen, Cat, Patrick, Enda and Laura.

Table of Contents

List of Figures

List of Tables

Nomenclature

Table of Symbols

$\%CH_4$	Methane percentage
$\boldsymbol{A_h}$	Area through which heat transfer occurs
$\boldsymbol{a_{ij}}$	Element from row i and column j in the branch nodal incidence matrix
Barg	Bar Gauge Pressure
$\boldsymbol{C_{Diesel}}$	Cost of diesel
$\boldsymbol{C_{NG}}$	Cost of natural gas
$\boldsymbol{C_{out}}$	Total cost of biomethane plant
$\boldsymbol{cp_{H_2O}}$	Specific heat capacity of water
$Capex_{AD}$	Capital cost anaerobic digester
$\boldsymbol{Capex_{CNG,I}}$	Capital cost CNG filling station
$\boldsymbol{Capex_{Diesel,V}}$	Capital cost of diesel vehicle
$Capex_{UP}$	Capital cost upgrader
$\boldsymbol{CE_{AD}}$	Cost of electricity for the anaerobic digester
$\boldsymbol{CE_{CNG}}$	Electrical cost of compressing CNG
$\boldsymbol{CE_{UP}}$	Cost of electricity for the upgrader
$\boldsymbol{CF_{Diesel}}$	Fuel cost of diesel
$\boldsymbol{CG_{AD}}$	Cost of heating anaerobic digester
CW_{UP}	Cost of water upgrader
d	Distance
D	Pipeline diameter
DP	Price of diesel
e	Internal energy per unit mass
$\boldsymbol{e_{bioCH4}}$	Energy content of biomethane
$\boldsymbol{E_{bioCH4}}$	Total energy produced by biomethane plant
$\boldsymbol{E_{CNG}}$	Total energy CNG
$\boldsymbol{E_{E,UP}}$	Electricity demand of upgrader
$\boldsymbol{E_{Th}}$	Thermal energy required to pasteurise the cattle slurry
f	Friction factor
FC	Feedstock cost
g	Gravitational acceleration

H	Efficiency factor of diesel vs CNG
h	Difference in elevation at pipe starting node and end node
$\boldsymbol{I_{bioCH4}}$	Incentives for biomethane
inc	Increment
l	Length of pipe
l_{AD}	Methane loss in the anaerobic digester
l_{up}	Methane loss in the upgrading system
LT	Lifetime of plant
m	Mass of feedstock
M	The number of branches
$\boldsymbol{Main_{up}}$	Maintenance cost of upgrader
MC_{CS}	Moisture content of cattle slurry
N	The number of nodes
N_{OH}	Number of operating hours of the plant
$Opex_{AD}$	Operational cost anaerobic digester
$\boldsymbol{Opex_{CNG,I}}$	Operational cost CNG filling station
$Opex_{UP}$	Operational cost upgrader
P	Pressure
$\boldsymbol{P_1}$	Pressure at pipe starting node
$\boldsymbol{P_2}$	Pressure at pipe end node
$\boldsymbol{P_{av}}$	Average pressure in pipe
$\boldsymbol{P_{bioCH4}}$	Price biomethane
$\boldsymbol{P_n}$	Pressure at standard temperature and pressure
PE	Price of electricity
PG	Price of gas
PW	Price of water
$\boldsymbol{Q_{bioCH4}}$	Volumetric quantity of biomethane
$\boldsymbol{Q_{biogas}}$	Volumetric quantity of biogas
$\boldsymbol{Q_j}$	Volume flow rate in branch j
$\boldsymbol{Q_n}$	Pipe volume flow at standard temperature and pressure
$\boldsymbol{Q_{net\ demand,j}}$	Net gas demand at node i
r	Discount rate
R	Specific gas constant
R_{in}	Revenue in.
s	Specific gravity
SE_{AD}	Specific electrical energy consumption anaerobic digester
$\boldsymbol{SEC_D}$	Specific energy consumption diesel
SO_{AD}	Specific operating cost of the anaerobic digester
SMY_{VSR}	Specific methane yield
T	Temperature
T_{CS}	Mass of cattle slurry
T_{GS}	Mass of grass silage
T_{max}	Maximum tonnage of feedstock
T_{min}	Minimum tonnage of feedstock
$\boldsymbol{T_n}$	Temperature at standard temperature and pressure
t	Time

t_{high}	Temperature to pasteurise cattle slurry
t_{base}	Base temperature of cattle slurry
TC	Transport cost
$Twwt$	Total wet weight tonnage
v	Velocity
$\boldsymbol{V_{w,UP}}$	Volume of water used by the upgrader
VS_{CS}	Volatile solids cattle slurry
VS_{GS}	Volatile solids grass silage
x	Distance
y	Year
Z	Compressibility factor
ρ	Density
$\boldsymbol{\Omega}$	Heat flow per unit length of pipe
$\boldsymbol{\theta}$	Angle of pipe inclination
$\boldsymbol{\Delta P_j}$	Pressure drop in branch
$\boldsymbol{\eta_{Boiler}}$	The thermal efficiency of a natural gas boiler
$\boldsymbol{\eta_{CNG}}$	Efficiency of a CNG euro VI long haul truck

Chapter 1 Introduction

1.1 Chapter Overview

This chapter will provide background and context to the key areas of interest explored in this thesis. It also outlines the objectives, and motivation behind the work, and gives a brief insight into the focus of each of the upcoming chapters.

1.2 Renewable Gas and Climate Targets

In 2015, the Paris agreement was signed by the members of the Conference of Parties (COP) 21 of the United Nations Framework Convention in Climate Change (UNFCC). This committed signatory members to limit global warming to a minimum of 2 ° C compared to pre – industrial levels [1]. In moving towards a climate neutral economy, the European Commission launched the EU Green Deal, which commits all 27-member states to achieve net – zero GHG emissions by 2050, and reductions of at least 55% by 2030, compared to 1990 levels [2]. The Energy Transitions Commissions predict that renewable electricity will be the main energy vector in the transition towards net – zero. However, it also notes that bioenergy (biomethane, bioSNG etc.), green hydrogen, and carbon capture utilisation and storage (CCUS) will play a key role in providing storage and flexibility to the power sector and in the decarbonisation of hard to abate sectors such as heavy- duty road freight, maritime and aviation fuels, high temperate heat for industry and chemical feedstocks [3].

Gas networks can have an important role to play in the decarbonisation of future energy systems. [4]. Natural gas accounted for 23.2% of the global total energy supply in 2019 [5]. It is key in meeting energy demands in many sectors including power generation, industrial heat and chemicals, residential heating, and as a vehicle fuel. Gas demand fluctuates significantly on hourly, daily and seasonal timescales, however this can be successfully managed by the storage flexibility of the gas grid infrastructure [6]. In contrast, the ability

of electricity grid infrastructure to handle energy demand fluctuations is more technically challenging and expensive [7]. In 2015, seven European transmission network operators, Energynet.dk (Denmark), Fluxys Belgium, Gasuine (Netherlands), Gaznat (Switzerland), GRTgaz (France), ONTRAS (Germany) and Swedegas (Sweden), signed a joint declaration committing themselves to the aim of achieving a CO_2 neutral gas supply by 2050 [8].

Another driver for the transition to renewable energy technologies are energy security concerns. The EU imports 90% of its natural gas consumption, with Russia providing approximately 45% of natural gas imported. In response to the Russian invasion of Ukraine, the European Commission has proposed REPowerEU, which will seek to diversify gas supplies and speed up the rollout of renewable gases. It has doubled the EU's ambition for biomethane, with the aim to produce 30 bcm by 2030, it also plans offset demand for Russian natural gas with 10 MT of imported hydrogen and an additional 5 MT of domestic renewable hydrogen [9].

1.3 Natural gas consumption in the Republic of Ireland

In 2020, natural gas provided 4564 ktoe (191 PJ), accounting for 34% of the total primary energy requirement in Ireland, of which 63.8 % was imported [10]. The quantity of imported gas has increased from a low of 34% in 2017, which is due to the depletion of Ireland's indigenous fossil natural gas resources [11]. The 4th of July 2020 marked the cessation of gas supply from the Kinsale gas field, leaving the Corrib Gas field as the primary supply of indigenous gas [12]. The Corrib Gas field was introduced in 2016 and is predicted to last 15 years, its production has already begun to decline, in 2020 it was 1654 ktoe, 42% below the 2017 peak [10].

Renewables contributed 13% of the total primary energy requirement in Ireland in 2020, bioenergy with a 32% share was the second largest renewable energy resource after wind [10]. Biomethane is a biogenic renewable gas with a composition of >95% methane making it compatible with existing gas network infrastructure and end user applications. Biomethane is produced through the process of anaerobic digestion (AD) and upgrading [4]. AD plants

can utilise a wide variety of feedstocks including food waste, animal slurries and manures, sewage sludge, slaughterhouse waste, algae and dedicated energy crops. Work by O'Shea et al estimated that the total biomethane resource in Ireland was 12.5 PJ from wastes and 128.4 PJ from grass silage [13], [14]. This has the potential to offset 6.5% and 67 % of natural gas demand respectively.

The first renewable gas injection facility in Ireland was introduced to the gas distribution (Dx) network in 2019 [12]. It will initially supply 36 GWh of biomethane to the Irish gas network. The Graze gas project launched by Gas Networks Ireland (GNI) in 2019 will introduce a central grid injection facility, with a capacity to inject 590GWh of biomethane into the transmission (Tx) network [15].

1.4 Bioenergy in Transport

Biomethane can play a key role in decarbonising hard – to – abate sectors such as heavy duty transport. Today there are over 22.4 million natural gas vehicles, and 26,677 natural gas refuelling stations distributed through 86 countries worldwide, with significant concentrations in Iran, China, Argentina, Brazil, India, Pakistan and Italy [16]. According to the Natural and bio Gas Vehicle Association (NGVA) Europe, there are currently 3,827 CNG stations in operation throughout Europe, one-third of which are in Italy [17].

Styles et al. investigated the environmental balance of the UK biogas sector, comparing a range of potential feedstocks and end uses. The results found that upgrading the biogas to biomethane, for use as a transport fuel would significantly improve the environmental profile of the AD sector, in comparison to the current dominant use for electricity generation or upgraded biomethane for injection into the gas grid [18]. Analysis by Börjesson et al. found that for light duty vehicle such as cars and vans, there is potential to reduce the well – to – wheel (WTW) greenhouse gas (GHG) emissions by 75% to 99% using bio-CNG in comparison to gasoline. For heavy duty vehicles including trucks, WTW GHG emissions savings were reported to be between 75% to 101% for bioCNG and bioLNG vehicles compared with

diesel vehicle [19]. Similarly, work by van den Oever et al., D'Adamo et al., and Ardolino et al. found that the use of biomethane as a transport is an effective option for mitigation of GHG emissions [20] [21] [22]. The results from these studies indicated GHG savings of between 131% and 79% when compared to fossil diesel, depending on the specific case study, feedstocks used and system boundary applied. In addition to providing significant GHG savings, work by Tratzi et al. and Hagos et al. showed that using biomethane as a vehicle fuel could significantly reduce NO_x emissions and particulate matter in comparison with diesel for heavy duty vehicles [23], [24].

However, while bio-CNG and bio-LNG can provide significant environmental benefits to the transport sector, the increased fuel and vehicle costs and decreased efficiency of natural gas engine technologies in comparison to diesel can form potential barriers to widespread adoption [25]. Gustafsson et al. found that for bio-LNG production from AD and upgrading, incentives are required for bio-LNG to be economically competitive with fossil LNG, even at large scale capacities of 100 – 120 GWh/a [26] .Similarly, in the case of bio-CNG Börjesson et al. found that WTW cost of a bioCNG heavy duty vehicle was between 11 % and 20% more expensive than its diesel equivalent [19].

1.5 Thesis Motivation

In 2018, a revision of the renewable energy directive 2018/2001/EU (RED II) was published. It established mandatory renewable energy targets for the European Union (EU) member states to achieve by 2030. The first target mandates at least 32% gross final energy consumption across the EU from renewable energy sources. The second target obligates fuel suppliers to ensure that at least 14% of final energy consumption in the EU transport sector comes from renewable sources [27]. Biomethane could play a significant role in helping Ireland achieve these targets, through decarbonisation of the gas and heavy duty transport industries. The Causeway projects aims to introduce a network of 10 grid connected CNG filling stations on to the TEN-T network, provide supports for a fleet of CNG HGV and

connect a biomethane to the Irish gas network [28]. The motivation of this thesis is to use a novel integrated modelling framework to investigated and discuss the opportunities and challenges of integrating biomethane production and injection facilities and CNG filling stations into gas networks from a technical, economic and environmental perspective.

1.6 Thesis Aims and Objectives

The aim of this work is to investigate the integration of biomethane production and injection facilities and compressed natural gas filling stations into existing gas distribution networks, in the specific case of Ireland. The work will considering the technical challenges imposed by gas networks, the economic viability and the environmental costs and benefits. The results of this work are of interest to gas network operators, interested in the deployment of cost effective renewable energy technologies to decarbonise their gas networks, as well as policy-makers, whose priority is to stimulate the transition to renewable energy technologies, with the aim of achieving emissions reductions targets. In order to create a comprehensive and robust model to achieve this aim, the following objectives must be met:

1. Simulation of a gas distribution network, giving consideration to the seasonal fluctuation of gas demand, and understanding the constraints this places on the quantity of biomethane which can be injected into the grid, for various levels of demand at a grid connected CNG filling station.
2. Modelling the biomethane supply chain, including feedstock supply and transportation, biomethane production, distribution and end use consumption.
3. Developing at techno-economic model to determine the optimum size and location of the biomethane production and injection facility based on its economic viability.
4. Conducting a lifecycle assessment to evaluate the overall environmental costs and benefits of the integration of biomethane production and injection facilities and CNG filling stations.

1.7 Thesis Overview

This thesis is written based on 3 journal articles, two of which are under review and one in preparation. The thesis subdivision of chapters is described as follows.

Chapter 2 presents a critical review of technical and economic assessments of biogenic renewable gas injection into the gas network, introducing and defining the main methodologies used. A number of complimentary elements are considered, (i) the technical constraints gas grids place on biogenic renewable gas injection, (ii) models for biogenic gas production and supply chains, (iii) the use CNG as a vehicle fuel, (iv) the optimisation of production and injection facility location, and (v) the incorporation of SCADA data recorded by gas network operators, in reviewing the state-of-the-art and limitations and gap are identified.

Chapter 3 presents a novel modelling approach to investigate the impact limitations imposed by the gas network can have on the quantity of biomethane that can be injected, under various levels of demand at grid connected CNG filling station. The model is applied to a representative Irish Dx network case study. Addressing objective (1) it takes into account seasonal variations in gas demand, and the location of the biomethane production and injection facility relative to major demand points on the network.

Chapter 4 presents a spatially explicit techno-economic assessment of a supply chain for deployment of a biomethane production and injection facility and a CNG station in an existing gas Dx network, addressing objective (2) and (3). The techno – economic model of biomethane production explores the relationship between the size and cost of the plant, giving particular consideration to the limitations imposed by the gas grid and variations in seasonal demand can have on the grid capacity to accept biomethane (sourced from Chapter 2). The cost-size relationship also incorporates a GIS-based model to minimise the transport distance of the feedstock required to supply the digester.

Chapter 5 presents a techno-econo-environmental analysis of the supply chain for biomethane production and injection into the gas grid for use as either a vehicle or heating fuel, addressing objective (4). The environmental impact of the supply chain, production and use of biomethane, assessed through a consequential life cycle assessment (LCA) methodology, is integrated with the techno-economic created in Chapter 4. The novelty of considering the seasonal variation in gas demand and the technical limitations imposed by the gas grid is carried through into this work.

Chapter 6 presents the overall conclusions and key takeaways from the results obtained, the contribution of this work to advancing the state-of-the-art, and an outline of potential areas of future work.

1.8 Chapter Summary

This chapter gives an introduction to climate targets and renewable energy technologies, with a specific focus on biomethane produced from anaerobic digestion, its potential in Ireland and use as a vehicle fuel. The chapter also discusses the thesis motivation, including the roll out of CNG filling stations and a biomethane facility to the Irish gas industry under the Causeway project. The specific objectives of this thesis are established and an overview of each of the upcoming chapters is given.

Chapter 2 conducts an in- depth review of the state-of-the-art literature on technical and economic assessments of the injection of biogenic renewable gas into the gas grid.

Chapter 2 Literature Review

Chapter Overview

Biogenic renewable gas, which includes biomethane from anaerobic digestion, and biomass-derived synthetic natural gas (bioSNG), can play a role to help decarbonise future energy systems and meet renewable energy targets. One way in which renewable gas can offset fossil use is by injecting it into natural gas networks. This chapter reviews 23 peer-reviewed journal papers that outline the state-of-the-art in technical and economic assessments of biogenic renewable gas injection. The review has particular focus on (i) the technical constraints gas grids place on biogenic renewable gas injection, (ii) models for biogenic gas production and supply chains, (iii) the use of compressed natural gas (CNG) as a vehicle fuel, (iv) the optimisation of production and injection facility location, and (v) the incorporation of SCADA data recorded by gas network operators.

2.1 Introduction

The EU renewable energy directive 2009/28/EC (RED) was introduced to promote the deployment of renewable energy sources in the EU energy system. The directive sets out mandatory renewable energy supply targets for the EU28, individual member states, and for energy types to be achieved by 2020 [29]. In 2018, a revision of the renewable energy directive 2018/2001/EU (RED II) was published. It established further binding renewable energy targets for the European Union (EU) member states to achieve by 2030. The first target mandates at least 32% gross final energy consumption across the EU from renewable energy sources. The second target obligates fuel suppliers to ensure that at least 14% of final energy consumption in the EU transport sector comes from renewable sources [27]. In 2018, the EU reached 18 % renewable energy share in gross final energy consumption, which was on track to meet the 2020 target of 20%. The main renewable energy sources were biomass for heating, wind and hydropower for electricity, and biodiesel for transport. Renewable gases also contributed to all three energy targets in smaller shares [30].

Renewable gases, such as renewably produced hydrogen, power to gas, biomethane and biomass-derived synthetic natural gas (bioSNG), are produced in several ways, as outlined in Figure 2-1. Biomethane is produced through anaerobic digestion (AD) and upgrading. This is a process whereby organic biomass and residues from agriculture, waste processing and food production are biologically broken down in the absence of oxygen to form biogas, a gaseous mixture comprising approximately 60% methane and 40% carbon dioxide. Carbon dioxide is then removed from the biogas during the upgrading process, leaving biomethane (approximately 94% methane) [4]. Additionally, oxygen, nitrogen, carbon monoxide, siloxanes, and other undesirable compounds are also removed during the upgrading process [31]. Alternatively, the biogas can be upgraded to biomethane by biological methanation. This is a process can be performed in-situ, where additional hydrogen is added to the digester where the biogas is produced or ex-situ, in an external reactor requiring the addition of hydrogen, carbon dioxide, hydrogenotrophic methogens and essential nutrients [32]. BioSNG is produced through gasification or pyrolysis of lignocellulosic feedstocks not suited for AD, such as forestry residues and woody crops including straw, willow and miscanthus [33]. Both gasification and pyrolysis produce a synthetic gas, which subsequently undergoes cleaning, upgrading to hydrogen or conversion to bioSNG via methanation. In the power to gas process, electrolysis is used to produce renewable hydrogen, by the splitting of water into oxygen and hydrogen. Electricity consumed in this process must be generated by renewably supplied electricity sources, such as wind and solar power, for this hydrogen to be considered renewable. It can be either used as a fuel itself or combined with carbon dioxide to produce methane, which could directly replace natural gas [34].

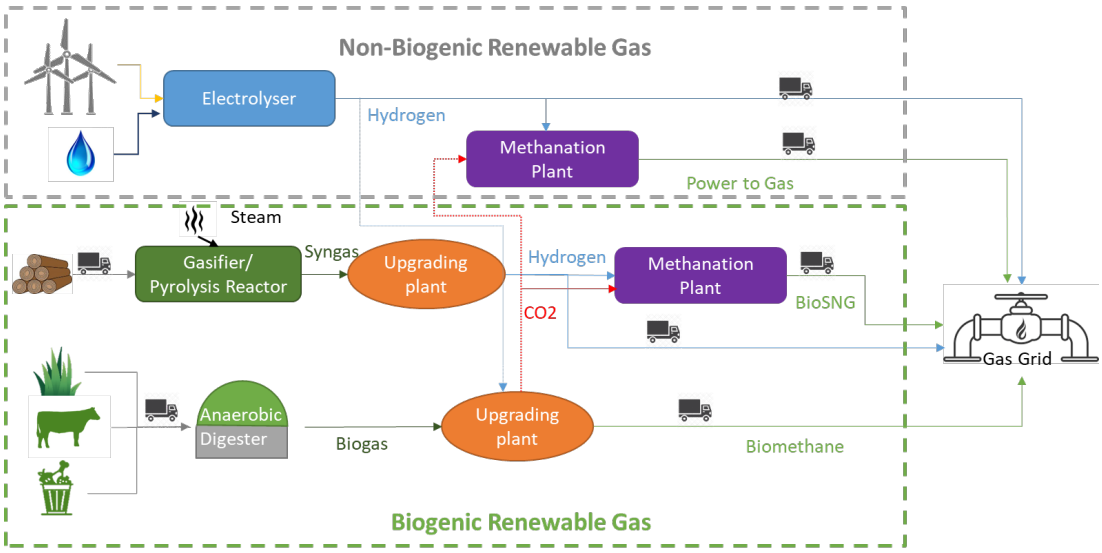

Figure 2-1:Schematic of renewable gas production pathways for injection into the gas network.

Historically in the EU, biogas from AD has been used for distributed electricity generation or combined heat and power. However, since 2013 there has been a significant increase in facilities upgrading biogas to biomethane for injection into the natural gas grid or use as a vehicle fuel [35]. Similarly, review by Quarton et al. found, in a study of over 130 power-to-gas facilities worldwide, that 19% of them injected hydrogen directly in to the natural gas grid, 8% converted the produced hydrogen into methane for subsequent grid injection, and the remainder did not involve grid injection [34]. Power-to-gas includes hydrogen produced via electrolysis or by steam methane reforming with carbon capture and storage (CCS), and synthetic methane which is form when hydrogen produced by electrolysis is combined with carbon dioxide in the methanation process. The majority of plants commenced operation from 2015 onwards.

Gas networks can have an important role to play in the decarbonisation of future energy systems. [4] Currently gas network infrastructure plays a critical role in supplying energy to consumers, typically delivering a greater quantity of energy than electricity networks and providing flexibility of supply [36]. Natural gas accounted for 24.6% of the EU's total primary energy supply 2018 [37]. It is key in meeting energy demands in many sectors including power generation, industrial heat and chemicals, residential

heating, and as a vehicle fuel. Gas demand fluctuate significantly on hourly, daily and seasonal timescales. This can be managed by the storage flexibility of gas grid infrastructure, including storage within the pipelines (linepack), dedicated storage, imports through interconnector pipelines from neighbouring countries and liquefied natural gas (LNG) import terminals [6]. In contrast, the ability of electricity grid infrastructure to handle energy demand fluctuations is more technically challenging and expensive [7]. In 2015, seven European transmission network operators, Energynet.dk (Denmark), Fluxys Belgium, Gasuine (Netherlands), Gaznat (Switzerland), GRTgaz (France), ONTRAS (Germany) and Swedegas (Sweden), signed a joint declaration committing themselves to the aim of achieving a CO_2 neutral gas supply by 2050 [8].

Figure 2-2 below outlines the configuration of the gas grid depicting the key infrastructure. Transmission (Tx) networks consist of steel pipelines designed to transport large quantities of high-pressure gas over considerable distances. Tx networks typically carry gas pressurised to between 5 and 70 bar with pipeline diameters of 152 mm to 1220 mm. Compressor stations are located at the entry to, and periodically along, Tx networks to ensure the natural gas remains pressurised. Tx networks supply gas to large industrial consumers, power generation plants and lower-pressure distribution (Dx) networks. City gate stations connect Tx networks to Dx Networks. Their primary function is to meter gas and reduce its pressure from the Tx level to the Dx level [38]. Dx networks are low pressure networks primarily composed of polyethylene pipes, typically below 4 bar [39, 40]. Dx networks deliver gas to CNG filling stations, residential, commercial and industrial consumers [41].

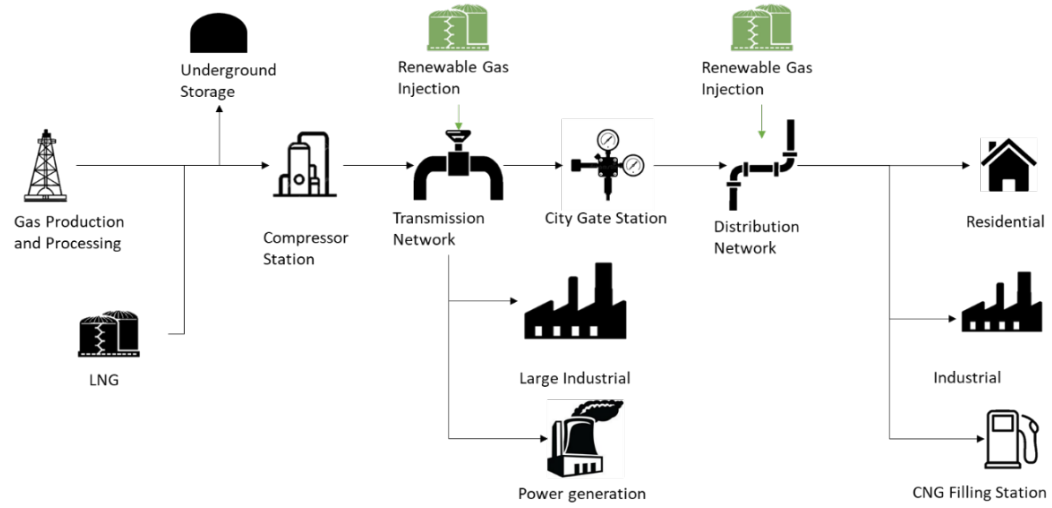

Figure 2-2:Outline of the major components in the gas network.

The integration of renewable gases into gas network infrastructure presents several challenges. These challenges include (i) compliance with gas injection standards, (ii) the supply chain and production of renewable gas, and (iii) the increased demand of using CNG as a vehicle fuel.

Firstly, for renewable gas to be injected into gas Tx or Dx networks, it must comply with gas standards. The European Committee for Standardisation has published three key standards (i) EN 16723-1:2016 – Part 1: Specification for biomethane for injection in the natural gas network, (ii) EN 16723-2:2017 – Part 2: Automotive fuel specification, and (iii) CEN/TR 17238:2018 – Proposed limit value for contaminants in biomethane based on health assessment criteria. These standards provide details on both the methods for testing and analysis of biomethane for contaminants, and the derivation of contamination limits based on their potential impact to human health. However, they do not cover gas quality, meaning national gas quality standards can differ significantly between countries [42]. Gas quality standards ensure the safe transportation of gas through the network and that the gas is compatible with end use appliances, such as gas turbines for power generation, central heating boilers, cookers, ovens and gas fireplaces. Gas quality is determined by the proportion of components present in the gas. Components can be classified as main, auxiliary or trace. The main components of natural gas are hydrocarbons, as they are present in the most

significant proportions. Auxiliary components include hydrogen, oxygen, carbon monoxide and helium. Trace components occur in very small concentrations and are undesirable from transportation and utilisation aspects (e.g. sulphur, hydrogen sulphide, mercaptan sulphur). From the gas composition, physical properties of the gas can be calculated, including Wobbe Index (WI) and higher heating value (HHV) [43]. WI is an indicator of the interchangeability of fuel gas, it is used to compare the combustion energy output of fuel gases with different composition. WI is calculated using Equation 2-1.

Equation 2-1: Wobbe Index

$$WI = \frac{HHV}{\sqrt{SG}}$$

where SG is the specific gravity of the fuel. HHV is the heat released when a fuel is fully burned and the products have returned to 25°C. Gas composition and physical properties of gas to be injected into gas networks are limited by gas quality standards to be in line with safety and integrity requirements of the network and end use applications [44]. Due to the differences in gas quality standards and variations in the compositions gas supplies across the EU, the WI can have an allowable range of 12.2 – 13.02 kWh/m^3 or 43.92 – 46.87 MJ/ m^3 (Belgium) to 13.38 – 16.02 kWh/m^3 or 48.17 – 57.67 MJ/ m^3 (Portugal) [40]. The injection of renewable gases that have a different compositional make up to the natural gas already in the network can significantly impact on important gas parameters such as pressure, WI and HHV [4] [45]. As well as technical specifications, a number of other key parameters were identified by the European Network for Transmission Systems Operators for Gas (ENTSOG) as requiring consideration when integrating renewable gas injection facilities. They include physical conditions (e.g. flow rate, pressure and temperature), the possible presence of sensitive consumers (e.g. gas power plants, chemical companies) downstream of the injection location, and the configuration of the gas network and its future developments [46]

Secondly, consideration must be given to the renewable gas supply chain. This encompasses a vast array of aspects. Ohemeng-Ntiamoah et al. evaluated

78 different papers that have assessed the digestibility and maximum biomethane production potential of commonly digested substrates [47]. Aghbashlo et al. assessed the current literature on exergoenvironmental analysis of bioenergy systems, discussing the pros and cons of the exergoenvironmental approach, and critically evaluating the role of its parent methods, exergy and life cycle assessment (LCA) [48]. Prussi et al. and Patterson et al. examined the state of the art in upgrading technologies for biogas or raw bioSNG to meet grid quality standards for gas grid injection [49] [50]. Work by O'Shea et al. used compromise programming to balance the benefits of AD of distillery waste (greenhouse gas (GHG) emissions savings and electricity savings) against its drawbacks (reduced animal feed and protein production, and import of animal feeds) [51]. Umar et al. proposed a novel approach to catalytic conversion of biomass, based on exsolved nanoparticles and basicity control [52]. Sansaniwal et al. reviewed the technical advancements in biomass gasification technology [53]. The authors determined that the optimum choice of gasification system is dependent on factors such as biomass characterization, required capacity and end use application. Speirs et al. conducted a review of technologies to produce renewable gas. The reviews concluded that there are significant variations in the literature concerning the range of costs and GHG emissions savings in the production of renewable gas. It established the need for further investigation to understand the suitability of the natural gas network to accept renewable gas, and to what extent decarbonisation of natural gas networks can be achieved [7].

Thirdly, the addition of a CNG filling station to the gas grid, in particular the distribution network, can add considerable demand to the network [54]. In 2020 there were 3,827 compressed natural gas (CNG) filling stations operating across Europe. Gas supply to the filling station can either be provided by trucks or by the natural gas grid [17].

The current state of the art has reviewed a number of the challenges associated with renewable gas integration as shown in Table 2-1. Tabatabaei et al. considered the biological approaches to improve biogas production pre- AD [55] and post-AD [56]. Singlitico et al. evaluated the state of the art in works

that conducted a LCA of biogenic renewable gas, with a focus on methodological choices including consideration of process models, geospatial models or uncertainty analysis [57]. In their recent paper, Quarton et al. comprehensively reviewed the role of non-biogenic renewable gas (i.e. hydrogen and power to methane) with a particular focus on injection into the gas grid [34]. Bekkering et al. evaluated the state of the art for biogenic renewable gas supply chains [58]. Ríos-Mercado et al. reviewed optimisation of natural gas transportations systems [59]. However, to the best of the authors' knowledge, there is no single study that reviews technical and economic assessments for biogenic renewable gases with a focus on gas grid injection. For the purposes of this paper, biogenic renewable gas gases will refer to both biomethane and bioSNG.

Table 2-1: Current state of the art in renewable gas review papers.

Review Paper	**Fuel Type**	**Paper Focus**	**Environmental**	**Technical**	**Economic**	**Upstream of Grid Injection**	**Downstream of Grid Injection**
Bekkering et al. **[58]**	$BioCH_4$	Green gas supply chain.		✓		✓	
Quarton et al. **[34]**	H_2, Power to X	Technical and economic assessments of power to gas for grid injection.		✓	✓	✓	✓
Ríos-Mercado et al. **[59]**	Natural gas	Technical studies assessing natural gas pipeline transportation systems.		✓			✓
Singlitico et al. **[57]**	$BioCH_4$, BioSNG	LCA studies considering process models, geospatial models or uncertainty qualification.	✓	✓		✓	
Speirs at al. **[7]**	$BioCH_4$, BioSNG, H_2, Power to X	Overview of renewable gas industry.	✓		✓	✓	✓
Tabatabaei et al. **[55]**	Biogas	Biological approaches to		✓		✓	

		improve biogas production pre AD					
Tabatabaei et al. **[56]**	Biogas	Biological approaches to improve biogas production post AD		✓		✓	

The overall aim of this paper is to review the state of the art in technical and economic modelling methodologies for assessing the impacts of biogenic renewable gas injection into the natural gas grid. This paper will have a particular focus on:

- Gas grid constraints on biogenic renewable gas injection, including limits on pressures and flowrates, and compliance with grid standards.
- The supply chain for biogenic renewable gas production, including feedstock availability, and transportation of feedstocks, non-upgraded biogas and/or biomethane to grid injection points.
- The impact to the grid of the use of CNG as a fuel for heavy vehicles.
- Optimisation of the location of biogenic renewable gas injection points on the gas grid from supply chain and grid constraint perspectives.
- The incorporation of CNG demand and real grid demand data also referred to as SCADA data, in the simulation to give accurate seasonal demand profiles, and to validate the model.

2.2 Materials and Methods

This is a review of the technical and economic assessments published in academic journals that modelled biogenic renewable gas injection into the natural gas grid. A literature search was preformed using the Scopus and Science Direct databases for the key terms “biomethane”, “bio-SNG”, “technical assessment”, “economic assessment” and “techno-economic assessment”. From this search, papers were filtered to exclude those that did not consider grid injection or bioCNG as end uses of the biogenic renewable gas. Overall, 23 papers were found, and the results summarised in Table 2-2.

The reviewed papers have been categorised by the type of renewable gas considered, biomethane (16 studies), BioSNG (3 studies), multiple gases (4 studies). The review then gives detail of the goal, type of model used, and whether the study was conducted for a transmission or distribution network. The next section contains a detailed review and discussion of the methods and findings of the literature.

Complimentary elements, which vary depending on the goal and type of study, are also described. These include, the type of feedstock used, consideration of the constraints imposed by the natural gas grid, inclusion of compressed natural gas as an end use, optimisation of the location of the injection point into the natural gas grid, inclusion of the supply chain for renewable gas production and the used of metered gas network data in modelling. A list of the acronyms and abbreviations used in Table 2-2 along with their explanations is contained in the footnotes.

Table 2-2: Summary of results from review of technical and economic assessments of renewable gas[1].

	Description	Model Type	Location	Tx / Dx	Feedstock	Grid constraints	Inclusion of CNG	Injection point location	Supply Chain	SCADA data	Ref.
Discussed in section of text	2.3.1	2.3.1		2.3.2	2.3.3	2.3.4	2.3.5	2.3.6	2.3.7	2.3.8	
Biomethane	Investigating the possibilities for designing a flexible BioCH4 supply chain to meet the varying gas demand.	Techno-economic	Netherlands	Dx	Manure, Maize				S	D	[60] (J. Bekkering et al.)
	Optimising locations for flexible production of BioCH4 for different levels of network penetration.	Techno-economic	Netherlands	Dx	Manure, Maize			ND	R,	D	[61] (J. Bekkering et al.)
	Economic comparison of BioCH4 as a transport fuel from different feedstocks.	Economic	Ireland		OFMSW, SHW, Slurry, Grass silage.		Yes		F		[62] (J. Browne et al.)
	Determining the impacts to the distribution network of biogas blending into the natural gas grid.	Steady state grid model. (non-isothermal)	Italy	Dx		Yes				V ,D	[63] (M. Cavana et al.)
	Evaluates the financial feasibility of BioCH4 plants as a function of plant size, feedstocks and end use.	Techno-economic	Italy	Dx	OFMSW, Maize, Manure		Yes		T, F, IS		[64] (F. Cucchiella et al.)
	Assessing the profitability of small-scale BioCH4 plants for grid injection.	Economic	Italy	Dx	OFMSW, Manure, Maize				S,T ,F		[65] (F. Cucchiella et al.)

	Assessment of mobile unit to upgrade and compress bioCH4 for grid injection from on farm digesters.	Techno-economic	Ireland	Tx	Cattle slurry, Food waste				IS, S, T, F		[66] (L. Gil-Carrera et al.)
	Economic feasibility of a bioCH4 plant as a function of feedstocks with vehicle fuel as the end use.	Economic	Mexico		Food waste, sewage sludge, pig manure.		Yes		F,IS,R,T		[67] (E. C. Gutiérrez et al)
	Comparison decentralized vs centralizer digesters for the bioCH4 supply chain.	Techno-economic	Netherlands	Dx	Manure, Maize				R,S,T,F		[68] (E. Hengeveld et al.)
	Optimisation of decentralised bioCH4 production plants as a function of feedstocks.	Techno-economic (BeWhere model)	Malaysia	Tx	POME, Food waste, Chicken Manure, Cattle Manure			RD	R,T,F		[69] (P. Y. Hoo et al.)
	Analysis of the bioCH4 supply chain with a focus on compression pressure and transportation.	Economic and grid simulation	Malaysia	Dx	Landfill gas	Yes			F,T,R		[70] (P. Y. Hoo et al.)
	Optimisation of feedstock source for potential bioCH4 plant locations.	Techno-economic	Ireland	Tx (at AGI)	Cattle Slurry, Grass Silage			RD	R,T, IS , S, F,		[14] (R. O'Shea et al.)
	Determining the optimal locations for centralised anaerobic digesters.	Techno-economic	Ireland	Tx	OFMSW, Slurry, Manure, Dairy waste, SHW			RD	R,T,S, IS,F		[71] (R. O'Shea et al.)
	Modelling the bioCH4 supply chain for end use as a vehicle fuel.	Techno-economic	California	Tx	Landfill gas, OFMSW,		Yes		R, T,		[72] (N. Parker et al.)

					WWTP, Manure (Dairy)						
	To optimise the location for biogas plants and determine the optimal end use.	Techno-economic (BeWhere model)	Italy	Dx	Cereals, Energy Crops, Manure		Yes	RD	S, IS, R,F		[73] (P. Patrizio et al.)
	Determining the local impacts of BioCh4 injection to gas quality under various levels of price and regulatory support scenarios.	Steady state grid simulation (isothermal) and economic	California	Tx	Results taken from [72].	Yes	Yes – in economic assessment as end use.		IS, F		[74] (G. A. Von Wald et al.)
BioSNG	Determining the potential locations and quantity of bioSNG that can be produced for grid injection.	Techno-economic	Ireland	Tx	Willow				R, T,S,F	D	[75] (C. Gallagher et. al.)
	Optimal integration of large-scale bioSNG production system into the existing gas network.	Techno-economic (Including thermal model)	Ireland	Tx	Forestry residues			RD	R, T, S,F	D.	[76] (A. Singlitico et al.)
	Optimisation of bioSNG production for use as a vehicle fuel in the EU.	Environmental and techno-economic (BeWhere model)	Europe		Forestry residues		Yes		R, T,S,F		[77] (E. Wetterlund et al.)
Multiple Gases	Investigates the impacts of centralised and decentralised injection of BioCH4 and H_2 on low-pressure networks.	Steady state grid simulation (isothermal)	UK	Dx		Yes					[78] (M. Abeysekera et al.)
	Optimising BioCH4 and bioSNG integration into the gas network	Environmental and techno-economic	UK	Dx	Farm waste, MSW, Sewage, Macro- algae				IS,F		[79] (T. Fubara et al.)

	with respect to feedstocks and conversion technologies.				Microalgae Energy Crop						
	Investigates the impacts of H_2 and BioCH4 injection on gas quality in the transmission network.	Steady state grid simulation (non-isothermal)	Italy	Tx		Yes				D.	[80] (S. Pellegrino et al.)
	Assesses the impact of energy recovery digestate on bioCH4 production. Including using the dried digestate to produce bioSNG.	Techno-economic and environmental	Ireland	Tx	OFMSW			RD	R, T,F		[81] (A. Singlitico et al.)

Acronym/ Abbreviation	*Explanation*
BioCH4	Biomethane
CNG	Compressed Natural Gas
D	Used to provide accurate profiles of gas demand
Dx	Distribution network
F	Includes production and upgrading related logistics and costs
H_2	Hydrogen
IS	Incentives and subsidies
MSW	Municipal solid waste
ND	Based on demand for natural gas
OFMSW	Organic fraction municipal solid waste
POME	Palm oil mill effluent
R	Includes assessment of feedstocks available
RD	Based on resource distribution
S	Includes sizing of plants
SHW	Slaughterhouse waste

T	Includes transport logistics costs
Tx	Transmission network
V	Used to validate model
WWTP	Wastewater treatment plant

2.3 Results and Discussion

2.3.1 Goal and Model Type

In the review, there are several different goals that correlate to the system boundaries, type of model and complimentary elements being employed in the paper. The papers in Table 2-2 can be divided into three main categories of system boundaries:

- Models that consider elements prior to (upstream of) injection of the renewable gas into the gas grid. (16 studies)
- Models that consider elements after (downstream from) the injection of the renewable gas into the gas grid. (3 studies)
- Models that consider a combination of the elements upstream and downstream from injection of renewable gas into the gas grid. (4 studies)

Works that are concerned with the elements upstream of injection are shown to include details on the type of feedstock used and the renewable gas supply chain. This is because they are typically more concerned with the production of the renewable gas than the impact it has on gas grid infrastructure. The review found that in the papers that focus upstream of grid injection, the type of model can be broken down into four main categories, economic models (3 studies), techno-economic models (10 studies), and techno-economic and environmental models (3 studies). Economic models examined the financial cost of producing renewable gas. Cucchiella et al. evaluated the profitability of small-scale biomethane plants according to discounted cash flow method, using net profit value, discounted payback time, internal rate of return and profitability index as indicators. Three different plant sizes (50 m^3/h, 100 m^3/h, 150 m^3/h) and two different feedstocks, OFMSW and a mix of 70% manure residues and 30% maize. The results showed that biomethane obtained from OFMSW substrate was financially feasible. However, the mixed manure and maize substrate was almost always unprofitable at this small scale, without gate fees or financial incentives [65]. Techno-economic models examined the financial cost of producing biomethane while also

considering logistical factors such as feedstocks distributions, supply chains and optimal locations and sizing for gas production facilities. Parker et al. estimated the potential quantity and production cost of biomethane for use as a vehicle fuel, from various sources distributed throughout California. Supply curves for production of biomethane and its delivery to California's transport fuel market are developed using a spatially explicit techno-economic model to estimate the economic potential. The study found up to 86 PJ/year of biomethane could technically be produced, 21.5 PJ/year could be produced below 9.5 USD/GJ, 43 PJ/year could be produced between 9.5 USD/GJ and 21 USD/GJ, however production cost of the final 21.5 PJ/year rapidly increases from 21 USD/GJ to over 80 USD /GJ [72]. Three of the techno-economic studies listed in Table 2-2 above also included an environmental analysis, with the aim to minimise greenhouse gas emissions. Singlitico et al. assessed the impact of energy recovery from digestate on the economics and carbon intensity of biomethane produced from OFMSW. The results found that if the digestate is dried, synthetic natural gas produced from steam gasification of the digestate presents the lowest levelised cost, highest net profit value and largest CO_2 emissions savings of the considered options [81].

Models that are concerned with elements downstream of grid injection consider constraints imposed by the natural gas grid as their focus is on the integration of renewable gas into currently existing gas networks. These studies are all technical assessments that consider the gas quality standards, gas compositions and demand within the gas network. There are two main types of downstream grid injection models, steady-state and transient gas network simulations, outlined in Table 2-3.

Table 2-3: Comparison of steady state and transient gas network models[2].

	Transient	Steady State
Governing Equations	Equation 2-2: Continuity Equation. $\frac{\partial \rho}{\partial t} + \frac{\partial (\rho v)}{\partial x} = 0$ Equation 2-3: Momentum Equation. $\frac{\partial (\rho v)}{\partial t} + \frac{\partial (\rho v^2)}{\partial x} + \frac{\partial P}{\partial x} + \frac{f \rho \lvert v \rvert v}{2D} + \rho g \sin\theta = 0$ Equation 2-4: Energy Equation. $\frac{\partial (\rho e)}{\partial t} + \frac{\partial (\rho v e)}{\partial x} + P\frac{\partial v}{\partial x} - \frac{f \rho v^3}{2D} - \frac{\Omega}{A_h} = 0$ Equation 2-5: Real Gas Equation of State. $P = \rho Z R t$	Equation 2-6: General Flow Equation. $Q_n = \sqrt{\frac{\pi^2 \rho_{air}}{64}} \frac{t_n}{P_n} \sqrt{\frac{\left[(p_1^2 - p_2^2) - \frac{2 p_{av} S g h}{Z \rho_{air} T}\right] D^5}{f S L T Z}}$ Equation 2-7 : Kirchhoff's First Law. $\sum_{i=1}^{m} a_{ij} Q_j = Q_{net\ demand,i} \quad j = 1, \dots, N$ Equation 2-8: Kirchhoff's Second Law. $\sum_{i=1}^{N} -a_{ij} P_i = \Delta P_j \quad j = 1, \dots, m$
Assumptions	Dynamic flow. Either isothermal or non-isothermal	Steady flow. Either isothermal or non-isothermal
Solution Method	Method of characteristics The Crank-Nicolson method Implicit finite differencing method.	Newton Nodal Method
Pros	Allows consideration for time variant impacts such as line pack, and fluctuations in gas demand.	Less complex simulation. Faster simulation computational time.
Cons	Complex simulation. Longer simulation computational run time.	Does not allow for time variant impacts.
References	[82], [83]	[78], [63], [80]

2

Acronym/ Abbreviation	*Explanation*
A_h	Area through which heat transfer occurs
a_{ij}	Element from row i and column j in the branch nodal incidence matrix
D	Pipeline diameter
E	Internal energy per unit mass
f	Friction factor
g	Gravitational constant
H	Difference in elevation at pipe starting node and end node
L	Length of pipe
M	The number of branches
N	The number of nodes
P	Pressure
P_1	Pressure at pipe starting node
P_2	Pressure at pipe end node
P_{av}	Average pressure in pipe

P_n	Pressure at standard temperature and pressure
Q_j	Volume flow rate in branch j
Q_n	Pipe volume flow at standard temperature and pressure
$Q_{net\ demand,j}$	Net gas demand at node i
R	Specific gas constant
S	Specific gravity
T	Temperature
T_n	Temperature at standard temperature and pressure
t	Time
v	Velocity
x	Distance
Z	Compressibility factor
ρ	Density
Ω	Heat flow per unit length of pipe
θ	Angle of pipe inclination
ΔP_j	Pressure drop in branch

A subcategory of steady state and transient gas network simulation is whether it used an isothermal or non-isothermal approach. The isothermal approach assumes that for slow transients caused by fluctuation in gas demand, gas in the pipe has time to come to thermal equilibrium with its constant temperature surroundings. For fast transients, such as a burst pipe, the isothermal approach assumes that the pressure change occurs instantaneously, leaving no time for heat transfer to take place between the gas pipe and the surroundings [84]. Non-isothermal models take into account heat transfer that may be caused by temperature differences between gas in the pipeline and the surrounding soil, after a compression station the gas temperature may be considerably higher that the external temperature, similarly at a decompression station the temperature of the gas can be lower that the external temperature [80]. Most models opted for an isothermal approach, as it simplified the model, and reduced computational time. However, Cavana et al. [63], and Pellegrino et al. [80] opted for a non-isothermal approach as it gave more accurate results for temperature and pressure, particularly for large flow rates or when modelling complex network scenarios [84]. Pellegrino et al. examined the impacts on pressure drops, WI, HHV, and gas gravity of hydrogen and bioSNG injection. The network case study chosen included compression and regulation stations. The results showed that the injection of bio-SNG has a negligible effect on the higher heating value, WI, and the gas gravity [80].

The advantage of models that focus on a combination of the elements prior to and after injection of renewable gas into the natural gas grid can give a better overall picture of full process chain from gas production to end user. However, they often do not contain the same level of detail on renewable gas supply chains, and gas blending within gas networks as dedicated upstream or downstream models. Hoo et al. considered an economic analysis to optimise biomethane injection from landfill gas into the different pressure regulation and metering stations for areas of industrial (20 psig /1.38 barg), commercial (4.3 psig / 0.3 barg) and residential (0.43 psig / 0.03 barg) demand on the Malaysian gas grid. The case study assumed industrial, commercial, and residential areas of gas demand were equally spatially distributed throughout Malaysia. This combined with the annual gas demand was used to estimate the hourly industrial, commercial and residential gas consumption. Injection through the pressure reduction station for industrial usage at 20 psig was the best option, with associated costs of 2.07 billion Malaysian ringgit/year. Bekkering et al. examined the ability of the biomethane supply chain to match the fluctuating nature of gas demand. The study investigated different possible ratios between minimum and maximum demand, called the seasonal swing factor. However, the study did not include a grid simulation to fully assess the impacts to the grid. The results suggested that flexible biogas production at a single digester was the cheapest option, followed by two biogas plants with constant biogas output, one of which was only operated during months of high demand. Gas storage was the most expensive option and had significant spatial disadvantages at seasonal swing factors above 2 [60].

2.3.2 Transmission and Distribution Network

With the exception of [62] [67] and [77], all the studies reviewed have specified as to whether the biogenic renewable gas being assessed is to be injected into a Tx or Dx network. This is an important distinction as it has several implications for the scope of the study. Dx networks operate at much low pressures, typically below 4 bar, in comparison to Tx networks, which typically operate between 5 bar and 70 bar. Dx networks also have lower gas

demands and flowrates than Tx networks, meaning that the potential quantity of renewable gas that can be injected into a Dx network is much lower than that of a Tx network and that Dx networks require smaller capacity and lower powered compressors to bring the biogenic renewable gas up to a suitable injection pressure. This in turn results in Dx network studies being on a smaller scale to Tx network studies. From technical and economic points of view, this means smaller plant capacities, shorter transport distances, and that local or regional areas are analysed in Dx network studies as opposed to nationwide studies in the case of Tx networks. Bekkering et al. considered a Dx network in the Netherlands where the total gas demand was $8x10^6$ Nm^3/a (approximately 84.4 GWh/a). The authors analysed a range of scenarios for biomethane to meet between 10% and 100% of the annual gas demand, using on-farm digesters located within an 8.5 km radius of the gas grid varying in the range 100 - 300 Nm^3/h (8.4 - 25.2 GWh/a) along with gas storage of 2 x 10^6 Nm^3 for the 100% scenario. [61]. O'Shea et al. assessed the total biomethane resource and developed a build order, ranked by profitability, for biomethane production facilities injecting into the Tx network for the Republic of Ireland. The results showed that 1.8% of Ireland's final thermal energy use could be met by 22 plants with maximum size 50 GWh/a, or 2% of final thermal energy use could be met by 18 plants with maximum size 200 GWh/a [71].

2.3.3 Feedstock

Feedstocks can help define the technical and economic parameters for upstream models as discussed in section 2.3.1. The first distinction used to categorise biomass feedstocks is their origin, which can be split into dedicated resources including short rotation forestry, maize, algae, and waste streams including forestry residues, food waste, slurry, sewage sludge. From this review, it is clear to see that feedstocks from waste streams are the most investigated and commonly used. There are several reasons for this, the first being that, unlike dedicated resources, wastes and residues are not considered responsible for any GHG emissions during their production process under RED II [27]. Secondly, they can be a more economical form of feedstock as

there can be low or zero cost associated with feedstock from waste sources. In some cases they can generate revenue through a gate fee [62] [67] [71].

Categorization by origin can also be broken down to include where in nature the biomass exists. In this case the biomass is split in to one of the following categories, wood and woody biomass (e.g. branches, foliage, bark, briquettes, sawdust etc.), herbaceous biomass (grasses and flowers, straw, crops etc.), aquatic biomass (microalgae, microalgae), and animal and human waste (slurry, manure, sewage sludge etc.).These classifications can be important in giving an indication of the chemical composition of the feedstock, which in turn can help determine the most suitable conversion technology and predict the biogas yield [85].

Biomass can also be characterised according to its physical condition. Dry biomass such as willow, forestry residues, typically presents with a moisture content of below 13%, while the moisture content of wet biomass such as algae, silage, SHW, OFMSW, generally varies between 15% and 90% [86]. This characterisation will impact on the method of gas processing. Wet biomass is more suited to biogas production via anaerobic digestion, where high water content is required in the digester for the decomposition of feedstocks [4]. Dry feedstocks are preferable for gasification and methanation to produce bioSNG. It is possible however, to pre-treat wet biomass to reduce its water content to levels suitable for gasification or pyrolysis [87]. In this case, the energy recoverable from the dried biomass must be considered relative to the energy required to pre-treat the wet biomass. Moisture content also effects harvesting, transportation and processing. Additional energy can be required for wet biomass as more water is being transported and it can require additional processing before storage such as drying or ensiling [86].

2.3.4 Technical Constraints Gas Grids Place on Biogenic Renewable Gas Injection

Gas that enters the natural gas network infrastructure must conform to strict quality standards. These are in place to ensure the safe transportation of gas within the network and that the gas delivered to consumers is within the

operating specifications of end use appliances, such as gas turbines for power generation, central heating boilers, cookers, ovens and gas fireplaces. Operating specifications ensure safe and efficient operation of the appliance. In 2016, the ISSAC project produced a report that outlined the regulatory framework including quality standards for biomethane for each EU member state that was producing biomethane at that time [88]. As the studies in this review are from several different counties, they each use the gas quality standard specific to the country being studied. However, despite the differences in the range of values specified for each parameter, there are a number of characteristics that are included in the majority of biomethane quality standards. These include physical properties such as WI (12.2 kWh/m^3 to 16.016 kWh/m^3), HHV (8.6 kWh/m^3 to 13.23 kWh/m3), water dew point (< -15 °C to < 2 °C). The water dew point is defined as the temperate at a given pressure that the water vapour will condense out of the gas. Biomethane standards also contain specifications for gas composition on allowable percentages of methane (> 78% to > 98.3%), carbon dioxide (< 2.5% to < 7%), hydrogen (< 12% to < 0.2%), and oxygen (< 0.5% to < 3% dry gas), and restrictions on undesirable compounds such as hydrogen sulphide (< 5 mg/m^3 to < 20 mg/m^3), sulphur (< 20 mg/m^3 to < 50 mg/m^3) , and ammonia (< 3 mg/m^3 to < 20 mg/$m^{3)}$ [40] [88]. Currently there is no gas quality standard in Ireland specific to biomethane.

It has been assumed by the biogenic renewable gas studies within this review that in the case of injection into the natural gas grid, the biogenic renewable gas has been upgraded to meet the gas composition and undesirable compound limits imposed by the gas quality standard. The sole exception to this is Cavana et al. [63], which considered the blending in a distribution network of biogas purified of sulphur compounds, O_2 and siloxanes, but not upgraded to biomethane by removing CO_2. Blending is the mixing of two gases of different compositions, it occurs in gas networks after injection of a renewable gas. The primary focus of the studies included in that work's review was to assess the impacts on WI, HHV, relative density and normal operating pressures and flowrates of blending renewable gas into the natural gas networks. Cavana et al. found that it was possible to inject up to 9% biogas

by volume into distribution network before the WI dropped below its minimum limit, offsetting 4.7% of natural gas demand due to biogas's high CO_2 content and low heating value [63]. Von Wald et al. [74] and Abeysekera et al. [78] both considered the injection of biomethane into low pressure distribution networks. The results showed that the distribution of the injected biomethane was not uniform and was concentrated in the pipeline near the injection point. As biomethane has a lower HHV than natural gas it results in a larger volume of gas being required to meet the consumers energy demand. However, biomethane has a similar composition to natural gas and thus the unmet energy demand by biomethane was relatively low when compared with natural gas blended with 10% hydrogen [78].

2.3.5 Compressed Natural Gas

CNG is a common choice of end use for biogenic renewable gases as it is an area in which significant greenhouse gas (GHG) savings can be made by the displacement of traditional vehicle fuels such as diesel and gasoline. When biogenic renewable gas is compressed and used as a transport fuel, it is often referred to as bioCNG. Analysis by Börjesson et al. found in a well-to-wheel life cycle analysis that bioCNG used in light duty vehicle, such as passenger cars and vans, can have a GHG emissions reduction of between 80% to 90% using the RED methodology or 75% to 99% using the ISO methodology. It also determined that bioCNG heavy duty vehicles, such as trucks and buses, could reduce GHG emission compared to diesel by 84% to 91% under the RED methodology or by 75% to 101% using the ISO methodology. Both RED and ISO are methods of calculating the GHG performance of a product. In the RED methodology GHG effects of potential by-products generated in the vehicle fuel production system are allocated by dividing the total GHG emissions between the biofuel and the by-product based on their lower heating value (LHV). For example, digestate from anaerobic digestion is 90% water and is thus assumed to have a LHV of zero, leading to 100% of GHG emissions being allocated to the biofuel. RED also does not include any indirect effects on soil carbon content due to biomass feedstock harvest. Comparatively, the ISO methodology includes the effects of potential by-

products generated in the vehicle fuel production system, by calculating the indirect GHG effects of the by-products when they replace an alternative product. For example, digestate for anaerobic digestion utilised as a replacement for mineral fertiliser, thus reducing the need for production of mineral fertiliser [19].

Today there are over 22.4 million natural gas vehicles, and 26,677 natural gas refuelling stations distributed through 86 countries worldwide, with significant concentrations in Iran, China, Argentina, Brazil, India, Pakistan and Italy [16]. According to the Natural and bio Gas Vehicle Association (NGVA) Europe, there are currently 3,827 CNG stations in operation throughout Europe, one-third of which are in Italy [17]. Patrizio et al. conducted an assessment of the various pathways for biogas production in the Po valley region in Northern Italy. The results showed that without a carbon price grid injection at a net cost of 5.18 €/GJ was most economically feasible end use of biomethane, followed by bioCNG with a net cost of 5.87 €/GJ. When a carbon price of 100 €/tCO_2 is included, combined heat and power plants at a net cost of -1.5 €/GJ became the most economically feasible, and bioCNG remained in second place with a net cost of -0.53 €/GJ [73]. Browne et al. investigated the availability and production cost of bioCNG for a number of different feedstocks in the Republic of Ireland. The study found that bioCNG produced from OFMSW was the cheapest to produce at a cost of 0.36 €/L diesel equivalent, when associated with a gate fee of 70 €/t. This was followed by SHW estimated at 0.65 €/L diesel equilavent. However, these feedstocks have a limited availability in Ireland, and between them only provided 1.4% of the renewable transport target. The cost of bioCNG from grass silage (surplus to animal feed) and slurry was found to be the highest cost at 1.41 €/L diesel equivalent, however they are the most abundant bioCNG feedstocks [62]. These papers show that with finacial supports and incentives such as gate fees, feed-in tarriffs or carbon taxes bioCNG is an economically viable end use for biogenic renewable gas, while also making a significant impact on GHG emissions reduction.

The Irish haulage sector is currently experiencing the roll out of a network of 14 public CNG filling stations for heavy trucks, all of which will be connected

to the Dx network [28]. However, CNG filling stations connecting to the gas grid can have a significant impact on the gas network [89]. The extra demand it places on the network can cause fluctuation in balancing patterns and network pressures. It will also limit the composition of the gas in the network, as it must conform to the EU standards for biomethane as an automotive fuel [42]. Perhaps the most significant of these restrictions from a renewable gas point of view is that the hydrogen component of the gas is restricted to 2% [45]. Currently the EU standard for biomethane as an automotive fuel and standards or biomethane injection into the gas grid are very similar and thus for this work the biomethane was modelled to be upgraded to be of a standard for injection into the gas grid and use as a vehicle fuel.

2.3.6 Injection Point Location

This review found that research to date has used resource-based allocation when selecting injection point locations. This means that locations for injection points are optimised based on distribution of feedstocks in the surrounding area. Geographical Information System (GIS) calculation tools are used to combine site specific data on biomass resources with the locations of gas network and road transportation infrastructure, to size and site plants and injection facilities [69] [73] [14] [71] [73] [81] [76] [81]. O'Shea et al. used this methodology combined with several different incentive scenarios and two different digester sizes to optimise the location for centralised anaerobic digesters and injection facilities, using the Republic of Ireland as a case study. The study also established an order in which to build the optimised facilities based on their profitability [71]. In a similar study, Singlitico et al. assess the locations that optimise net profit value (NPV) and minimise the levelised cost of energy (LCOE) for centralised forest residue gasification plants and bioSNG injection facilities for the Republic of Ireland [76].

Bekkering et al. [61] adopted a version of this approach, in which it was combined with consumer demand data from the natural gas grid to highlight areas of large gas demand. The work examined a case study of a Dx network in the Netherlands, to optimize the supply chain for biomethane injection into

the grid for a number of possible injection facility locations and biomethane demand scenarios. The DSO supplied a list of several possible injection facilities, located at pressure reduction stations on the Dx network where the pressure was reduced from 8 bar to 300 mbar and where a significant gas demand was measured. The model assessed several scenarios in which 10% - 100% of the annual gas demand was replaced with biomethane. The injection facility used was selected based on which station was closest to the digesters that could supply the required quantity of biomethane to be injected into the gas grid in that scenario.

As noted by Bekkering et al. [60] [61] the large fluctuations in gas network demand throughout the year meant that a constant rate of renewable gas injection into the gas grid was not practical. These studies also illustrated the value of including network demand data on choosing the location of injection points to maximise renewable gas injection into the gas grid. However, further work is required account for other impacts to grid operation, such as pressure drops and changes to gas quality as discussed in section 2.3.4 above.

2.3.7 Supply Chain

The supply chain for biogenic renewable gas production can encompass a wide range of elements. These elements are broken down into the following headings: feedstock availability, transport logistics and costs, production and upgrading related logistics and costs, sizing of plants, and incentives and subsidies. Each of these can play important roles in optimising the renewable gas supply chain. O'Shea et al. [71] [14] combined all of these elements to optimise biomethane injection locations, plant sizes and build order while maximising plant profitability. Singlitico et al. [76] used a similar approach to assess the potential for bioSNG. Both studies assumed the renewable gas produced could be injected into an above ground installation (AGI). AGI is the term used to describe city gate stations on the Irish gas network. They are pressure reduction stations connecting the Tx network to the Dx network. Singlitico et al. [76] took the maximum injection capacity of the AGIs set by the Irish gas Tx systems operator. The results found that the minimum

levelised cost of energy is achieved with one centralised plant at 86.3 €/MWh and increased to 89.5 €/MWh, 93.7 €/MWh and 97.1 €/MWh for two, three, and four plants, respectively. On the other hand, the net present value for the two-plant configuration, 165.8 M€, is greater than that for one plant,129.9 M€ as it used a larger portion of the available biomass. It was also greater than the three plant 129.3 M€ and four plant 98.9 M€ scenarios, due to its greater economies of scale. However, that study did not consider the large fluctuation in gas network demand, which could limit the quantity of renewable gas that can be injected as noted by Bekkering et al. [60] [61]. To fully assess the relationship between the grid constraints discussed in the previous section and the supply chain, further research is needed.

Hengeveld et al. [68] studied the biomethane supply chain with a particular focus on economic optimisation of centralised versus decentralised AD for a number of different scenarios. The centralised and decentralised layouts for biomethane production are outlined in the schematic in Figure 2-3 below. This schematic in general terms can also be applied to bioSNG. In the centralised scenario, feedstocks are trucked to a large-scale gas production and upgrading plant, located at the injection site, and by-products are then removed from the plant. In the case of anaerobic digestion, digestate is transported back to farms to be used as a substitute for mineral fertiliser. For bioSNG, by-products such as ash are transported for disposal [76]. In the decentralised scenario, small-scale gas production and upgrading plants are located on-farm. The upgraded gas is then transported either by pipeline or virtual pipeline to the injection facility. A virtual pipeline is system that allows liquid or compressed natural gas to be transported by road, rail or sea.

The results found by Hengeveld et al. [68] indicated that when producing a given amount of biomethane, the production cost was lower for a centralised digester than for decentralised digesters. This was due to the increased investment, operational and biogas transportation cost being larger than the decreased feedstock transportation cost found for decentralised digesters compared to a centralised digester. However, work by Singlitico et al. which examined the supply chain and location of gasifiers to produce bioSNG in the republic of Ireland found that for a single plant, with no injection capacity

limits, the optimal size which minimised the levelised cost of energy was 102 MW_{SNG} as the feedstock transportation cost increased steeply for capacities larger than this [76]. Hengeveld also noted that the number of transport movements could be higher for a centralised digester, which is undesirable from an environmental point of view. Also, from a maintenance point of view, it may be desirable to have alternatively scheduled maintenance of decentralised digesters, especially if a certain minimum supply is always required. Further research is required to fully assess the advantages and disadvantages of centralised versus decentralised digesters.

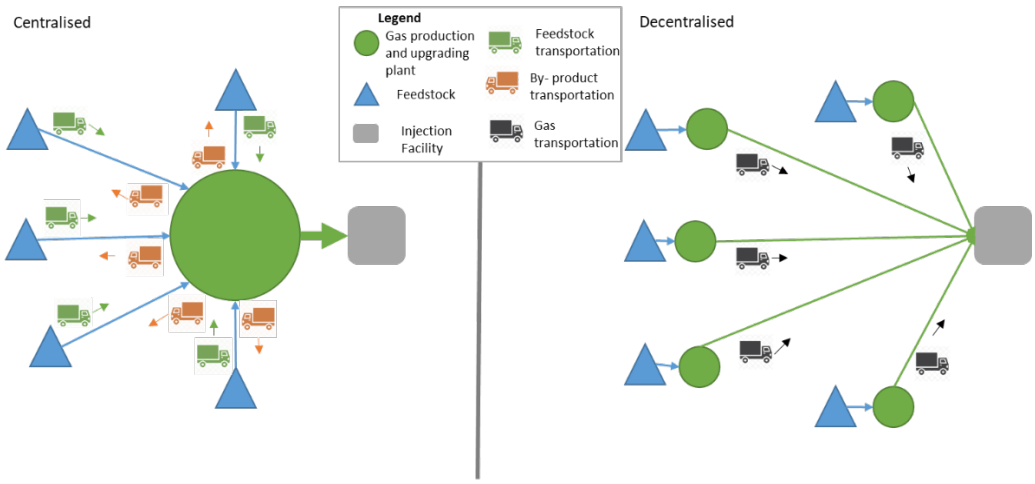

Figure 2-3:Schematic of centralised vs decentralised renewable gas production.

2.3.8 Use of SCADA Data in Model

The use of SCADA data in modelling studies has two primary functions: to validate simulation results, and to provide accurate representations of gas demand profiles for a network. Cavana et al. benchmarked their model against results obtained from Marte R2 by DEK S.r.l currently used by the Italian distribution network operator (DSO), comparing the results at a number of key nodes in the network [63]. This then lends credibility to the model when it is used to assess the injection of biogas, not biomethane, into the distribution network.

The use of gas grid data is almost exclusively used in models that consider the renewable gas after downstream of injection into the network; however, there are four exceptions to this. Singlitico et al. [76] takes into consideration limits imposed on injection capacity at AGIs on the Irish gas network. Gallagher et al. [75] used grid demand data to determine that it was more suitable to inject into Tx over Dx for an assessment of bioSNG production, considering plants at a scale of $50MW_{th}$ and $300MW_{th}$. Bekkering et al. used gas demand for a Dx network in the Netherlands to assess the potential penetration of biomethane, giving particular consideration to the fluctuation of gas demand against the production of biomethane throughout the course of a year for a number of different user scenarios [60] [61]. The study found that depending on the scenario, the maximum gas demand in a year was between 6.8 and 23.3 times the minimum gas demand recorded in the same year. This highlights challenges associated with the assumption of renewable gas injection into the natural gas network at a constant rate if high levels of penetration are to be achieved.

2.4 Conclusions and recommendations

Technical and economic assessments play an important part in characterising the role that biogenic renewable gas can play in the decarbonisation of energy systems. This work has reviewed 23 journal papers assessing the technical and economic impacts of biogenic renewable natural gas with a focus on gas grid injection. The work has also identified five key complimentary elements (i) the technical constraints gas grids place on biogenic renewable gas injection, (ii) models for biogenic gas production and supply chains, (iii) the use of compressed natural gas (CNG) as a vehicle fuel, (iv) the optimisation of injection facility location, and (v) the incorporation of SCADA data.

Several papers have used a combination of these elements to create upstream models that focus on the optimisation of biogenic renewable gas supply chains and the location of renewable gas injection locations. O'Shea et al. [14] [71] , Singlitico et al. [76] [81] and Cucchiella et al. [64] [65] used techno-economic models that aimed to identify the most profitable supply

chains and injection locations for renewable gas. Patrizio et al. [73] also focused on the most profitable solution. However, their primary focus is on comparison between different end uses for biogas in the Po valley. Other authors developed models that concentrated on maximising the quantity of renewable gas production [75] [77]. Bekkering et al [60] [61] also included the fluctuating pattern of gas demand in their model to determine the maximum quantity of biomethane injection.

Downstream models also used a combination these complimentary elements to simulate the dispersion of renewable gas once it has been injected into the natural gas grid. They have considered the effects on key gas quality standard parameters including WI, HHV, gas composition and normal operating pressures and flowrates [78] [63].

However, the review also found that there are several gaps in the state of the art. Firstly, Singlitico et al. [76], [81], O'Shea et al. [14], [71], and Hoo et al. [69] incorporated elements (iv), the optimisation of injection facility location, and (ii), models for biogenic gas production and supply chains to optimise the integration of biogenic renewable gas into gas networks by determining the most financially viable injection locations and supply chains. Patrizio et al. [73] and Parker et al. [72] also took into account element (iii), the use of compressed natural gas (CNG). On the other hand, Abeysekera et al. [78], and Von Wald et al [74], used element (i), the technical constraints gas grids place on biogenic renewable gas injection, to examine the impact to pressures, flow rates and gas quality of biogenic renewable gas blending in gas networks. Element (v), the incorporation of SCADA data is also included in similar studies by Cavana et al. [63], and Pellegrino et al. [80]. A combination of these modelling approaches including all elements would enable consideration to be given to the interaction between upstream and downstream models and depict a clearer picture of the overall integration of biogenic renewable gas with gas networks.

Secondly, the integration of renewable gas has been assessed from several standpoints, including feedstock availability, fluctuating seasonal gas demand, but consideration has yet to be given to the ability of the natural gas

grid to receive biomethane. This may also be extended to the optimisation of locations for the injection of renewable gas into the gas network. Previous studies have optimised injection locations from a feedstock distribution point of view, with Bekkering et al. [61] also giving some consideration to gas demand. However, to date, research has not taken into account the optimum location from a gas network point of view, including giving consideration to grid constraints including pressures, flowrates, HHV and WI.

Thirdly, while several studies have included the use of gas network SCADA data for either validation or accurate profiling purposes, the incorporation of CNG demand profiles has yet to be investigated. CNG stations connected to distribution networks can significantly increase the overall demand on the network [89]. Collantes et al. examine the experience of Argentina with CNG. As part of this, they show the monthly gas demand between 2001 and 2007 [90]. Comparing this with the annual gas demand presented by Bekkering et al. for a Dx network in the Netherlands [60], it is evident that there is slightly different seasonal variation between CNG and most industrial and residential gas demand. Future work should assess the impacts CNG demand can have on gas networks and their ability to accept renewable gas.

Further investigation of these areas could greatly assist network operators and renewable gas producers to make better informed decisions when locating and sizing renewable gas production plants and injection facilities on natural gas infrastructure.

2.5 Chapter Summary

This chapter reviewed 23 peer – reviewed journal papers that outline the state-of-the-art in technical and economic assessments of biogenic renewable gas injection. The review found that the state-of-the-art literature highlighted the importance of models that analyse the production, injection, and distribution of biogenic renewable gas in the gas grid. Research to date has developed models to optimise biogenic renewable gas supply chains and injection points. These optimisation models have been approached from several different perspectives, including (a) maximising renewable gas production,

(b) minimising the cost of energy, and (c) matching the variable nature of gas demand. Models have also been created to determine the impacts of biogenic renewable gas injection on gas networks. These models have been used to assess gas blending in the network, including pressures, WI, HHV and gas composition. However, it also identified several gaps in the literature that should be addressed in future work. Firstly, the state of the art does not include a comprehensive study where all the potential impact factors associated with biogenic renewable gas injection are considered. Secondly, studies that model and optimise the locations for renewable gas injection facilities have not given consideration as to how the injected gas will affect gas flow within the network. Finally, the impact of CNG demand on gas networks and their capacity to accept renewable gas injection should be determined.

Chapter 3 will build on the gap identified in this literature review by simulating a gas Dx network to investigate the impact of limits imposed by the gas network operator on the quantity of biomethane that can be injected.

Chapter 3 The Technical Feasibility for Biomethane and Compressed Natural Gas in a Gas Distribution Network

3.1 Chapter Overview

Chapter 2 identified several gaps in literature on technical and economic assessments of biogenic renewable gas injection, including the need to consider how seasonal demand, gas grid technical constraints and grid connected CNG filling stations affect the injection of biomethane into gas Dx networks. This chapter details the simulation of a gas distribution (Dx) network to investigate the impact of limits imposed by the gas network operator on the quantity of biomethane that can be injected. The results calculated the grid's capacity to accept biomethane on an hourly basis over the course of a year. Scenarios of maximum, minimum and no demand at a Dx-connected compressed natural gas (CNG) filling station were computed for the three potential locations being investigated for the biomethane production and injection facility.

3.2 Introduction

Extensive research has been done on the simulation of gas networks and the technical impacts of biomethane injection. Pellegrino et al. developed a steady-state mathematical model simulating the injection of renewable gas into the transmission (Tx) network. The results showed that the injection of biomethane had a negligible effect on key gas quality parameters including Wobbe Index (WI), higher heating value (HHV) and gas gravity [80]. Von Wald et al. [74] and Abeysekera et al. [78] both investigated the injection of biomethane into a low-pressure distribution network. The studies found that the distribution of the injected biomethane was not uniform and was concentrated near the injection point. The results also determined that the injection of biomethane had a localised effect on pressure and required a larger volume of gas to meet the same energy demand, as biomethane has a slightly lower HHV than natural gas [78].

However, these studies assume a fixed injection of biomethane and do not consider the impact of diverse seasonal demand on operating conditions within the gas network. This is of key importance when considering the overall gas supply chain, as highlighted in work by Bekkering et al. Their work used measured grid data to create an annual profile for gas demand on a distribution (Dx) network in the Netherlands. It investigated the ability of the biomethane supply chain to meet different ratios between maximum and minimum demand, called the seasonal swing factor. The work is based on the assumption that flexible biogas production is possible, which is supported by [91] but acknowledges that further research is needed. The results found that flexible biogas production from a single digester was the cheapest option, followed by two digesters producing biogas at a constant rate, one of which operated year-round, while the second was only operated during certain periods of high demand. Storage was the most expensive in all cases and had significant spatial disadvantages at seasonal swing factors above 2 [61]. However, the analysis does not include a grid simulation to full assess the impact to the Dx network.

To the best of this author's knowledge, there have been no studies to date that have considered the impact of constraints within the natural gas grid on its ability to accept biomethane. The aim of this chapter is to assess the biomethane capacity from a gas grid perspective by analysing supply and demand patterns. This work is of importance as it demonstrates the necessity for prior network planning to maximize the quantity of renewable biomethane that can be injected into the network. The addition of a CNG filling station to the gas network could add substantial demand, potentially affecting pressures and flowrates within the grid [89]. However, to date no study has attempted to characterize this impact.

This chapter proposes a novel modelling approach to quantify the grid capacity for biomethane. For this work, the grid capacity for biomethane will be defined as the maximum quantity of biomethane that can be injected into the network while maintaining pressures and flowrates within normal operating limits. It will also assess the impact the additional demand from the CNG filling station has on the Dx network.

3.2.1 Initial Modelling Work

To gain an understanding of the equations and methodology used to simulate gas network, MATLAB was used to create both steady-state and dynamic models of basic gas distribution networks. These models were validated using examples from the literature.

The steady-state model simulated a Dx network operating at both medium and low pressures. The method consists of a set of algebraic equations equal in number to the number of state variables to be calculated. They are formulated using standard gas flow equations and Kirchhoff's first and second laws applied at all nodes. Initial approximations of the pressures at each node are iteratively corrected using the Newton-Raphson method. The specific gravity, calorific value and flowrate in each pipeline are calculated for each iteration. Further detail on this model can be found in the appendices in section A.1.1 Steady-State Model.

The dynamic model simulated a branch of a Dx network operating at a medium pressure. Under the assumption of isothermal flow, unsteady gas dynamics are governed by the conservation of mass Equation A-9 and momentum Equation A-10. The equations are rearranged into two partial differential equations, which were then solved using MATLAB ode15s solver to find the pressures and flowrates on the network. Further detail on this model can be found in the appendices in section A.1.3 Dynamic Model.

These MATLAB models allowed the author to gain an in-depth understanding of the theory behind steady-state and dynamic gas network simulation. However, when investigating the grid capacity to accept biomethane, Synergi gas modelling software [92] is used. This software is the software used by Gas Networks Ireland (GNI), the Irish Tx and Dx network operator. An existing but anonymised Dx network was chosen as a case study and the simulation was based on an initial steady-state template of the network created by GNI. This was determined to be the best approach as the novelty of this work is based in the methodology of assessing the potential

for biomethane injection and not the underlying mathematical theory of gas network simulation.

3.3 Methodology

3.3.1 Case Study

An existing but anonymised Dx network, supplying an Irish town of 17,000 inhabitants and a smaller town of 4,400 inhabitants, with a mix of industrial, residential, and commercial demand is chosen as a case study. The Dx network consists of both 2 and 4 barg networks. The surrounding area has high potential for biomethane production due to the town's location in a highly productive agricultural region. There is also potential for significant demand at a CNG filling station, located on a nearby motorway, which is part of the TEN-T Core Network [93]. Figure 3-1 is a schematic of the representative Dx network and surrounding area. To assess the impact of the biomethane production and injection facility location on the grid capacity for biomethane, three potential injection sites were chosen in key locations of supply/demand on the Dx network. The first was located close to the above ground installation (AGI). The AGI is a pressure reduction station, which connects the Dx network to the Tx network, thus acting as the current gas supply to the Dx network. The second potential production and injection facility site was located near the proposed CNG filling station, which may add substantial demand to the network. The third potential production and injection facility site was located near the larger town's centre, as this is currently the area with maximum demand on the network. Each candidate biomethane production and injection facility is connected to the Dx network by a hypothetical pipeline with a length of 60m.

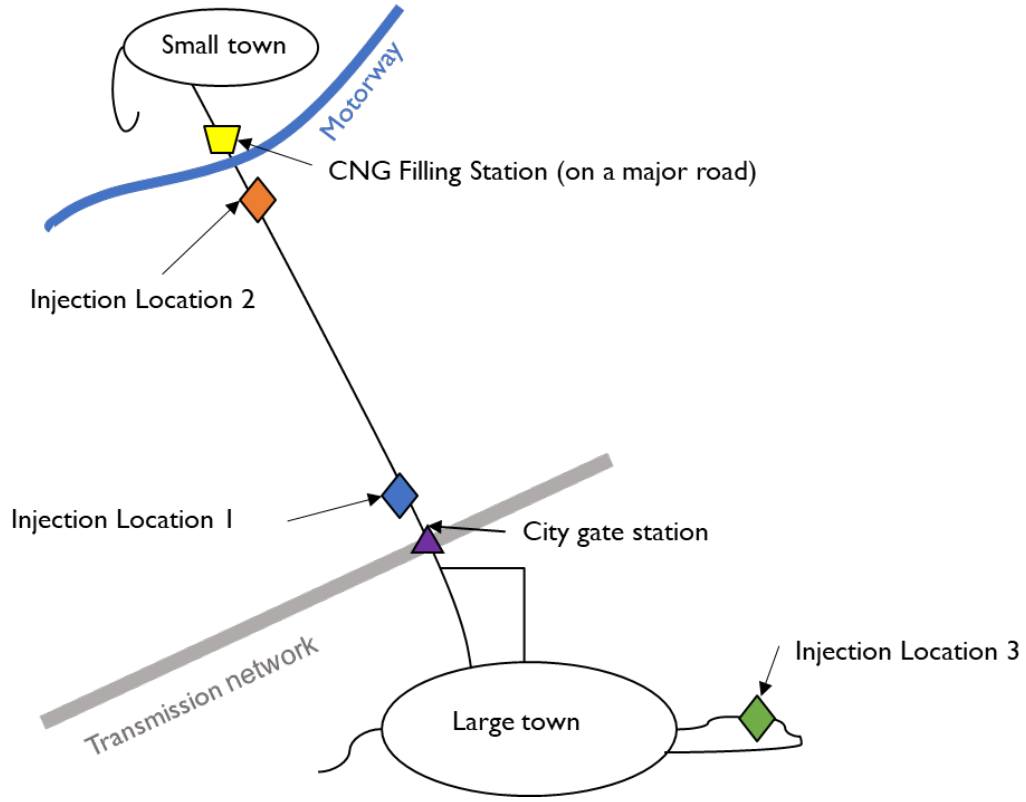

Figure 3-1: Schematic of the representative Dx network.

3.3.2 Dx network Model Overview

Synergi gas modelling software is used to create the simulation of the representative Dx network [92]. This software was chosen as it is the modelling software used by the Gas Networks Ireland (GNI), the Irish gas systems operator, to analyse their Dx networks. An unsteady-state or transient approach is used in the Dx network simulation. Unsteady gas dynamics in a pipe are governed by the Euler equations for compressible fluids. These equations are expressed below, under the assumption of isothermal flow, Equation 3-1 shows the conservation of mass, while the momentum balance is expressed in Equation 3-2.

Equation 3-1: Continuity equation

$$\frac{\partial \rho}{\partial t} + \frac{\partial (\rho u)}{\partial x} = 0$$

Equation 3-2: Momentum equation

$$\left(\frac{\partial \rho u}{\partial t} + \frac{\partial \rho u^2}{\partial x}\right) + \frac{\partial p}{\partial x} + \frac{f \rho |u| u}{2D} + \rho g \sin\theta = 0$$

where ρ is the density of the gas, t is the time, u is the velocity, x is the distance, p is the pressure, f is the friction factor, D is the pipe diameter, g is the gravitational constant, and θ is the angle of inclination of the pipe.

Synergi uses the method of characteristics to solve for unknown pressures and flowrates within the network. This method assumes that:

(i) Δx is constant for all pipe lengths.

(ii) Δt is constant.

(iii) The isothermal wave speed of the gas (B) is constant.

(iv) $\Delta x/B$ must be an integer.

The isothermal wave speed is given by

$$B = \sqrt{gZRT}$$

where g is the acceleration due to gravity, Z is the gas compressibility factor, R is the gas constant and T is the temperature.

Annual gas demand profiles are created for each consumer demand point on the network using SCADA data from GNI. SCADA data is the actual metered pressure and flowrate data recorded at meter points, such as the AGI or large industrial consumers on the Dx network. For this case study, SCADA data was recorded on an hourly basis. Figure 3-2 below shows the total annual demand for the Dx network case study throughout 2018. The significant variation in demand between the summer and winter months is apparent. The demand depicted in Figure 3-2can be divided into to two categories, daily metered (DM) and non-daily metered (non-DM). DM demand includes demand from industrial and large commercial consumers, whose gas usage is monitored on an hourly basis. Non-DM is composed of demand from small commercial and residential consumers. DM demand accounted for 54% of the total annual gas demand on the case study Dx network in 2018, while non-DM demand makes up the remaining 46%. It is evident that DM demand

remains relatively constant throughout the year, while non-DM demand varies significantly between the winter and summer months.

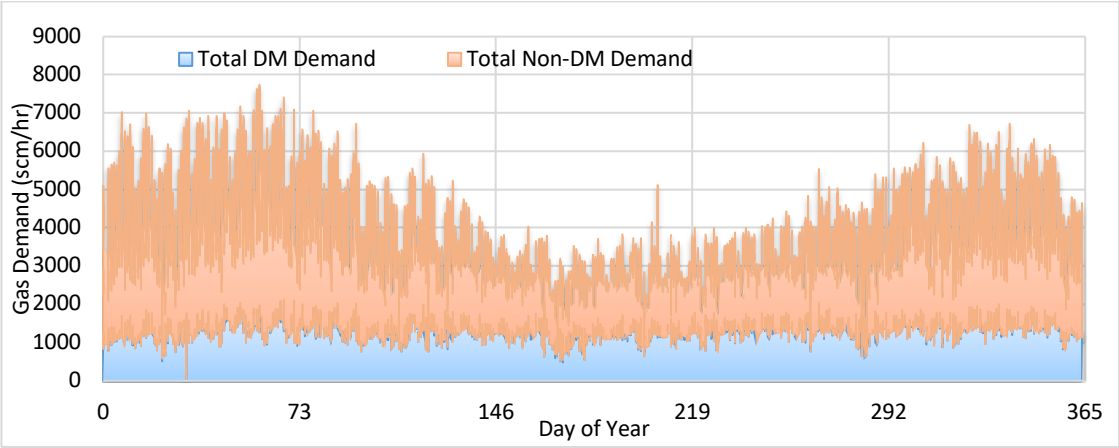

Figure 3-2: Total annual gas demand profile for the representative Dx network in 2018

This variation is further highlighted in Figure 3-3, which depicts the daily demand profiles for days on which the maximum, minimum and an average demand was experienced by the Dx network. Differences between DM and non-DM demands are also evident at a daily timeframe in Figure 3-3; DM demand maintains a steady level over the 24hr period, comparatively non-DM demand increases considerably between 7am and 11pm with notable spikes at 8am – 9am and 6pm – 8pm.

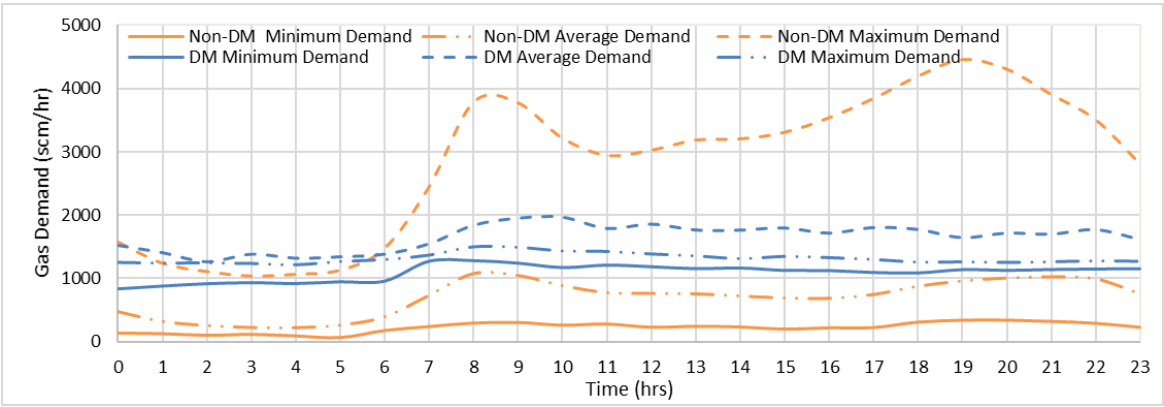

Figure 3-3: 24-hour DM and non-DM gas demand profiles for the representative Dx network in 2018.

Table 3-1 below outlines the different modelling scenarios examined to assess the impacts of adding a CNG filling station and biomethane production and

injection facility to a Dx network. The model is initialised with the SCADA data described above. The potential demand from the CNG filling station was then estimated using the method described in section 3.3.3 below. This demand was then added to the model to assess its impact on the Dx network. Each candidate biomethane production and injection facility is then analysed at its base and optimum conditions, as outlined in section 3.3.4.

Table 3-1 : Description of different modelling scenarios.

Scenario	Demand	CNG	Injection Point	Injection Diameter	Purpose
1	Winter Max	No	N/a	N/a	Validation of modelling framework
2 3 4 5 6	Summer Min Average Day Winter Max Summer Min Average Day	No No Yes Yes Yes	N/a N/a N/a N/a N/a	N/a N/a N/a N/a N/a	Impact of CNG on Network
7-25	Winter Max Summer Min Average Day	Yes/No	1,2,3	Baseline (72.9mm)	Impact of injection location on grid capacity for biomethane
26-44	Winter Max Summer Min Average Day	Yes/No	1,2,3	77.9 mm	Impact of injection pipeline diameter on grid capacity for biomethane
45-60	Winter Max Summer Min Average Day	Yes/No	1,2,3	Optimised	Find location and diameter that maximises grid capacity for biomethane
60 - 72	Year Run (2018)	Yes/No	1,2,3	72.9mm/ Optimised	Quantify annual capacity for biomethane

3.3.3 CNG demand submodel

The method outlined in Figure 3-4 was proposed to approximate the CNG demand. This method can apply to any location in which a CNG station is proposed but not yet built. Traffic flow patterns of HGVs on the motorway that passes the proposed CNG filling station in both directions were determined using data from Transport Infrastructure Ireland [94]. A tank with a capacity of 96kg CNG for trucks and 303kg for buses, reported by Hagos et al. [24] is used to calculate the CNG demand at the station. This concurs with the average tank size of 100kgs estimated by GNI for CNG trucks purchased in Ireland. Approximated maximum and minimum CNG demand profiles were created to give an estimate of the upper and lower bounds to the CNG demand which could be experienced at the CNG filling station. The GNI projection for CNG uptake in HGVs, of 24% of trucks and 13% of buses by 2030 are used to estimate to proportion of CNG HGVs in the traffic flow passing the CNG filling station. It is assumed that 50% of CNG HGVs that passed the filling station would stop and refuel to an average of 50% of the maximum tank capacity. This is to account for the fact that most HGVs passing the station will do so twice in a round trip and also that many haulage companies in Ireland have their own depots where the HGVs will return to refuel. The minimum CNG demand profile was determined using the minimum contracted station demand of 7525 m^3/day at standard temperature and pressure, specified by GNI for the Causeway filling stations. This corresponds to 52 heavy duty truck per day, which was determined to be the minimum demand at the station for commercial viability. It is assumed that the distribution throughout the day would be a constant percentage of the hourly traffic flow. The annual network demand increases by 24% and 13% respectively with the addition of the maximum and minimum CNG demands.

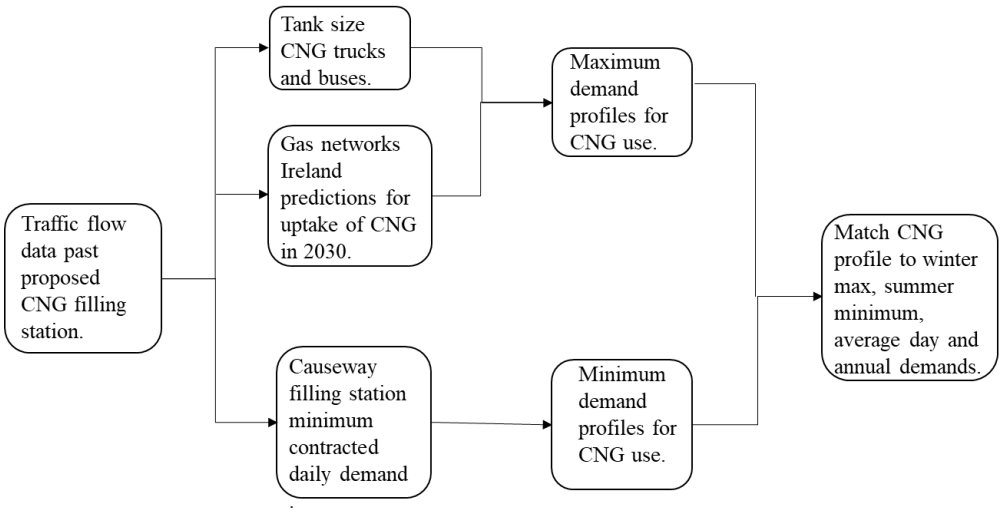

Figure 3-4: Outline CNG filling station demand submodel.

Figure 3-5 shows the annual demand profile for the representative Dx network the scenarios with no CNG, minimum CNG and maximum CNG demand at the grid connected CNG filling station. It is evident the addition of the CNG demand is significant to the overall dx network demand, particularly in the periods of lower network demand.

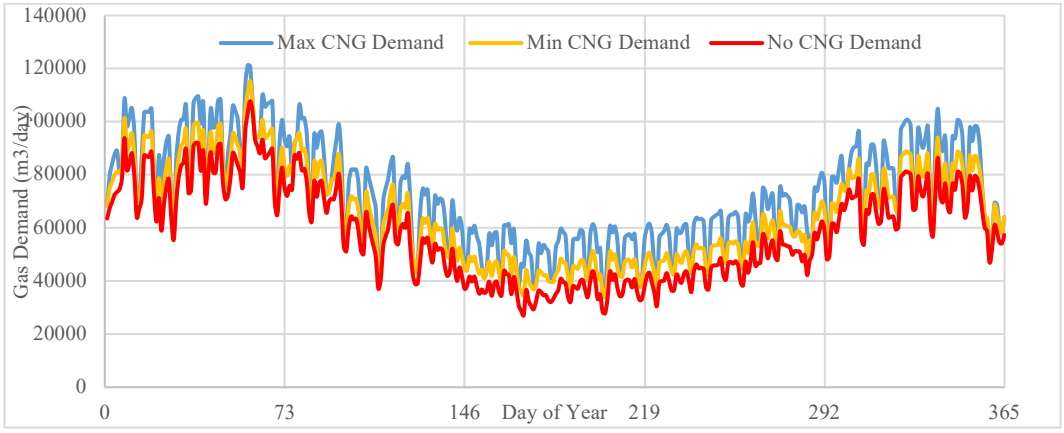

Figure 3-5: Annual profile for the no CNG (red), minimum CNG (orange) and maximum CNG (blue) demands for representative Dx network.

3.3.4 Optimisation Process

Figure 3-6 depicts the method used to optimise the injection pipeline diameter, with the objective function being the grid capacity for biomethane at each potential biomethane production and injection facility location. First, the gas demand profiles for the minimum demand day are loaded into the

model, the CNG demand scenario being analysed is set at the CNG filling station and the location of the biomethane production and injection facility being analysed is selected. The biomethane production and injection facility and AGI are set to have a constant pressure of 4 barg and 3.9 barg respectively. Setting the biomethane production and injection facility to a higher constant pressure than the AGI, means that the biomethane production and injection facility will supply a larger proportion of the gas demand establishing it as the dominant source of gas to the Dx, while still maintaining the AGI as close as possible to its normal operating pressure. The pipeline length connecting the biomethane production and injection facility to the grid is fixed at 60m. Initially the injection pipeline inner diameter is set to a predetermined baseline of 72.9mm, which is chosen, as it is the smallest standard pipeline diameter used on the medium pressure Dx network in the case study. By constructing the model in this way, it enables a calculation of the maximum flowrate of biomethane for the conditions set by the pipeline diameter and grid configuration. The simulation is run for the 24-hour period of the minimum demand day. After the simulation is run, checks are completed to ensure all pressures and flowrates on the network are within normal operating limits and that the pressure at the AGI remains constant. Normal operating pressures for the Dx network are between 2 barg and 4 barg for the medium pressure network and 60 mbarg 2 barg for the low-pressure network. If all conditions are met, the injection pipeline diameter is changed to the next standard size up and the simulation is re-run. This continues in an iterative manner until one of the conditions is violated, this establishes that the optimum injection pipeline diameter had been reached in the previous run and the maximum grid capacity for biomethane is determined. This optimization method was carried out for all three potential injection locations for the scenarios both with and without CNG at the summer minimum demand state. Once the optimum injection pipeline diameter has been determined for each injection location, the simulation is run for the maximum, average day, and annual demand scenarios, with the baseline and the optimised injection pipeline diameter, for each of the injection locations.

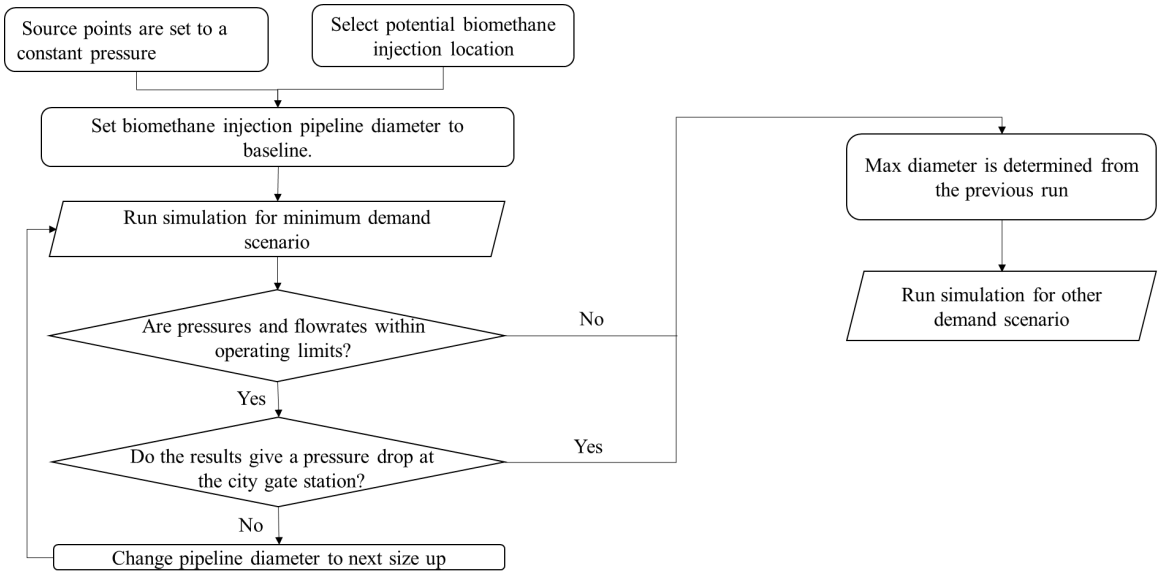

Figure 3-6: Method for optimising the injection pipeline diameter.

3.4 Results and Discussion

Figure 3-7 shows the resulting flowrate from the each of the candidate biomethane production and injection facilities during the maximum demand day. Figure 3-7 (a) considers the scenario of maximum CNG demand at the CNG filling station, Figure 3-7(b) considers the scenario of minimum CNG demand and Figure 3-7 (c) considers the scenario of no CNG demand. Results are shown for the three potential production and injection facility locations, for both the 72.9mm base injection pipeline diameter and the optimised injection pipeline diameter. It is apparent that optimising the injection pipeline diameter and location can have a significant impact on the grid capacity for biomethane. This is also evident in the results obtained for the minimum and average demand days, which are included in the Appendices in Figure A.2- and Figure A.2- respectively.

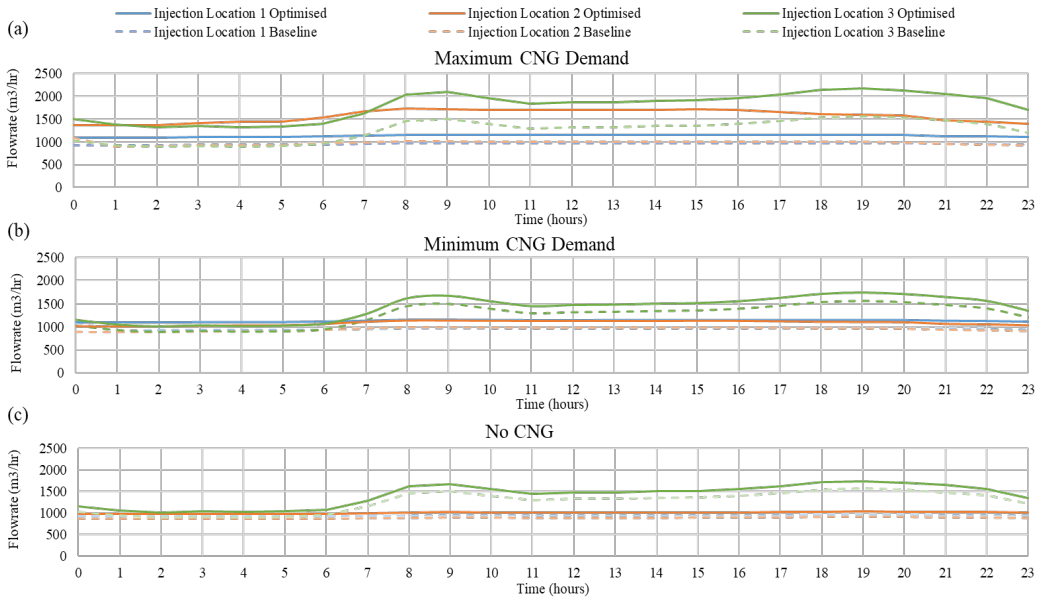

Figure 3-7: Results for the maximum demand day scenario with (a) the minimum CNG demand, (b) maximum CNG demand, and (c) no CNG demand, for the candidate biomethane production and injection facility at Location 1 (blue), Location 2(orange) and Location 3(green).

For the maximum demand day, it is evident that regardless of the CNG demand scenario, injection location 3 results in the maximum grid potential for biomethane. This is because in the maximum demand scenario, the demand of non-DM consumers increases significantly, while the CNG demand and the DM consumer demand remains relatively consistent with the minimum and average demand days. Out of the three potential injection locations, injection location 3 is closest to the large town centre when the non-DM demand is centralised. For the minimum and average day demand scenarios, injection location 3 remains the optimum location in the scenario where the is no CNG demand at the CNG filling station, as demand on the Dx network is concentrated in the large town. However, when analysing the scenario with maximum CNG demand at the CNG filling station, injection location 2 becomes the optimum location. This is due to location 2 being closest to the CNG filling station where the demand accounts for a significant percentage of the total network demand. Similarly, in the scenario where the minimum CNG demand being considered, injection location 1 becomes the optimum location, as it is situated between the CNG filling station and the large town centre.

This highlights the importance of reviewing the network being studied under several different demand scenarios. Current distribution network operator best practice conducts a steady state analysis at a 1 in 50 winter scenario to examine the impact to pressures and flowrates in the Dx network when upgrading the network or adding demand points, such as a CNG filling station. In the case where the addition of a biomethane production and injection facility is being considered, a steady state analysis for a summer minimum demand scenario is used to assess the location suitability and maximum hourly injection rate. However, these simulations alone do not account for the variation in demand experienced by the gas network. For example, if a steady-state analysis for the minimum summer demand was used to site and size a biomethane production and injection facility in the scenario of no CNG demand on the network, location 3, is the optimum location. However, as the biomethane injection into the network is constrained at the minimum flowrate, this results in an estimated potential of 82 GWh/a, in comparison to the 102 GWh/a estimated in Figure 3-8 below when biomethane injection is allowed to vary with grid demand. It also demonstrates the advantage of considering the development of the CNG market when planning for the addition of biomethane production and injection facilities to the gas network, to maximise the quantity of biomethane that can be injected into the network.

Figure 3-8 shows the annual cumulative biomethane injection determined by simulation results for the annual demand state. It is evident that optimising the injection pipeline diameter and injection location can significantly increase the grid capacity to accept biomethane. In the scenario where there maximum CNG demand at the CNG filling station, depicted in Figure 3-8 (a), there is an increase of approximately 18% in the grid capacity to accept biomethane in between the worst (Location 1, baseline diameter) and best (Location 2, optimised diameter) scenarios. For the minimum CNG demand scenario, shown in Figure 3-8 (b) the grid capacity for biomethane increased by approximately 7% from the worst (Location 2, baseline diameter) and the best (Location 1 or 3, optimised diameter) scenarios. In Figure 3-8 (c) for the scenario of no CNG demand at the CNG filling station, the rid capacity to

accept biomethane increases by approximately 12% from the worst (Location 2, baseline diameter) to the best (Location 3, optimised diameter) scenarios.

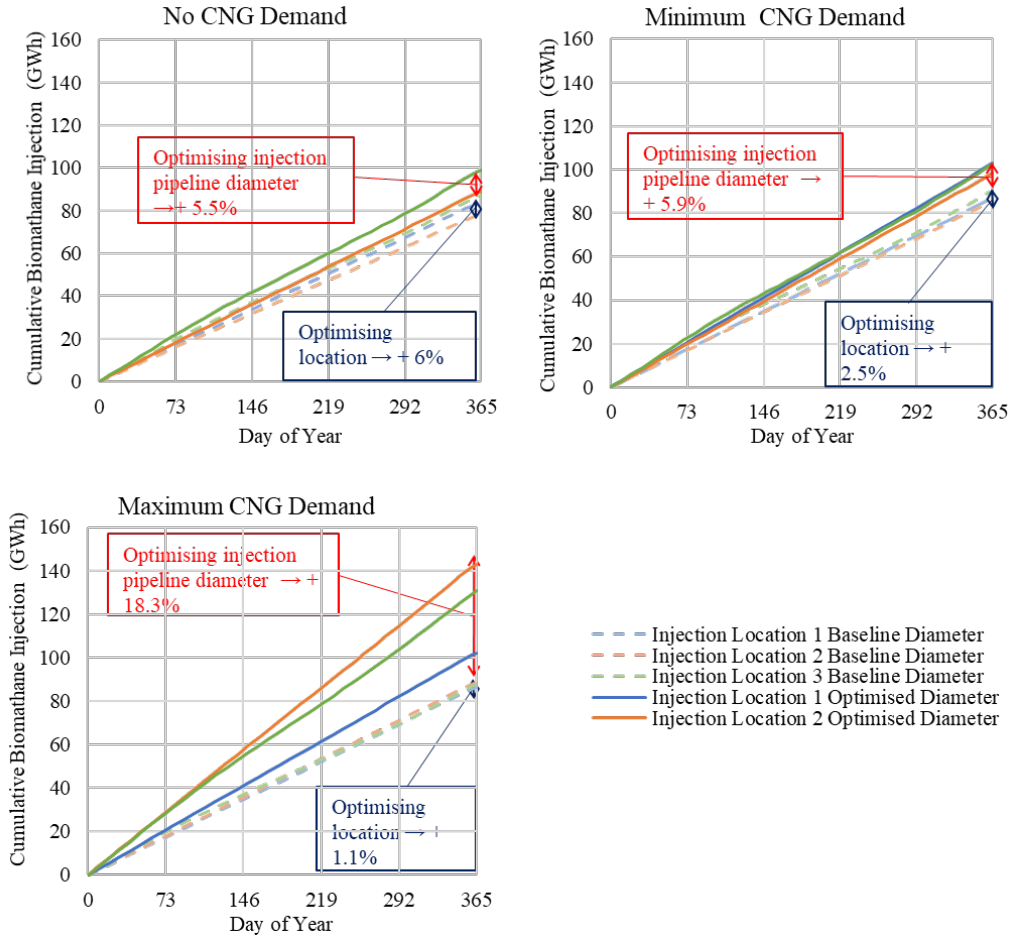

Figure 3-8: Results of the gas network demand submodel showing the optimised annual cumulative biomethane injection for each potential injection location, with (a) maximum demand at the CNG filling station, (b) minimum demand at the CNG filling station and (c) no demand at the CNG filling station.

It is evident from the results that the potential of biomethane injection into the grid cannot solely be based on resource availability, as has been assumed in previous work [14], [69]. Neither is the assumption of a constant injection rate used by other studies [80], [74], [78], practical if the priority is to maximise the quantity of biomethane being injected into the natural gas grid.

In this case study, the pressure at the AGI was fixed at 3.9 barg to keep it as close to its normal operating pressure, while still allowing the biomethane production and injection facility to supply the network. The reduction of pressure at the AGI could potentially increase the supply from the biomethane production and injection facility. However, it may also cause large drops in

pressure during periods of high demand. An area of potential interest for future work may be investigating to what extent the pressure at the AGI can be reduced without having adverse effects on the network.

This work assumes that the biomethane production plant is operated with flexible production, to match demand throughout the year. While Bekkering et al. determined that storage was a more expensive solution than flexible biomethane production [61], integrating storage with flexible biomethane production to allow greater biomethane production during periods of low demand and provide a reserve to biomethane for peak demand periods is an another possible area of interest for future work.

3.5 Conclusions

The integration of biomethane production and injection facilities and CNG filling stations into gas network infrastructure presents many challenges. One of the main challenges that has not previously been explored is the ability of the natural gas grid to accept biomethane while maintaining pressures and flowrates within normal operating conditions. This study quantified the grid capacity for biomethane while giving particular consideration to the location of the biomethane production and injection facility in relation to the location of the CNG filling station and the location of other major demands on the network. It also determined that to give a full overview of how best to integrate the biomethane production and injection facility into the network several different demand scenarios must be analysed to represent the variation in both the demand on the natural gas network and the demand at the CNG filling station.

This work presents a novel method for determining the maximum amount of biomethane that can be injected into the grid by optimising the injection pipeline diameter for the three potential injection locations. The results show the annual quantity of biomethane that can be injected into the gas grid can be increased significantly by optimising the injection pipeline diameter and the location of the biomethane production and injection facility. It determined that optimising the location could increase the grid capacity for biomethane

by between 1.1% and 6%, and that optimising the injection pipeline diameter could increase the grid capacity for biomethane by between 5.5% and 18.3%. The results found, for this case study, that by using the optimisation method, the quantity of biomethane injected into the grid as a percentage of the overall Dx network annual demand, could be increased from 35% to 43% with no CNG demand, 33% to 42% with minimum CNG demand, and 31% to 49% with maximum CNG demand. Building on these results, Chapter 3 considers the ability of the biomethane supply chain to match the varying gas demand throughout the year.

3.6 Chapter Summary

The integration of biomethane production and injection facilities and CNG filling stations into gas Dx networks presents several technical challenges to the operation of distribution (Dx) networks, including changing load-balancing patterns, and determining optimum locations for biomethane production and injection facilities. In this work, a representative gas Dx network, for an Irish town of 17,000 inhabitants in an area of high potential for both CNG and biomethane was chosen as a case study. The results found that by optimising the biomethane production and injection facility location and injection pipeline diameter, the quantity of biomethane injected into the grid as a percentage of the annual demand, could be increased from 35% to 43% with no CNG demand, 33% to 42% with low CNG demand, and 31% to 49% with high CNG demand.

Chapter 4 uses the results from this Dx network simulation to determine a range of possible plant sizes for each potential facility location and CNG demand scenario and assess the techno-economic impacts.

Chapter 4 A Techno-economic Case Study for Biomethane Injection and Natural Gas Heavy Goods Vehicles

4.1 Chapter Overview

This chapter used the results from the Dx network simulation in Chapter 3 is used to determine a range of possible plant sizes for each potential facility location and CNG demand scenario. Next, a spatially explicit geographical information systems (GIS) model is created to map the distribution of feedstock suitable for biomethane production in the surrounding area and determine transportation distances. These two submodels feed into a techno-economic model that calculates the net present value (NPV) and levelised cost of energy (LCOE) for each configuration.

4.2 Introduction

The total final energy consumption in Ireland in 2019 was approximately 520 PJ, 42.1 % of which can be attributed to transport. Within the total final energy consumed by transport, 96.4% originated from fossil fuels [95]. The recast of the renewable energy directives 2018/2001/EU (RED II) set two mandatory targets to be achieved by the 27 European Union (EU) member states by 2030. The first target mandates that at least 32% of gross final energy consumption across the EU must be from renewable sources. The second target obligates fuel suppliers to ensure that a minimum of 14% fuel consumption in the EU transport sector comes from renewable sources [27]. For a fuel to be counted towards the transport targets of RED II, it must meet the sustainability criteria of 65% greenhouse gas emissions savings compared to the standard fossil fuel comparator by 2030 [35]. The production of biomethane for use as a vehicle fuel for heavy goods vehicles (HGVs) could be a significant step towards meeting these targets.

Biogas is produced through the process of anaerobic digestion, whereby organic biomass and resides from food production, waste processing and agriculture are broken down biologically in the absence of oxygen. The

biogas produced is approximately 60% methane and 40 % carbon dioxide. Biogas can itself be used to produce heat and electricity or can be upgraded, by removing the carbon dioxide, to produce biomethane suitable for gas grid injection or used as a vehicle fuel [4]. Since 2013, there has been significant growth in the number of facilities throughout Europe that are upgrading biogas to biomethane for grid injection and use as a vehicle fuel [35]. European transmission network operators, Energynet.dk (Denmark), Fluxys Belgium, Gasuine (Netherlands), Gaznat (Switzerland), GRTgaz (France), ONTRAS (Germany) and Swedegas (Sweden), signed a joint declaration with the aim of achieving a carbon dioxide neutral gas supply by 2050 [8]. The Irish transmission (Tx) and distribution (Dx) network operator, Gas Networks Ireland (GNI) estimates that biomethane will meet 37% of annual gas demand by 2050. GNI is currently in the process rolling out the EU-funded Causeway project, which will deploy a network of 14 public compressed natural gas (CNG) filling stations for heavy goods vehicles, all of which will be grid connected, as well as the first biomethane production and injection facility to the Irish gas network [28]. However, the introduction of a CNG filling station and biomethane production and injection facility can significantly affect the operation of the gas network in a location. The extra supply and demand can cause fluctuations in network pressures and load balancing patterns [63] [78] [80] [89]. Ranges of gas composition within the network may also be limited, as biomethane will be required to conform to the EU standards for biomethane as an automotive fuel [42].

In a well–to–wheel lifecycle assessmrnt of bioCNG (biogenic conpressed natural gas), HGVs, Börjesson et al. found that they could reduce greenhouse gas (GHG) emissions by 84% to 91% under the RED methodology and 75% to 100% under the ISO methodology. RED [27] and ISO [96] [97] are widely used methods of calculating the GHG performance of a product. The RED method allocates GHG emissions of potential by-products generated during the production of vehicle fuel by allocating the total GHG emissions between the biofuel and the by-product, proportional to their lower heating value. For example, digestate from anaerobic digestion has 90% moisture content and is thus assumed to have a lower heating value of zero, leading to 100% of GHG

emission being allocated to the biofuel. RED also does not include any indirect effects on soil carbon due to biomass feedstock harvest. Comparatively, the effects of potential by-products generated in the production of vehicle fuel are included under the ISO methodology. This is done by calculating the indirect GHG effects of the by-products when they replace an incumbent product. For example, digestate from anaerobic digestion can be utilised in place of mineral fertiliser, thus reducing the need for mineral fertiliser production [19].

The state of the art has examined various aspects of the biomethane and bioCNG production and supply chains. Patrizio et. al investigated the economic viability of different potential end uses of biogas for the Po valley region in Northern Italy. The authors found that without a carbon tax, grid injection at a net cost of 18.65 €/MWh to the plant owner was the most economically feasible end use, followed by bioCNG at a net cost of 21.13 €/MWh However, when a carbon tax of 100 €/tCO_2 was introduced combined heat and power plants became the most economically feasible end use at a net cost of -5.4 €/MWh, with bioCNG remaining in second place at a net cost of-1.91 €/MWh [73].

O'Shea et al. used a spatially explicit model to determine that across Ireland there was 12.5 PJ/a of biomethane available from animal slurries and manure, food processing waste, and source separated household waste organic waste [13]. Browne et al. examined the availability and cost of various feedstocks for bioCNG production in the Republic of Ireland. The results found that bioCNG produced from organic fraction municipal solid waste (OFMSW) was the cheapest option at a cost of37.55 €/MWh, followed by slaughterhouse waste, and grass silage and cattle slurry at a cost of 67.55 €/MWh and 145.45 €/MWh respectively. However, the production potentials of bioCNG from OFMSW and slaughterhouse waste were limited to 1.14 PJ and 1.36 PJ respectively, contrasting with 27.55 PJ from grass silage (surplus to animal feed) and cattle slurry [62].

Bekkering et al. investigated flexible biomethane supply chains to match the fluctuations in seasonal gas demand. The authors analysed different possible

seasonal swing factor, which is the ratio between minimum and maximum demand. The study used measured grid data for a Dx network in the Netherlands to create a profile for annual demand. However, it did not include a grid simulation to fully assess the impacts on the Dx network. The work is based on the assumption that flexible biogas production is possible, which is supported by [91] but acknowledges that further research is needed. The results showed that flexible biomethane production from a single digester was the most economical option, followed by two biogas plats operating at a constant rate, one running year-round, with the second only operating during periods of high demand. A single digester operating with a constant biogas output and gas storage was the most expensive option, with significant spatial disadvantages at a seasonal swing factor above two [61].

Pellegrino et al. used a steady-state, non-isothermal model to simulate the injection of renewable gas into the Tx network. The results found that biomethane injection had a negligible effect on key gas parameters such as Wobbe Index (WI), gas gravity and higher heating value [80]. Abeyskera et al. [78] and Von Wald et al. [74] investigated the effects of biomethane injection on a low-pressure Dx network. It was determined that the distribution of the injected biomethane was not uniform and was concentrated near the injection location. The results also showed that the injected biomethane required a larger volume of gas to meet the same energy requirement as the heating value (HHV) of biomethane is lower than that of natural gas and that there was a localised increase in pressure near the injection point. In the case study investigated by Abeyskera et al. [78] natural gas was determine to have a HHV of 41.04 MJ/m^3, while biomethane had a HHV of 37.40 MJ/m^3, while on the case study analysed by Von Wald et al. [74] the HHV of natural gas was 39.12 MJ/m^3, with a HHV of biomethane between 35.40 MJ/m^3 to 36.89 MJ/m^3. However, these studies consider the gas grid at a particular instant and do not account for fluctuation in gas demand.

The current literature that consider the production of green gas for grid injection can predominantly be divided into two main categories [98]. The first consider elements upstream of gas grid injection. These studies focus on

optimising the biomethane supply by analysing feedstock distributions, the sizing of anaerobic digesters and upgrading facilities, and the potential biomethane end uses. Techno-economic models were used in works by Cucchiella et al. [64] [65], and O'Shea et al. [14] [71] to identify the most economically viable locations and supply chain for the production of biomethane. Hengeveld et al. [68] focused on the economic optimisation of supply chains with decentralised versus centralised biomethane production. Parker et al. [99] assessed the economic feasibility of biomethane to be used as transport fuel, transport to the station via gas grid, evaluating a number of different feedstocks. However, these studies do not consider the technical constraints imposed on biomethane injection by the gas grid.

The second category of literature concerning green gas injection is concerned with elements downstream of grid injection. They simulate the dispersion of biomethane once it has been injected into the gas network. These studies analyse the impacts on key gas parameters including WI, HHV, gas composition, and normal operating flowrates and pressures. Cavana et al. [63] used a steady-state, non-isothermal model to investigate the maximum quantity of raw biogas that can be injected into a Dx network. Pellegrino et al. [80] examined the impacts of biomethane and hydrogen injection on the pressure, WI, gas gravity and HHV of gas within the grid.

To the best of the authors' knowledge there has been no study that has combined both upstream and downstream elements to give a full overview of biomethane production and injection. This work presents a novel approach that incorporates both the biomethane supply chain and a gas network simulation. The method is applied to a case study, a representative Irish Dx network, to illustrate the importance of considering elements both upstream and downstream of the injection point.

The aim of this chapter is to create a model to determine the techno-economic optimum site and size of a biomethane production and injection facility based on the grid's ability to accept biomethane and the distribution of feedstock in the surrounding area.

4.3 Materials and Methods

4.3.1 Model Overview

Figure 4-1 outlines the top-down techno-economic modelling approach used to determine the optimum site and size for a biomethane production and injection facility. The model is divided into three submodels: the gas network demand submodel (highlighted in purple), the transportation submodel (highlighted in yellow), and the techno-economic submodel (highlighted in blue).

The gas network demand submodel uses a Dx network grid simulation, which incorporates a CNG filling station, to determine the grid capacity to accept biomethane. The grid capacity to accept biomethane is defined as the maximum quantity of biomethane that can be injected into the grid while maintaining pressures and flowrates within normal operating limits. Further information on this model can be found in chapter Chapter 2.

The techno-economic sub model uses the results from the gas network demand submodel and the transport submodel, along with various cost factors to determine the levelised cost of energy (LCOE) and net present value (NPV) of the biomethane production and injection facility. The cost factors and equations used in the techno-economic submodel are detailed on section 4.3.2.

The transportation submodel uses the grid capacity for biomethane, the feedstock geospatial distribution and the road network, to determine the total feedstocks transport distance and transport cost to supply the AD plant. Section 4.3.3.6 presents the geographical information system (GIS) model used to allocate feedstock to the AD and calculate transport distances.

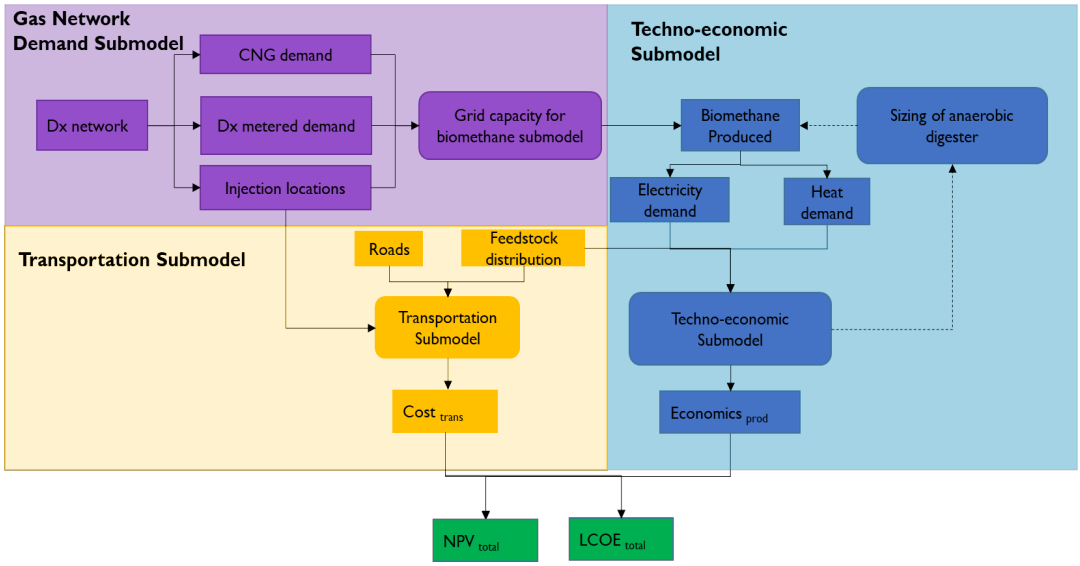

Figure 4-1: Overview of techno-economic model, incorporating the grid simulation and transportation submodels, where CostTrans is the cost of transporting feedstocks, Economics~Prod is the cost of biomethane production.

4.3.2 Case Study

As described in in section 3.3.1, an existing but anonymised Dx network, supplying an Irish town of 17,000 inhabitants and a smaller town of 4,400 inhabitants, with a mix of industrial, residential, and commercial demand is chosen as a case study. The Dx network consists of both 2 and 4 barg networks. The surrounding area has high potential for biomethane production due to the town's location in a highly productive agricultural region. There is also potential for significant demand at a CNG filling station, located on a nearby motorway, which is part of the TEN-T Core Network [93]. Figure 4-2 is a schematic of the representative Dx network and surrounding area. Chapter 3 investigated the grid capacity to accept biomethane at three potential injection sites, the first located near the AGI, the second situated close the proposed CNG filling station and the third located near the large town centre. The Dx network simulation described in Chapter 3 also consider the scenarios of maximum, minimum and no demand at the grid connected CNG filling station. The results from the analysis in Chapter 3 determined the range of biomethane plant sizes and the potential plant location to be considered in this techno-economic evaluation.

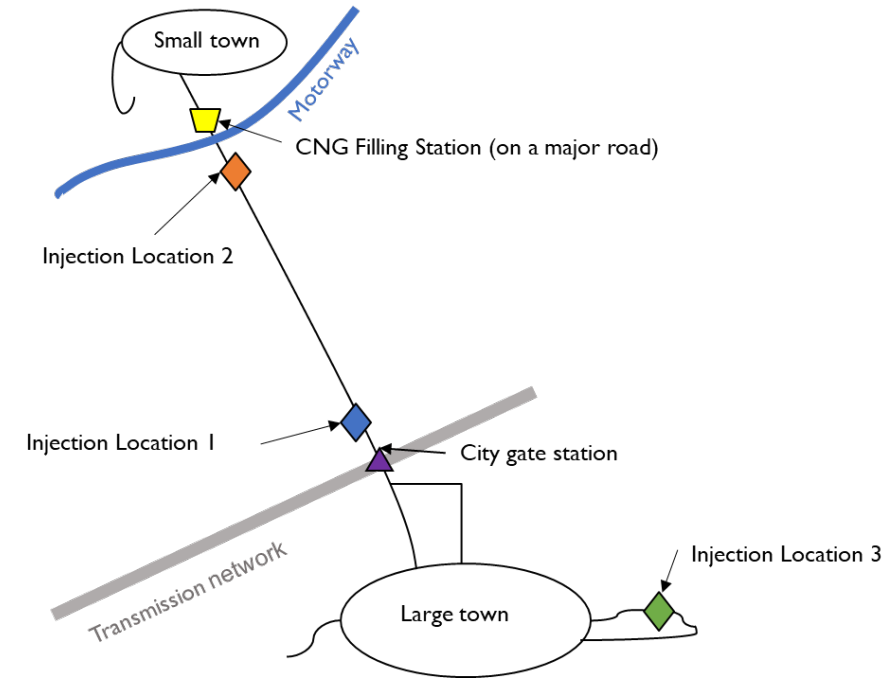

Figure 4-2: Schematic of the representative Dx network.

4.3.3 Techno-economic and Transportation Submodel

4.3.3.1 *Input Values*

Table 4-1 gives a list of the techno-economic model input parameters, the values used for this analysis and their sources.

Table 4-1: List of input values for the techno-economic model.

Parameter	Value	Reference
Anaerobic Digester		
Volatile Solids Cattle Slurry (CS) (%)	6.23	[100], [101]
Volatile Solids Grass Silage (GS) (%)	26.8	[100]
Specific operating Cost of AD Facility (€/twwt)	5	[14]
Electrical Energy Consumption AD plant (kWhe/twwt/a)	10	[14]
Gas Price (€/MWhth)	41.60	[102]
Electricity Price (€/MWhe)	164.30	[102]
Thermal Efficiency of Gas Boiler (%)	90	[14]
Base temp & temp to pasteurise cattle slurry. (°C)	10 , 70	[103]
Feedstock cost cattle slurry (€/twwt)	0	[62] [14]
Feedstock cost grass silage (€/twwt)	19	[104]
% vol CH4 in biogas from cattle slurry and grass silage	55	[100]
Losses in Biogas System (%)	6	[65]
Moisture Content of Cattle Slurry (%)	90	[100]
Upgrader		

Specific Methane Yield GS: CS (20:80, volatile solids ratio), (80:20, volatile solids ratio) (L CH_4 kg^{-1} VS)	271 , 369	[100]
Number of Operating Hours	8000	[65]
Losses in Upgrader (%)	1	[105]
Cost of water supply and wastewater disposal (€/m^3)	3.12 + standing charge of 249.10 (€/year)	[106]
Transportation Cost		
Specific Energy Consumption Diesel (L/tkm)	0.074	[14]
Diesel Price (€/L)	1.34	[107]
Revenue		
Biofuels Obligation Cert (€/MWh)	72	[108]
Market price of Natural gas (€/MWh)	24.9	[102]
Additional Premium for Biomethane (€/MWh)	60	[14]
Other		
Discount rate %)	8	[14]
Lifetime of the Project (Years)	20	[65]

4.3.3.2 *Sizing*

Using the results from the grid simulation, the required quantity of biogas can be calculated using the following formula [64]:

Equation 4-1: Required quantity of biogas.

$$Q_{biogas} = \frac{\left(\frac{Q_{bioCH4}}{\%CH_4 \times (1-l_{up})}\right)}{(1-l_{AD})}$$

where, Q_{bioCH4} (m^3/h) is the hourly quantity of biomethane, $\%CH_4$ is the percentage of methane in the produced biogas, l_{up} (%) is loss of methane in the upgrading system, and l_{AD}(%) is the methane loss in the anaerobic digester. From this, the quantity of grass silage and cattle slurry needed can be determined, using Equation 4-2 [14],

Equation 4-2: Quantity of cattle slurry and grass silage.

$$Q_{biogas} = \frac{(T_{GS} \times VS_{GS} + T_{CS} \times VS_{CS}) \times SMY_{VSR}}{\%CH_{4\ CS\&GS}}$$

where, T_{GS} (t) is the mass of grass silage, T_{CS} (t) is the mass of cattle slurry, VS_{GS}(%) is the volatile solids percentage in grass silage, VS_{CS} (%) is the volatile solids percentage in cattle slurry, SMY_{VSR} (L CH_4 kg^{-1} VS) is the specific

methane yield, and $\%CH_{4\,CS\&GS}$ is the percentage of methane in the biogas produced from cattle slurry and grass silage.

It is assumed that the AD would operate at a volatile solids ratio of 80:20 cattle slurry to grass silage during the 16 week period between October and February when cattle are housed indoors and slurry is collected and stored [109]. Using this volatile solids ratio Equation 4-2 can be rearranged to solve for the total tonnage of grass silage Equation 4-3 and total tonnage of cattle slurry Equation 4-4. For the remainder of the year the volatile solids ratio was taken to be 20: 80 cattle slurry to grass silage, in which case the total tonnage of grass silage and cattle slurry can be found from Equation 4-5 and Equation 4-6 respectively. This is done to minimise the storage of cattle slurry and associated cost and methane leakage.

Equation 4-3: Quantity of grass silage for a volatile solids ratio of 80:20.

$$T_{GS} = \frac{Q_{biogas} \times \%CH_{4\,CS\&GS}}{SMY_{1:4} \times 5VS_{GS}}$$

Equation 4-4: Quantity of cattle slurry for a volatile solids ratio of 80:20.

$$T_{CS} = \frac{4 \times T_{GS} \times VS_{GS}}{VS_{CS}}$$

Equation 4-5: Quantity of grass silage for a volatile solids ratio of 20:80.

$$T_{GS} = \frac{Q_{biogas} \times \%CH_{4\,CS\&GS}}{SMY_{4:1} \times 1.25\,VS_{GS}}$$

Equation 4-6: Quantity of cattle slurry for a volatile solids ratio of 20:80.

$$T_{CS} = \frac{0.25 \times T_{GS} \times VS_{GS}}{VS_{CS}}$$

The plant size in terms of total tonnage of feedstock that can be accepted at the AD is obtained from Equation 4-7.

Equation 4-7: Total tonnage of feedstock at plant.

$$T = \sum_{i=1}^{N_{OH}} T_{GS_i} + \sum_{i=1}^{N_{OH}} T_{CS_i}$$

where i is the specific hour of operation of the anaerobic digester, and N_{OH}(h) is the number of operating hours.

4.3.3.3 *Anaerobic Digester*

The capital cost of the AD is calculated using a linearized AD capex function proposed by O'Shea et. al [14].

Equation 4-8: Capital cost of anaerobic digester.

$$Capex_{AD} = M_{AD} \times T + C_{AD}$$

M_{AD} is the slope of the linearized AD capex function in €/tonne, and C_{AD} is the constant term of the linearized AD capex function in €, which can be calculated from Equation 4-9 and Equation 4-10 respectively. M_{AD} represents the increase in capital cost proportional to the digester size, while C_{AD} represents the minimum capital cost for the range of digesters being analysed.

Equation 4-9: Slope of the linearized AD capex function.

$$M_{AD} = \frac{\left(554.89 \times T_{max}^{0.841} - 554.89 \times T_{min}^{0.841}\right)}{\left(T_{max} - T_{\min}\right)}$$

Equation 4-10: Constant term of the AD linearized capex function.

$$C_{AD} = 554.89 \times T_{max}^{0.841} - M_{AD} \times T_{max}$$

T_{max} and $T_{\min}$ are maximum and minimum plant tonnages with a tolerance of $\mp$ 5% of the calculated plant size, allowed in the model.

The annual operating cost and annual electricity cost of the AD can be determined from Equation 4-11 and Equation 4-12 respectively.

Equation 4-11: Operational cost of anaerobic digester.

$$Opex_{AD} = SO_{AD} \times T$$

Equation 4-12: Annual electricity cost of anaerobic digester.

$$CE_{AD} = T \times SE_{AD} \times PE$$

where, SO_{AD}(€/twwt) is the specific operating cost of the AD, SE_{AD} (kWhe/twwt/a) is the electrical energy consumption of the AD plant and PE (€/kWhe) is the price of electricity.

The thermal energy required to pasteurise the cattle slurry, which is mandatory for AD plants in Ireland as the slurry is originating from multiple farms [110], can be calculated using the moisture content of cattle slurry, MC_{CS} (%), the mass of cattle slurry accepted by the AD, T_{CS} (t), the specific heat capacity of water, cp_{H_2O} (J $kg^{-1}K^{-1}$), the base temperature of the cattle slurry t_{base}(K), and the temperature it must reach to be pasteurised, t_{high} (K).

Equation 4-13: Thermal energy demand of the anaerobic digester.

$$E_{Th} = MC_{CS} \times 1000 \times T_{CS} \times \frac{cp_{H_2O}}{3.6} \times (t_{high} - t_{base})$$

When mixing the grass silage with the cattle slurry that has been heated through the pasteurisation process, the resultant temperature was above 37 °C, so the thermal energy requirement of heating grass silage to the digester temperature could be neglected [14].

Using the thermal energy requirement to pasteurise the cattle slurry, the annual cost to heat the AD plant can be calculated, where η_{Boiler} (%) is the thermal efficiency of a natural gas boiler and PG (€/kW_{th}) is the price per unit of natural gas.

Equation 4-14: Annual cost of heat to the anaerobic digester.

$$CG_{AD} = \frac{E_{Th}}{\eta_{Boiler}} \times PG$$

4.3.3.4 *Upgrader*

A water scrubber was selected as the most suitable technology as it is commercially mature, available for a wide range of capacities (350 m^3/h – 2800 m^3/h), produces biomethane with greater than 97% methane content, and has a low methane slip (< 1%) [111] [105] [112] [113]. The biomethane from the water scrubber process is produced at a pressure of 4 barg – 8 barg, meaning that for injection into a Dx network there is no additional compression required [111].

The capital cost for a water scrubber upgrader was determined as per Bauer et al. [105].

Equation 4-15: Capital cost of the upgrader.

$$Capex_{UP} = \left(25433 \times Q_{biogas}^{-0.376}\right) \times Q_{biogas} \times N_{OH}$$

The operating cost of the water scrubber comprised the maintenance, electrical and water costs of the upgrader. The annual maintenance cost of the upgrader was estimated to be 3% of the capital cost [105]. The annual electrical demand of the upgrader could be calculated from Equation 4-16 [105]. Using this demand, the annual electrical cost of the upgrader could be found from Equation 4-17.

Equation 4-16: Annual electrical demand of the upgrader.

$$E_{E,UP} = (1.2448 \times Q_{biogas}^{-0.236}) \times Q_{biogas} \times N_{OH}$$

Equation 4-17: Annual cost of electricity to the upgrader.

$$CE_{UP} = E_{E,UP} \times PE$$

Bauer et al. found that between 0.5 m^3/day ($V_{w,min}$)and 5 m^3/day ($V_{w,max}$) of water is required by a water scrubbing upgrader, depending on its capacity

[105]. As the capacity of the upgraders ranged between 350 m^3/h (Q_{min}) and 2000 m^3/h (Q_{max}), a linearized function was created to estimate the water demand of the upgrader Equation 4-18. From this, the cost of the water required to supply the upgrader is calculated from Equation 4-21.

Equation 4-18: Annual quantity of water required by the upgrader.

$$V_{w,UP} = M_W \times Q_{biogas} + C_W$$

M_w is the slope of the linearized function to estimate the water required to supply the upgrader. It represents the increasing amount of water required proportional to the increasing scale.

Equation 4-19: Slope of function for annual quantity of water at upgrader.

$$M_w = \frac{V_{w,max} - V_{w,min}}{Q_{max} - Q_{min}}$$

C_W is the constant term of the linearized function to estimate the water required to supply the upgrader. It represents the minimum amount of water required for the upgrader.

Equation 4-20: Constant term of function for annual quantity of water at upgrader.

$$C_W = V_{w,max} - M_w \times Q_{max}$$

Equation 4-21: Annual cost of water required by the upgrader.

$$CW_{UP} = 365 \times V_{w,UP} \times PW$$

4.3.3.5 *CNG Filling Station and Biomethane Injection Facility*

The Irish gas Tx and Dx networks operator, Gas Networks Ireland (GNI), provided cost data for the CNG filling station and biomethane injection facility. The capital cost for the CNG filling station was taken to be €1,250,000, with an operation and maintenance cost of 50,000 (€/a). This concurs with a report by the US Department of Energy, which estimated that a large CNG filling station would cost between $1,200,000 and $1,800,000 (€1,000,000 to €1,540,000) [114].

The biomethane injection facility is estimated to have a capital cost of €648,000, with an annual operation and maintenance cost of 80,000 (€/a).

4.3.3.6 *Transportation submodel and Feedstock Cost*

Electoral divisions, of which there are 3409, are the smallest areas for which detailed data on livestock numbers are available in Ireland. The quantities of grass silage and cattle slurry available in each electoral division is sourced from O'Shea et al. [13] [14]. That work used the Irish census of agriculture to determine the number of cattle in each electoral division and thus calculated the available slurry resource that could be collected during the 16-week period in which cattle are housed indoors. However, as the last Irish census of agriculture was in 2010, in the current work a scaling factor is applied to data from O'Shea et al. to allow for the significant growth in the Irish herd since 2010. This scaling factor is calculated by obtaining the livestock figures for each cattle type in the counties that make up the area surrounding the case study every year for 2010 – 2020 from the CSO Statbank database [115]. The average year-on-year increase or decrease in livestock numbers for each county are established. The year-on-year livestock numbers in each electoral division are assumed to vary uniformly with the county to which they belong, thus the values can be adjusted to represent 2020 values.

The availability of grass silage is assumed to be the same as in 2010, as there is a lack of land use data on county level, which could indicate otherwise.

(a 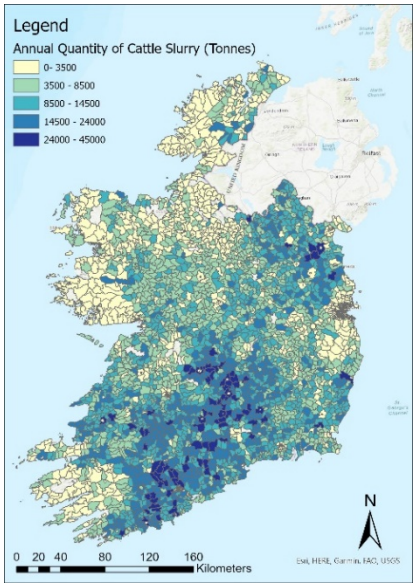

(b 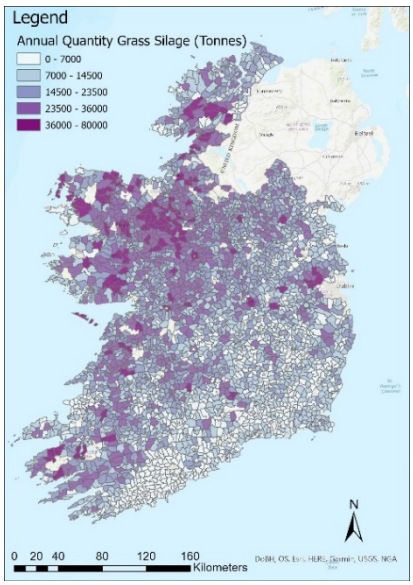

Figure 4-3: Spatially explicit representation of (a) the annual quantity of cattle slurry and (b) the annual quantity of grass silage available throughout the Republic of Ireland.

The allocation of feedstock to the biomethane plant is performed in ArcGIS Pro 2.7 [116], using a location-allocation algorithm with the maximum capacitated coverage constraint. Singlitico et al. used this algorithm to determine the optimum siting and sizing of gasification plants in Ireland, minimising the levelised cost of energy [76]. Comber et al. optimised the location of anaerobic digesters to maximise biogas production in the East Midlands of the UK, using a location-allocation algorithm [117].

Location-allocation is a solver based on Hillsman theory [118] for the facility location problem: given K candidate facilities, J origin points with a weight of m, the algorithm determines a subset of facilities P such that the sum of the weighted distances d between each J and P is minimised.

However, in the case of this analysis, there is only one facility L being considered at any given time. The addition of the maximum capacitated coverage constraint allows a capacity c to be assigned to the facility. Thus, the algorithm will instead determine a subset of origin points I such that the sum of m's is equal to c and the weighted distance between I and L is minimised.

Figure 4-4 shows a simplified example of the results that can be obtained when using the location-allocation algorithm in conjunction with the

maximum capacitated coverage constraint for a singular facility with different capacities. Where C is the capacity of the plant, and m is the feedstock quantity. The algorithm determines which feedstock sources will meet the capacity of the plant while minimising the transportation distance between the feedstock sources and the plant.

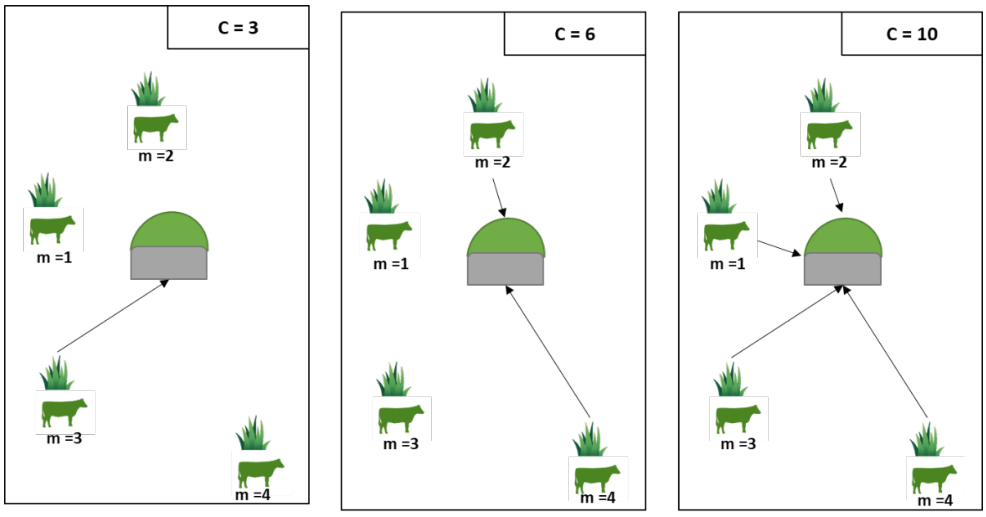

Figure 4-4: Simplified representation of the location-allocation algorithm with the maximum capacitated coverage constraint for a single facility with different capacities.

Once the optimal location of the biomethane plant has been achieved, the resultant weighted transport distance can be used to calculate the transport costs of cattle slurry and grass silage. To ensure farmers are not deprived of the fertiliser value of the cattle slurry they provided to the anaerobic digester, it was assumed that an equal mass of digestate was returned to each ED from which the feedstock was sourced [119]. The cost of transporting the feedstock to the facility and returning the digestate, for use as a bio-fertilizer, to the farmer was determined to be the responsibility of the operator of the biomethane production and injection facility.

Based on the literature, 40km was maximum collection radius for sourcing feedstock for this work [14] [120] [121]. The total transportation cost can be calculated from Equation 4-22.

Equation 4-22: Annual cost for the transportation of cattle slurry and grass silage.

$$TC = \sum_{i=1}^{N_{CS}} m_{CS,i} \times d_{CS,i} \times 2 \times SEC_D \times FC_D + \sum_{i=1}^{N_{GS}} m_{GS,i} \times d_{GS,i} \times 2 \times SEC_D \times DP$$

where, m (t) is the mass of the feedstock, d is the distance from ED to the biomethane production facility, SEC_D (L/tkm) is the specific energy consumption of diesel and DP (€/L) is the average price of diesel in 2020.

Along with the transportation cost, the cost of the feedstock (FC) itself must be considered. The feedstock cost is determined from Equation 4-23.

Equation 4-23: Annual feedstock cost.

$$FC = T_{GS} \times FC_{GS} + T_{CS} \times FC_{CS}$$

where, FC_{GS} (€/t) is the price of grass silage and FC_{CS} (€/t) is the price of cattle slurry.

4.3.3.7 *Outputs*

Net present value (NPV) and levelised cost of energy (LCOE) were chosen as the parameters by which to assess the economic viability of the biomethane production facility. NPV is the difference between the present value of inflows and outflows of cash over the lifetime of the plant. NPV is used to evaluate the profitability of the plant, a positive NPV means that the total income is greater than the total expenditure over the lifetime of plant. LCOE is the present cost to produce a unit of energy, (in this case biomethane) over the lifetime of the plant. LCOE gives an indication of the average price at which the biomethane must be sold to break even over the lifetime of the plant. It can also be used to compare the competitiveness of biomethane / bio-CNG to other fuels in the market such as natural gas and diesel.

NPV and LCOE are calculated from Equation 4-24 and Equation 4-25 respectively.

Equation 4-24: Net present value.

$$NPV = \sum_{y=0}^{LT} \frac{R_{in\,y} - C_{out\,y}}{(1+r)^y}$$

Equation 4-25: Levelised cost of energy.

$$LCOE = \frac{\sum_{y=0}^{LT} \frac{C_{out\,y}}{(1+r)^y}}{\sum_{y=0}^{LT} \frac{E_{bioCH4\,y}}{(1+r)^y}}$$

The total revenue, R_{in} (€), total costs, C_{out} (€) and total energy produced by biomethane plant E_{bioCH4} (MWh), are determined by Equation 4-26, Equation 4-27, and Equation 4-28 respectively. When calculating the total revenue, the gas demand of the CNG filling station is given priority in the allocation of the biomethane produced, while the remaining biomethane is assumed to be delivered by the gas grid for end uses such as heating. In Ireland, biomethane that is used as a transport fuel is eligible for a biofuels obligation certificate (BOC). BOCs can be traded between transport fuel suppliers and have a value of 54 €/MWh from 2010-2021, 72 €/MWh from 2022 – 2029 and 108 €/MWh from 2030 onwards [108]. For the remaining biomethane it was assumed that incentive of €60/MWh could be applied, the median price used by O'Shea et al. [14]. Both the BOC and biomethane incentive were additional to the market price for natural gas.

Equation 4-26: Total revenue of the plant.

$$R_{in} = (E_{bioCH4} - E_{CNG}) \times (P_{bioCH4} + I_{bioCH4}) + E_{CNG} \times (P_{bioCH4} + BOC)$$

Equation 4-27: Total cost of the plant.

$$C_{out} = Capex_{AD} + Opex_{AD} + CE_{AD} + CG_{AD} + Capex_{UP} + Main_{up} + CE_{UP} + CW_{UP} + C_{CNG} + O_{CNG} + C_{INJ} + O_{INJ} + TC + FC$$

Equation 4-28: Total energy produced by the plant.

$$E_{bioCH4} = \frac{e_{bioCH4}}{3600} \times \sum_{i=1}^{N_{OH}} Q_{bioCH4\,i}$$

where, e_{bioCH4} (MJ/m^3) is the energy content of biomethane.

4.3.4 Integration of Gas Network Demand Submodel and Techno-economic and Transportation Sub- Model.

The gas network demand submodel outputs a profile of the grid capacity for biomethane for the particular scenario being analysed. The grid capacity for biomethane is the quantity of biomethane that can be injected into the gas network while keeping pressures and flowrates within normal operating limits. Figure 4-5 is an example of this, showing the profile of the grid capacity to accept biomethane over the course of the year, at injection location 3, with maximum CNG demand. From this, a maximum hourly flowrate and minimum hourly flowrate are determined. This sets the upper and lower bounds of the biomethane production facility sizes, which will be investigated to determine the economic optimum. When sized using the minimum hourly injection rate, the biomethane production facility can run at its full capacity throughout the year, however it restricts the quantity of biomethane that can be injected into the network. Use of the minimum hourly injection rate in this example only allows 71% of the grid's capacity to accept biomethane. Comparatively, when sized using the maximum hourly flowrate, the biomethane production facility can reach the full grid capacity to accept biomethane. However, the production facility will only operate at its full capacity one hour per year, which impacts on economic viability.

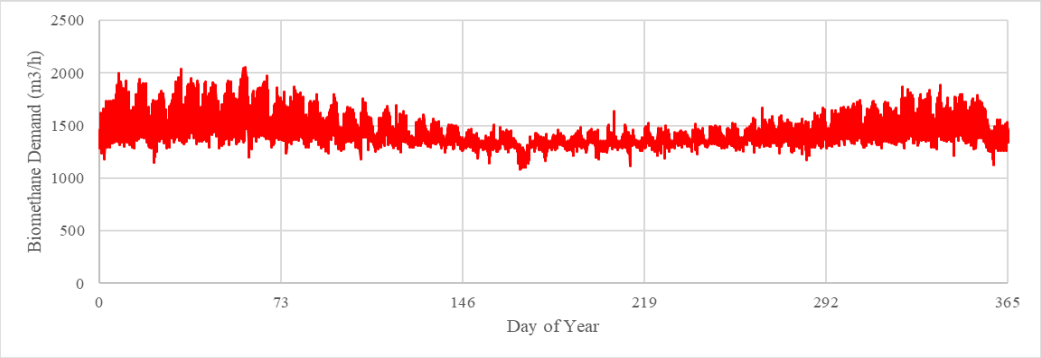

Figure 4-5: Annual profile for the hourly biomethane demand for injection location 3, with maximum CNG demand at the CNG filling station.

Thus, to determine the optimum size, the techno-economic model is run iteratively for a number of plant sizes, starting with the minimum flowrate and increasing in increments (inc) determined by Equation 4-29, until the maximum flowrate is reached. For each iteration (j) the new maximum facility flowrate is calculated from Equation 4-30. This is the maximum hourly flowrate of the biomethane production facility ($Q_{bioCH4,fmax,_j}$), and is used when calculating the size and associated costs of the anaerobic digester and the upgrader. However, when determining the feedstock cost, transport cost and annual energy output of the biomethane production facility, the hourly injection profile is used with values being restricted by $Q_{bioCH4,fmax,_j}$ as per Equation 4-31.

Equation 4-29: Model incremental increase.

$$inc = 0.05 \times (Q_{bioCH4,max} - Q_{bioCH4,min})$$

Equation 4-30: Maximum biomethane facility flowrate.

$$Q_{bioCH4,fmax,_j} = Q_{bioCH4,min} + j(inc)$$

Equation 4-31: Biomethane hourly flowrate restriction.

$$Q_{biomethane} = \begin{cases} Q_{bioCH4}, & Q_{bioCH4} < Q_{bioCH4,fmax,_j} \\ Q_{bioCH4,fmax,_j}, & Q_{bioCH4} \geq Q_{bioCH4,fmax,_j} \end{cases}$$

4.4 Results and Discussion

4.2.1 Net Present Value

Figure 4-6 depicts the results of the NPV calculated for each potential injection location, for the scenarios of maximum CNG demand, minimum CNG demand and no CNG demand on the gas network. A trend that is apparent across all locations and filling station demand scenarios is that the NPV gradually increases to a maximum before rapidly decreasing. This sharp decrease in NPV occurs at the point where the increase in the size of the biomethane production plant has minimal impact on increasing the actual

energy output, due to it becoming significantly restricted by the limits imposed by the gas grid. For example, this can clearly be seen in Figure 4-6(a) where the NPV drops from €4,067,660 at 93.2 GWh/a to €455,199 at 94.77 GWh/a for injection location 1, from €9,561,163 at 114.4 GWh/a to € -9,419,415 at 128.77 GWh/a for injection location 2, and from €2,392,712 at 105 GWh/a to € -23,949,866 at 121.76 GWh/a at injection location 3. This clearly shows the necessity of considering the restrictions imposed by the gas network of the quantity of biomethane that can be injected.

Another trend that is evident for all injection locations is that as the CNG demand at the filling station increases, so too does the NPV. This can be attributed to two factors, firstly the increase in CNG demand, increases the overall network demand and thus grid capacity to accept biomethane. This means that the plant sizes being analysed are larger and the economies of scale implied by the power law relationship in the CAPEX values in Equation 4-27 apply. Secondly and possibly more impactful, the BOC has a higher value per unit biomethane than the incentive for biomethane used in traditional grid end uses such as heating. Hence, the larger the percentage of produced biomethane that can be sold as a vehicle fuel, the greater the revenue stream.

When comparing the different injection locations, it is evident that injection location 2 is the most profitable across all scenarios of CNG demand, followed by injection location 1, with injection location 3 being the least profitable. This is primarily due to the difference in transportation distances of feedstocks to the biomethane production facilities. Injection location 3 is located on the outskirts of a large town centre, while injection locations 1 and 2 are located on more rural sections of the Dx network. As the feedstock in this case is grass silage and cattle slurry, injection locations 1 and 2 are substantially closer to the feedstock sources than injection location 3. Another factor that may contribute to injection location 3 being less profitable than injection location 1 or 2, is that in every CNG demand scenario, injection location 3 has a larger range between its minimum hourly flowrate and maximum hourly flowrate. This means that increasing the capacity of the plant does not have as great an impact on the annual energy output.

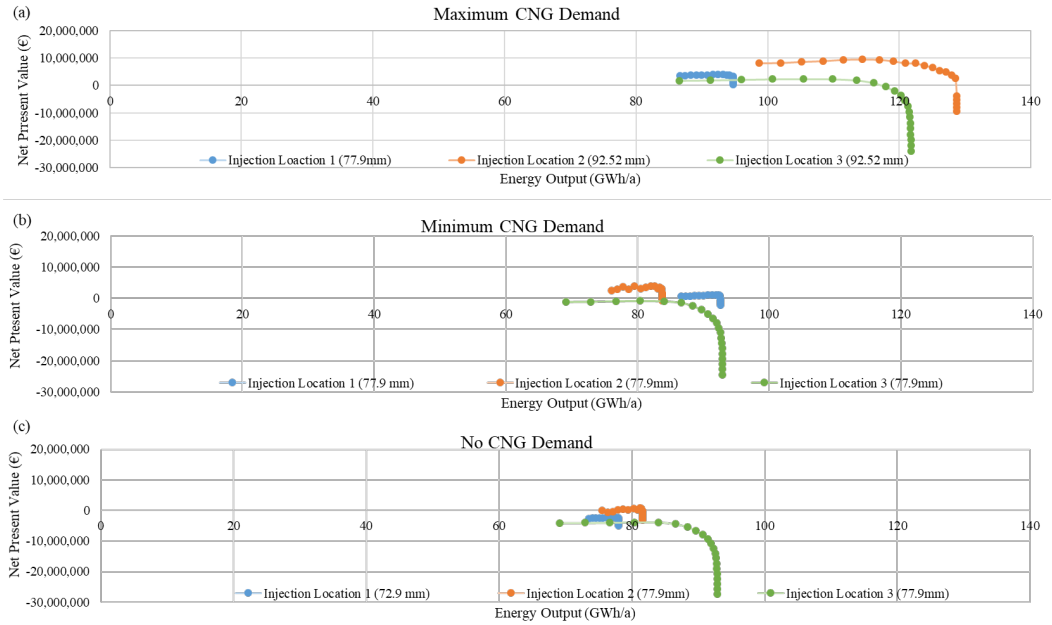

Figure 4-6:Results of the net present value calculated for each potential injection location, with (a) maximum demand at the CNG filling station, (b) minimum demand at the CNG filling station and (c) no demand at the CNG filling station.

4.2.2 Levelised Cost of Energy

Similar trends are observed in Figure 4-7, which shows the LCOE calculated for each potential injection location, for the scenarios of maximum demand at the CNG filling station, minimum demand at the CNG filling station and no CNG demand on the Dx network. Across all potential injection locations and CNG demand scenarios, the LCOE curve increases dramatically as it approaches the maximum grid capacity for biomethane. The LCOE decreases with increased CNG demand at the filling station across all potential injection locations. For each CNG demand scenario the injection location 2 results in the lowest LCOE, followed by injection location 1and lastly injection location 3. The potential causes for each of these trends has been discussed in section 4.2.1.

The results show that the LCOE ranged between 81.61€/MWh (injection location 2) and 109.84€/MWh (injection location 3) for the scenario with maximum demand at the CNG station, from 83.59 €/MWh (injection location

2) to 114.90 €/MWh (injection location 3) for the scenario with minimum demand at the CNG station, and from 83.73 €/MWh (injection location 2) to 114. 97 €/MWh (injection location 3) for the scenario with no CNG demand. These results are slightly higher than the 50.2 €/MWh to 109 €/MWh reported by O'Shea et al. [14] or the 70 €/MWh to 92 €/MWh reported by Cucchiella et al. [65]. This may be due to the inclusion of the gas network demand submodel, as it means the annual energy output is not directly proportional to the size of the biomethane production facility. Another factor, which may contribute to a higher LCOE, is the inclusion of the CNG filling station cost in this analysis. In other work the cost of the CNG filling station is assumed to be borne by the filling station operator [73] [14]. However, the CNG filling station costs has been included in this work, as the construction of CNG filling stations under the Causeway project in Ireland is being undertaken by GNI, the gas networks operator. The exception to this is the scenario where there is no CNG demand on the network.

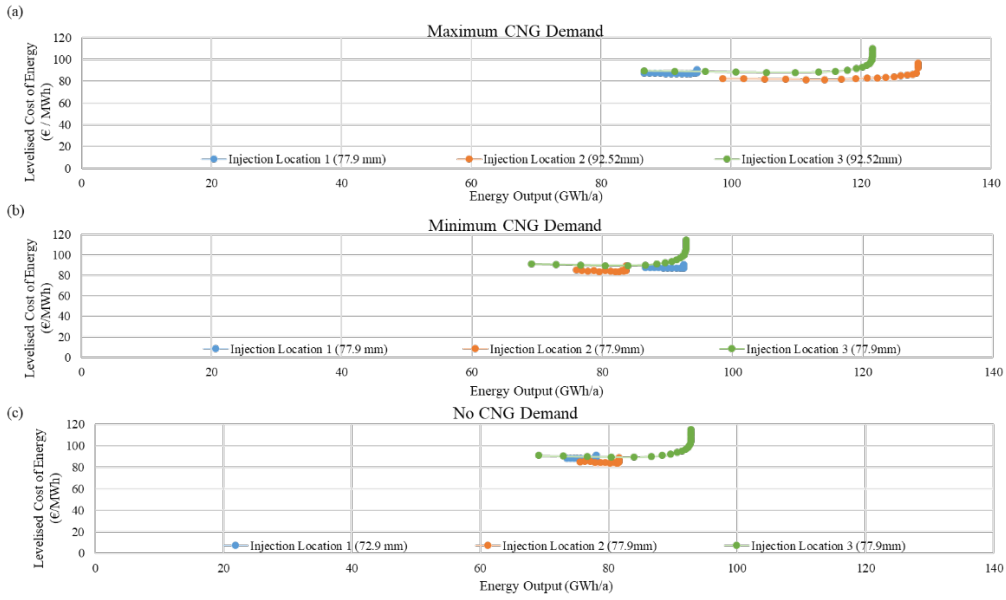

Figure 4-7:Results of the levelised cost of energy calculated for each potential injection location, with (a) maximum demand at the CNG filling station, (b) minimum demand at the CNG filling station and (c) no demand at the CNG filling station.

4.2.3 Limitations and Future Work

The inclusion of the gas network demand submodel considers the seasonal fluctuation of gas demand, adding a more realistic perspective of the operation of biomethane production plants. However, it also opens the model to variation. The grid capacity for biomethane is dependent on the distribution of demand throughout the gas grid, and the pressure of the AGI. In this case study the AGI was set to 3.9 barg. Decreasing this pressure could allow for the grid capacity for biomethane to be increased at each injection location. However, it may also result in large pressure drops on the network during periods of high demand. Investigating the maximum pressure reduction at the AGI without causing adverse effects on the network may be an area of future work. The sensitivity of the results to the gas network demand submodel means that detailed network data is required to apply the method to other case studies.

This work assumes that the end use for all of the biomethane produced in this case study is injection into the gas grid for use as a vehicle fuel or residential heating. The coupling gas grid demand with off-grid gas demand could provide additional use for the biomethane during periods of low demand, potentially reducing the gap between the peak demand and lowest demand points, possibly increasing the profitability of the biomethane plant. This is an area which may be of interest in future work.

The work assesses a relatively small geographical region surrounding a Dx network in Ireland, thus only road transportation was considered due to the lack of infrastructure in the surrounding area. While the biomethane facility location selected was seen to have a small influence on the transportation costs, if applied to a larger area impacts of site selection may be more significant and alternative routes of transport might be considered.

4.5 Conclusions

This work presented a novel method for considering the impacts of seasonal demand variation within the gas grid when evaluating the economics of a biomethane production and injection facility. A grid simulation model of a

representative Dx network was created to determine the annual grid capacity for biomethane. Three potential injection locations were evaluated for the scenarios of maximum, minimum and no CNG demand at the grid connected CNG filling station. The results from this sub model were used to determine a range of plant sizes for each potential injection location and CNG scenario. This along with a spatially explicit feedstock distribution model was used to determine the NPV and LCOE for each configuration.

The results convey the importance of considering the technical limitations the gas grid imposes on the quantity of biomethane that can be injected into the grid, when assessing the location and size of a biomethane production and injection facility. In the maximum CNG demand scenario the LCOE ranged from 81.61 €/MWh at injection location 2 for an energy output of 114.4 GWh to 109.84 €/MWh injection location 3 for an energy output of 121.76 GWh. The results showed that for all CNG demand scenarios location 2 was the most economically viable option. For this case study, location 2 was the most profitable location for all scenarios of CNG demand. The optimum plant sizes are determined to be 115 GWh for the maximum CNG demand, 82.2 GWh for the minimum CNG demand and 81.8 GWh/a for no CNG demand, resulting in an energy output of 114.5 GWh/a, 82 GWh/a and 81.2 GWh/a respectively replacing 34% - 40% of the Dx network natural gas demand with biomethane. Determining the optimum location and size for biomethane plants, whilst considering the impact of seasonal demand is of key importance to maximise decarbonisation of the gas network in an economically viable way.

4.6 Chapter Summary

This chapter presents a novel method for incorporating the seasonal variations in gas demand into an assessment of the economic viability of a biomethane production and injection facility. Notably, the profitability of the plant was seen to increase proportionally with an increase in demand at the CNG filling station. Location 2 was determined to be the most economically viable site for the biomethane production and injection facility. The most economically

competitive configurations resulted in an LCOE of 83.16 €/MWh, 85.76 €/MWh, and 83.73 €/MWh, with corresponding NPVs of € 7,820,265, € 2,238,675 and € 935,481, for maximum, minimum and no demand at the CNG filling station respectively. The most competitive configurations are achieved at a plant size of 115GWh/a for the maximum CNG demand, 82.2 GWh/a for the minimum CNG demand, and 81.8 GWh/a for no CNG demand replacing 40%, 34%, and 35% of annual natural gas demand in the Dx network respectively.

Chapter 5 builds on this work, using a consequential life cycle assessment to evaluate the overall environmental impacts of production and usage of biomethane as a vehicle fuel for HGVs replacing fossil diesel or offsetting natural gas for residential heating.

Chapter 5 An Environmental and Economic Assessment for Biomethane Injection and Natural Gas Heavy Goods Vehicles

5.1 Chapter Overview

This chapter presents a novel method to incorporate the seasonal variations in gas demand into the assessment of environmental sustainability and economic viability of biomethane production and injection into the grid for either use as a vehicle or heating fuel. The results from the Dx network simulation in Chapter 3 are used to determine a range of possible plant sizes for each potential facility location and CNG demand scenario. The transportation distances and operational burdens such as heat and electricity demands are taken from the techno-economic model detailed in Chapter 4. They feed into a consequential life cycle assessment to determine the overall environmental impacts of the biomethane production and usage. The environmental impacts can then be combined with the total cost of the plant calculated in Chapter 4 to calculate the total cost of carbon abatement (TCA).

5.2 Introduction

In 2019 the European Commission launched "The European Green Deal", a set of policy initiatives, setting targets for clean energy, the circular economy, biodiversity and farming, all with the overarching goal of achieving net zero greenhouse gas emissions by 2050 [2]. Anaerobic digestion is promoted as an effective option to improve the circular economy and mitigate greenhouse gas emissions through the production of renewable energy via biomethane and nutrient cycling in digestate co-product [122], [13].

Life cycle assessment (LCA) is a methodology that can be applied to assess the environmental impacts associated with the production and utilisation of biomethane as an energy carrier [123]. LCA results are critically dependent on the system boundaries used, notably the choice between attributional and consequential modelling [124]. The attributional approach is defined as a system modelling approach where input and outputs are attributed to the

functional unit of a product system. The consequential approach is a system modelling approach in which activities in a product system are linked so that activities are included in a product system to the extent that they are expected to change as a consequence of a change in demand of the functional unit [125].

In a review of 15 attributional LCA studies of biogas systems, Hijazi et al. found that in all cases the biogas system showed a significant savings in greenhouse gas (GHG) emissions. However, in the case where crops cultivation is the feedstock for biogas production, the acidification and eutrophication impacts can be higher than the reference system [126].

Beausang et al. considered a consequential LCA to assess the environmental impacts of mono digestion of cattle slurry and co-digestion with grass silage in different ratios on a volatile solids (VS) basis, for the production of renewable electricity and heat. The results determined the optimum environmental performance to be achieved at a VS ratio of 0.4:0.6 for silage to slurry. However, the author notes that the choice of marginal technologies displaced and assumption about the source of the grass silage can have a significant impact on the results [127].

Work by Styles et al. investigated the environmental balance for the UK biogas sector, considering a range of different feedstocks and end uses. The authors concluded that to maximise the emission savings potential, the digestion of food waste and manures should be encouraged, while the digestion of crops and wastes that could be used as animal feed should be restricted. The analysis also found that upgrading the biogas to be used as a transport fuel considerably improved the environmental profile of AD compared to electricity generation or upgrading and injection into the grid [18].

Similarly, van den Oever et al., D'Adamo et al., and Ardolino et al. found that the use of biomethane as a transport is an effective option for mitigation of GHG emissions [20] [21] [22]. The results from these studies indicated GHG savings of between 131% and 79% when compared to fossil diesel, depending on the specific case study, feedstocks used and system boundary applied.

D'Adamo et al. also used a discounted cash flow methodology to assess the economic feasibility. Their work determined that biomethane is a cost-effective pathway to decarbonise urban transport systems, with increased profitability at large scale deployment [21]. Rehl et al. considered the carbon abatement cost of GHG mitigation for different biogas conversion pathways, using life cycle costing and LCA methodologies. The study found the use of biogas in a CHP for heat and electricity generation resulted in the lowest abatement cost of between -196 €/tCO_2 for a heat-scaled system to 69 €/tCO_2 for an electricity-scaled system, and that use as a vehicle fuel resulted in the highest abatement cost with a ranger of 228 €/tCO_2 to 240 €/tCO_2 [128]. This shows the importance of considering both the economic and environmental impacts.

Figure 5-1 shows the wheel – to – wheel (WTW) greenhouse gas emissions of CNG, BioCNG, LNG, BioLNG and diesel euro VI heavy duty trucks. Euro VI is a mandatory vehicles emissions standard for heavy duty vehicles, introduced by the European Commission in 2013 [129]. The Euro VI standard for heavy duty vehicle sets limits on the tailpipe emissions including carbon monoxide (1.5 g/km-steady-state testing, 4 g/km-transient testing for diesel engines), hydrocarbons (0.13 g/km-steady-state testing, 0.16 g/km-transient testing for diesel engines), methane (0.5 g/km-transient testing for diesel engines), nitrogen oxides (0.4 g/km-steady-state testing, 0.46 g/km-transient testing for diesel engines), particulate matter (0.01 g/km-steady-state testing, 0.01 g/km-transient testing for diesel engines), particulate number (8 x 10^{11} particles/km-steady-state testing, 6 x 10^{11} particles/km-transient testing for diesel engines), ammonia (0.01 ppm-steady-state testing, 0.01 ppm-transient testing for diesel engines), and fuel sulphur limit (10 ppm-steady-state testing, 10 ppm-transient testing for diesel engines) [130]. The results show the highest and lowest value reported for the well – to – tank (WTT) and tank – to – wheel (TTW) greenhouse gas emissions values in technical reports for the different engine technologies including spark ignition (SI), high pressure direct injection (HDPI), dual fuel (DF) and diesel combustion ignition [131]. These results are compiled from a review of technical reports and industry trials [19], [25], [131], [132], [133], [134]. It is evident that bioCNG and

bioLNG can offer significant greenhouse gas savings in comparison to diesel, while fossil CNG and LNG can be more carbon intensive than diesel on the high end or offers marginal carbon saving on the lower end.

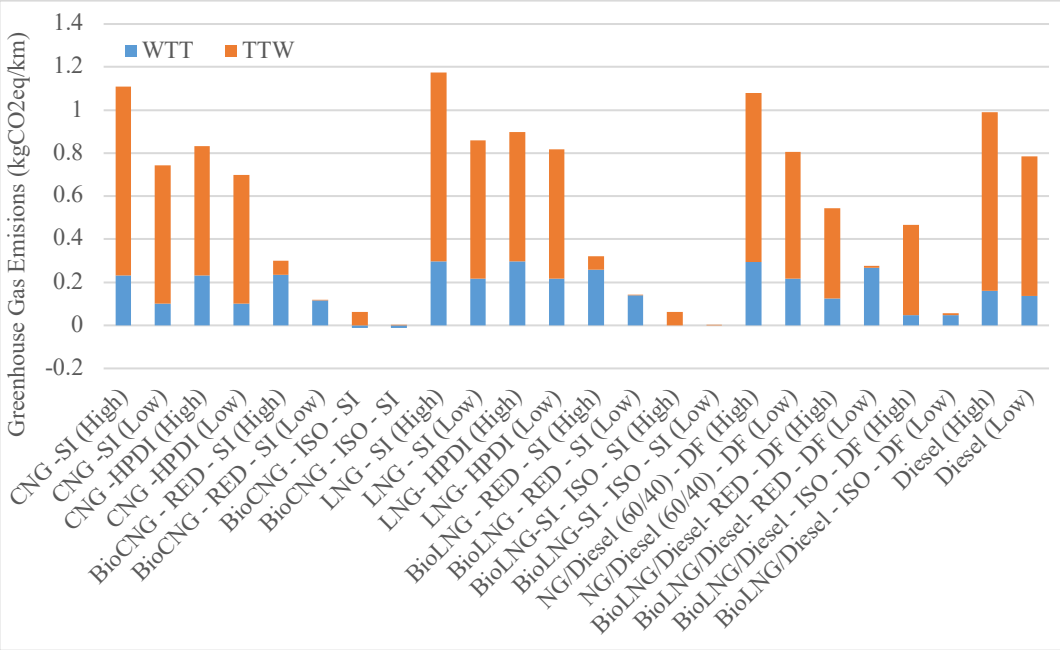

Figure 5-1: The well - to- wheel emissions of for diesel, CNG and LNG Euro VI trucks. Where SI is spark ignition, HPDI is high pressure direct injection, DF is dual fuel, RED is renewable energy directive and ISO is international organisation for standardisation.

The current literature has extensively explored the environmental impacts of biomethane as an energy carrier, while considering the potential feedstocks and different end uses. This chapter will build on the previous work described in this thesis to determine the environmental impact of integrating a biomethane production and injection facility and CNG filling station into a gas Dx network. The novelty of considering the fluctuation of gas demand throughout the year and the technical constraints the gas grid places on the injection will carry through in this analysis. The main aims of this chapter are to:

- Quantify the environmental impact of bio-CNG offsetting diesel as a transport fuel for HGVs and biomethane offsetting natural gas as a source of residential heating.
- Calculate the cost of carbon abatement for different scenarios of demand at the grid connected CNG filling station.

5.3 Methodology

5.3.1 Model Overview

Figure 5-2 gives an overview of the top-down modelling approach used to evaluate the environmental and techno-economic impacts of the integration of CNG filling stations and biomethane production and injection facility into gas Dx networks. The model consists of four submodels: the gas network demand submodel, the transportation submodel, the techno-economic submodel and the environmental submodel.

The gas network demand submodel simulates annual demand of a real by anonymised Irish gas Dx network, taking into consideration the fluctuation of gas demand throughout the year. It calculates the grid capacity to accept biomethane under various demand scenarios at the grid connected CNG filling station. This submodel is described in detail in Chapter 3.

The transportation submodel maps the distribution of feedstocks in the area surrounding the biomethane production and injection facility. It determines from where to source the feedstocks to minimise the transport distance, further information on this model can be found in section 4.3.3.6.

The techno-economic submodel uses the results from the gas network demand submodel and the transportation sub model to calculate the levelised cost of energy (LCOE) and the net present value (NPV). Further details and the results of this model can be seen in Chapter 4.

The environmental submodel uses a lifecycle assessment to determine the overall greenhouse gas emissions. Details of the methods and the emissions factors used are described in section 5.3.2. The lifecycle assessment is then combined with the cost factors detailed in section 5.3 total cost of carbon abatement (TCA).

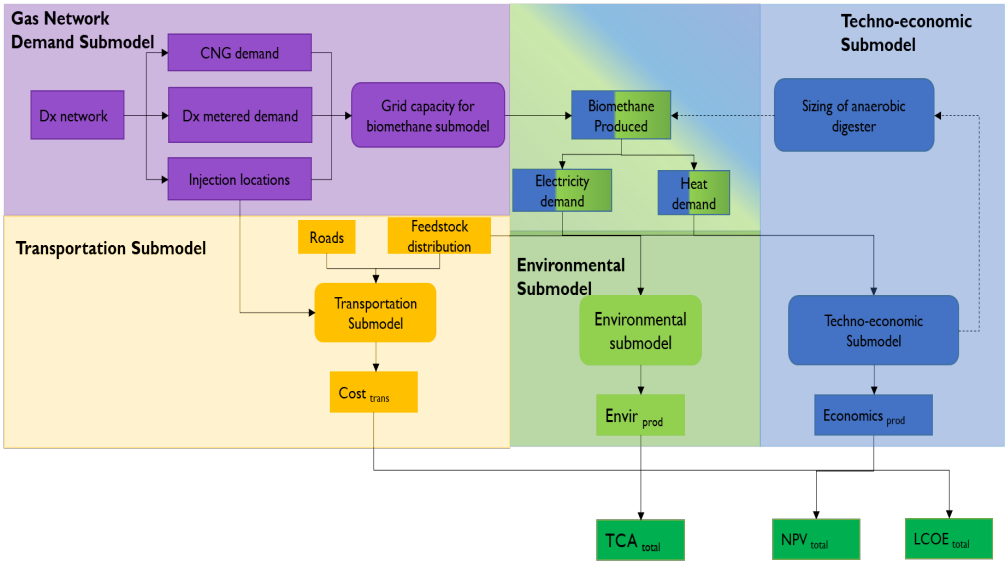

Figure 5-2:Overview of environmental and techno-economic models, incorporating the grid simulation and transportation submodels, where $Cost_{Trans}$ is the cost of transporting feedstocks, $Economics_{Prod}$ is the cost of biomethane production, and $Envir_{prod}$ is the environmental impact of the fuel production and use.

5.3.2 Life Cycle Assessment

5.3.2.1 *Goal, Scope and Boundary Definition*

The goal of this LCA is to assess the environmental impacts of biomethane production from cattle slurry and grass silage, to offset diesel as a transport fuel for HGVs and fossil natural gas as a source of residential heating. The range of AD and upgrader sizes to be investigated and the corresponding feedstock requirement are determined from using the same method as the techno-economic model described in section 4.3.3. The functional unit is defined as "one year of biomethane plant operation".

Figure 5-3 show the system boundaries for both an attributional and consequential LCA for the biomethane plant, along with the incurred and avoided processes. A consequential LCA was determined to be the most suitable for this analysis as it includes the impact of using digestate as a replacement fertiliser [124]. The incurred processes includes feedstock transportation, operation of the biomethane plant (digester and upgrader operation, digestate storage and application). The avoided processes are those that are displaced by the production of biomethane. The storage and land

spreading of cattle slurry are avoided as the using the cattle slurry in the digester offsets it's use as a fertiliser, the fertiliser value is replaced by the use of digestate. However, due to co-digesting the cattle slurry with grass silage, there is a large quantity of digestate produced, with a higher fertiliser value than the avoided cattle slurry, thus the extra digestate is assumed to replace the use of mineral fertiliser. The production of bioCNG and biomethane also offsets the use of diesel and fossil natural gas respectively. As is typical for bioenergy systems, the construction and manufacture of buildings and equipment are excluded from the scope of this study [135].

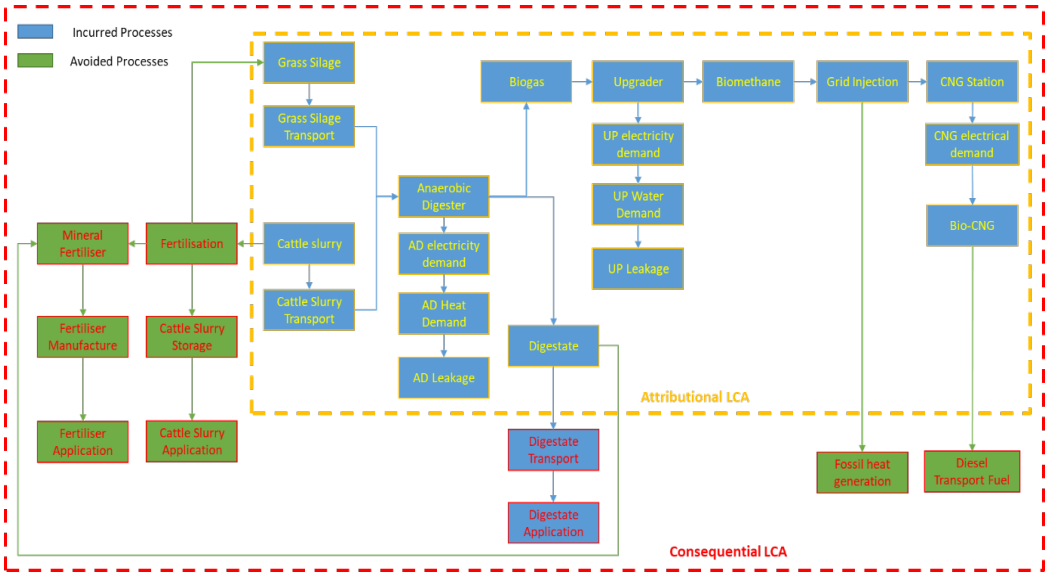

Figure 5-3: Schematic representation of the major processes considered within consequential LCA boundary of biomethane produced from AD compared with an attributional LCA boundary.

OpenLCA v1.10.3 is the software chosen to conduct the lifecycle assessment [136]. ReCiPe 2016 is chosen as the life cycle impact assessment (LCIA) method, the selected characterisation factors are at the midpoint level, under the hierarchist scenario, as they have a strong relation to the environmental flows and relatively low uncertainty [137]. The results are expressed in relation to four environmental impact categories: global warming potential (GWP) expressed as CO_2eq, freshwater eutrophication (EP) expressed as Peq, terrestrial acidification (AP) expressed as SO_2eq, and fine particulate matter formation (PM) expressed as PM2.5eq. These impact categories are chosen,

as they are the most important in relation the biomethane supply chain and transport fuels [22], [127], [18].

5.3.2.2 *Case Study Description*

As described in in section 3.3.1, an existing but anonymised Dx network, supplying an Irish town of 17,000 inhabitants and a smaller town of 4,400 inhabitants, with a mix of industrial, residential, and commercial demand is chosen as a case study. The Dx network consists of both 2 and 4 barg networks. The surrounding area has high potential for biomethane production due to the town's location in a highly productive agricultural region. There is also potential for significant demand at a CNG filling station, located on a nearby motorway, which is part of the TEN-T Core Network [93]. Figure 5-4 is a schematic of the representative Dx network and surrounding area. Chapter 3 investigated the grid capacity to accept biomethane at three potential injection sites, the first located near the AGI, the second situated close the proposed CNG filling station and the third located near the large town centre. The Dx network simulation described in Chapter 3 also consider the scenarios of maximum, minimum and no demand at the grid connected CNG filling station. Chapter 4 evaluates the techno-economic impacts of integrating a CNG fillings station and biomethane production and injection facility into a Dx network, for the range of plant sizes and locations determined in Chapter 3. This chapter assesses the techno-econo-environmental impacts of producing biomethane and bioCNG to offset fossil natural gas for residential heating and diesel as a fuel for HGVs respectively.

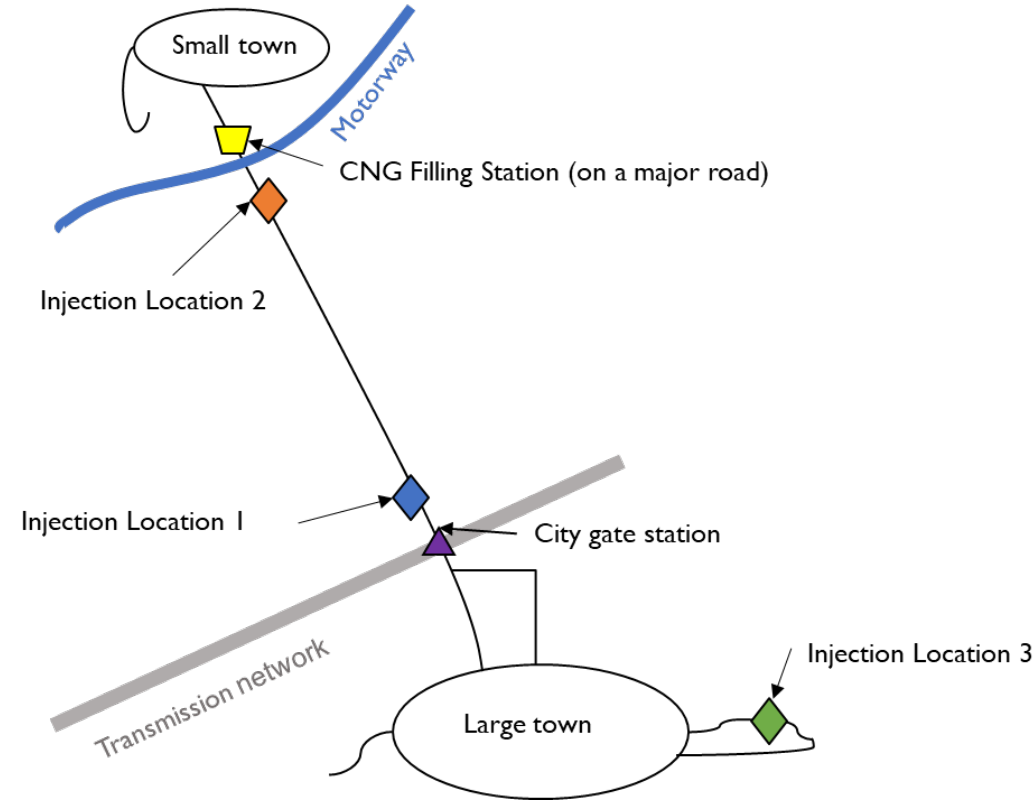

Figure 5-4: Schematic of the representative Dx network.

5.3.2.3 *Inventory Compilation*

Table 5-1 outlines the methods to calculate the emissions for each of the incurred and avoided processes shown in Figure 5-3Figure 5-3: Schematic representation of the major processes considered within consequential LCA boundary of biomethane produced from AD compared with an attributional LCA boundary. It also details the required input parameters and their sources.

Table 5-1: Equations for the lifecycle assessment.

Parameter	***Formula***	***Reference***	***Input Values***	***Reference***
Incurred Processes				
GS transport	=tkm from GIS model * Ecoinvent burden per tkm for tractor trailer			
CS transport	=tkm from GIS model * Ecoinvent burden per tkm for tractor trailer			
AD electrical demand	= AD gas demand *Ecoinvent burdens for Irish gas mix			

AD gas demand	= AD electrical demand *Ecoinvent burdens for Irish electricity mix			
AD leakage	kg CH4 = m3 of CH4 yield * density CH4 * % Digester loss		Density CH4 = 0.67 kg/m3, Losses in Digester = 1%	Styles et al. [18]
Upgrader electricity demand	= UP electrical demand *Ecoinvent burdens for Irish electricity mix			
Upgrader water demand	= UP water demand *Ecoinvent burdens for water			
Upgrader leakage	kg CH4 = (m3 of CH4 yield - CH4 loss at AD)* density CH4 * % upgrader loss	Styles et al. [18]	Density CH4 = 0.67 kg/m3, Losses in UP = 1%	Styles et al. [18]
Digestate Transport	=tkm from GIS model * Ecoinvent burden per tkm for tractor trailer			
Digestate Storage	kgCH4 = m3 CH4 yield * density CH4 * 1.5%	Styles et al. [18]	Density CH4 = 0.67 kg/m3	
	kg NH3-N = MgDM * total N, kg/MgDM *%total N as NH4-N * 2%/10%/52% (closed tank/ open tank/ lagoon)	Styles et al. [18]	kg N/Mg DM for GS = 21.5 , kg N/Mg DM for CS = 40.7, %total N as NH4-N GS = 37, %total N as NH4-N CS = 75,	Styles et al. [18]
	Indirect N2O-N = NH3-N * 0.01	Styles et al. [18]		
Digestate Application	kg NH3-N and kg NO3- N = Mg DM * total N, kg/Mg DM* % total N as NH4-N - NH3 storage loss * MANNER NPK EF	Styles et al. [18]	kg N/Mg DM for GS = 21.5 , kg N/Mg DM for CS = 40.7, %total N as NH4-N GS = 37, %total N as NH4-N CS = 75,	Styles et al. [18]
	kg N2O-N = Mg DM * total N, kg/MgDM - NH3-N storage loss * 0.01 + NH3-N *0.01 +NO3-N*0.0075	Styles et al. [18]	kg N/Mg DM for GS = 21.5 , kg N/Mg DM for CS = 40.7, %total N as NH4-N GS = 37, %total N as NH4-N CS = 76,	Styles et al. [18]
	kg P leached = Mg DM * P content, kg/Mg DM* 001	Styles et al [18].	kg P/Mg DM GS = 9.4, kg P/MgDM CS = 17.8,	Styles et al. [18]
CNG Station electricity demand	= CNG electrical demand *Ecoinvent burdens for Irish electricity mix			
Avoided Processes				

CS storage	Kg CH4 = MgDM * 800 kg/Mg volatile solids * CH4 producing capacity for manure type * density CH4 * CH4 conversion factor by system type	Styles et al. [18]	CH4 producing capacity for manure type = 0.24 (Dairy), 0.18 (non-dairy), CH4 conversion factor by system type = 37% (slurry pit storage below confinement 6 months)	Styles et al. [18] IPCC 2019 [138]
	Kg N2O-N = Mg DM*total N, kg/MgDM * storage system EF	Styles et al. [18]	kg N/Mg DM for CS = 40.7, storage system EF= 0.05,	Styles et al. [18] IPCC 2019 [138]
	kg NH3-N = Mg DM *total N kg/MgDM * % total N as NH4-N * storage system EF	Styles et al. [18]	kg N/Mg DM for CS = 40.7, %total N as NH4-N CS = 60, storage system EF= 5%,	Styles et al. [18] DEFRA 2019 Webb et al. [139]
CS application	kg NH3-N and kg NO3-N = Mg DM * total N, kg/MgDM * % total N as NH4-N * MANNER NPK EF	Styles et al. [18]	kg N/Mg DM for CS = 40.7, %total N as NH4-N CS = 60,	Styles et al. [18]
	kg N2O-N = Mg DM*total N kg/MgDM - storage NH3-N loss * 0.01 +NH3-N*0.01+NO3-N *0.0075	Styles et al. [18]	kg N/Mg DM for CS = 40.7,	Styles et al. [18]
	kg P leached = Mg DM * P content, kg/MgDM * 0.01	Styles et al. [18]	kg P/MgDM CS = 17.8,	Styles et al. [18]
	Fertilizer replacement credits = Mg DM * nutrient contents, kg/MgDM - storage NH3-N loss * MANNER NPK availability factors * fertilizer manufacture and application credits	Styles et al. [18]		
Oil/Gas heating	=(CH4 yield - AD losses - UP losses-CNG demand)*LHV*Ecoinvent oil/gas heat burdens per MJ			
Diesel	=CNG demand*LHV*Ecoinvent diesel burdens per MJ*H			Börjesson et al. [19]
NPK fertiliser manufacture	= Ecoinvent burdens for Can and DAP, per kg N,P and K	Beausang et al. [127]		

NPK fertiliser application	Direct kg N2O = fertiliser kg N * EF * (44/28)	Beausang et al. [127]	EF for CAN: kg N2O–N/kg N = 0.0140, EF for protected urea: kg N2O–N/kg N = 0.0040,	EPA 2019 [140]
	Indirect kg N2O (volatilisation) = fertiliser kg N * 0.1 * 0.01*(44/28)	Beausang et al. [127]		
	Indirect kg N2O (leaching) = fertiliser kg N * 0.3 * 0.0075*(44/28)	Beausang et al. [127]		
	kg NH3 = fertiliser kg N *EF* (17/14)	Beausang et al. [127]	EF for CAN: kg NH3/kg N = 0.008	EPA 2019 [140]
	kg P leached = Mg DM * P content, kg/Mg * 001	Styles et al. [18]		

To determine the consequential environmental impact of bioCNG as a transport fuel versus biomethane for residential heating the following assumptions are made:

- The biomethane plant size was set to be 4,741,032 m^3/annum, which is the maximum annual demand at the CNG filling station.
- MANNER-NPK software is used to determine the fertiliser replacement value of cattle slurry and digestate, assuming February application by broadcast spreading, to grass on sandy loam solids.
- The transportation distance for grass silage and cattle is averaged from the three-biomethane production and injection facility locations.
- The feedstock requirement and transportation distance, heat demand, and electricity demand of the anaerobic digester and upgrader are calculated using the methodology outlined in section 4.3.

5.3.2.4 *Sensitivity Analysis*

The current literature has reported a variety of values for the methane leakage from biomethane for high pressure water scrubbers systems, with a rage of 1% to 6% for anaerobic digesters [18], [65], [71], [127] and 1% to 1.5% [113]. An increase in the methane leakage not only increases the methane emissions released into the atmosphere, it also means that a greater quantity of

feedstocks are required to produce the quantity of biomethane and bioCNG. This in turn means the environmental burdens from the feedstock transportation, heat demand and electricity demand are increased. The impact the methane leakage percentage has on the overall environmental impacts is examined using the consequential LCA model described.

5.3.3 Total Cost of Carbon Abatement

The TCA is used to as a parameter to compare the overall techno-econo-environmental performance of different technologies. In this case, the TCA is used to investigate impact of integrating a biomethane production and injection facility into a Dx network. In this case study as well as biomethane to offset natural gas for residential heating, the biomethane production and injection facility produces bioCNG to offset diesel as a fuel for HGV, 4,741,032 m^3/annum in the scenario of maximum and 2,367,677 m^3/annum in the scenario of minimum demand at the CNG filling station . Thus both the environmental impacts of both bioCNG and biomethane must be considered. The range of plant sizes to be looked at for each potential injection location, under the conditions of maximum, minimum and no demand at the grid connected CNG filling station, is taken from the results of the Dx network simulation detailed in Chapter 3, using the method outlined in 4.3.4. The TCA calculation is expressed in Equation 5-1.

Equation 5-1: Total Cost of Carbon Abatement.

$$TCA = \frac{\sum_{y=0}^{LT} \frac{C_{Diesel\ y}}{(1+r)^y} + \sum_{y=0}^{LT} \frac{C_{Natural\ gas\ y}}{(1+r)^y} - \sum_{y=0}^{LT} \frac{C_{BioCNG,\ Biomethane\ y}}{(1+r)^y}}{\sum_{y=0}^{LT} \frac{(GWP_{WTW\ bioCNG} + GWP_{WTW\ biomethane})_y}{(1+r)^y}}$$

The cost of diesel is represented by C_{Diesel}, it is calculated using Equation 5-2 where, CF_{Diesel} (€/MWh) , is the price of diesel, H is the efficiency factor, which is equal to the efficiency of a diesel euro VI long haul truck divided by the efficiency of a CNG euro VI long haul truck, E_{BioCNG} (MWh) is the bioCNG produced by the plant, $Capex_{Diesel,V}$ (€), is the capital cost of a euro VI long haul diesel truck, ηCNG (MJ/km), is the efficiency of a CNG euro VI

long haul truck and d(km), is the average distance travelled by a CNG euro VI long haul truck in Ireland.

Equation 5-2: Cost of diesel.

$$C_{Diesel} = (CF_{\ Diesel} \times \mathrm{H} \times E_{BioCNG}) + \left(Capex_{Diesel,V} \times \frac{E_{BioCNG} \times 3600}{\eta CNG \times d}\right)$$

$C_{Natural\ gas}$ represents the cost of natural gas, it is determined using Equation 5-3, where $CF_{\ NG}$ (€/MWh), is the cost of natural gas and E_{BioCH4}(MWh), is the biomethane produced by the plant.

Equation 5-3: Cost of Natural Gas.

$$C_{Natural\ gas} = CF_{\ NG} \times E_{BioCH4}$$

The cost of biomethane and bioCNG produced by the plant, $C_{BioCNG,\ Biomethane}$ is calculated using Equation 5-4 where, $Capex_{AD}$(€), is the capital cost of the anaerobic digester, $Opex_{AD}$ (€/a), is the operational cost of the anaerobic digester, CE_{AD} (€/a), is the electrical cost of the anaerobic digester, CG_{AD}(€/a) is the natural gas price of the anaerobic digester, $Capex_{UP}$(€), is the capital cost of the upgrader, $Main_{up}$ (€/a) is the maintenance cost of the upgrader, CE_{UP} (€/a), is the electrical cost of the upgrader, CW_{UP}(€/a), is the water cost of the upgrader, TC (€/a), is the feedstock transportation cost, $Capex_{CNG,I}$(€), is the capital cost of the CNG filling station, $Opex_{CNG,I}$ (€/a), is the operational cost of the CNG filling station, $Capex_{CNG,V}$(€), is the capital cost of a euro VI long haul CNG truck. Further details on the majority of these cost factors can be found in section 4.3.3, the additional cost factors for the cost of carbon abatement are given in Table 5-2 . The CNG filling station and vehicle cost are included in the scenarios of maximum and minimum demand at the CNG filling station but not in the scenario of no demand at the CNG filling station.

Equation 5-4: Cost of biomethane and bioCNG production.

$$C_{BioCNG,\ Biomethane} = Capex_{AD} + Opex_{AD} + CE_{AD} + CG_{AD} + Capex_{UP} + Main_{up} + CE_{UP} + CW_{UP} + TC + FC + Capex_{CNG,I} + Opex_{CNG,I} + CE_{CNG} + \left(Capex_{CNG,V} \times \frac{CNG\ Demand}{\eta CnG \times d}\right)$$

$GWP_{WTW\ bioCNG}$(kg CO_2 eq.) and $GWP_{WTW\ biomethane}$ (kg CO_2 eq.) are the WTW GWP emissions of bioCNG and biomethane respectively. Due to the fact that a consequential method has been used for this analysis the results outputted include the offsetting of fossil diesel and natural gas.

Table 5-2: Cost factors for the total cost of carbon abatement.

Parameter	*Value*	*Reference*
Diesel Price (€/MWh)	93.44	[141]
Efficiency Diesel truck (MJ/km)	9.68	Börjesson et al. [19]
Efficiency CNG Truck (MJ/Km)	11.75	Börjesson et al. [19], Ricardo Energy & Environment [25]
Capital cost of a Diesel truck (€)	135,000	Discussion with Irish hauliers and GNI.
Capital cost of a CNG truck (€)	162,000	Discussion with Irish hauliers and GNI.
Annual distance travelled by a CNG truck (km)	99,107	Discussion with Irish hauliers and GNI.

5.4 Results and Discussions

5.4.1 Life Cycle Assessment

Figure 5-5, Figure 5-7, Figure 5-8, Figure 5-9 shows the results of the LCIA of biomethane and bioCNG presented per MJ of fuel produced, the contribution of the system processes highlighted. The results for each of the selected impact categories are discussed in detail below.

5.4.1.1 *Global Warming Potential*

The results found that for bioCNG there is a potential net reduction of -0.02272 kg $CO_{2\ eq.}$ /MJ for bioCNG and -0.01899 kg $CO_{2\ eq.}$ /MJ for biomethane. The processes with the largest incurred emissions are the digestate storage, transport and application, followed by the transportation of feedstocks, they accounted for 30.1% and 25.8% of the bioCNG incurred emissions and 30.5% and 26.1% of biomethane incurred emissions respectively. While the incurred emissions have a significant impact, they do not exceed the avoided emissions, giving an overall negative result. The

processes with the largest avoided emissions are manure storage, fossil fuel offset (i.e. diesel or natural gas), and manure application, they accounted for 40.8%, 22.6% and 21.8% of bioCNG avoided emissions and 43.4%, 17.6% and 23.2% of biomethane avoided emissions respectively. The primary difference between the GWP of bioCNG and biomethane is that the value of offsetting diesel offers a greater emissions saving than offsetting fossil natural gas, despite the increased electricity burden required to compress the bioCNG.

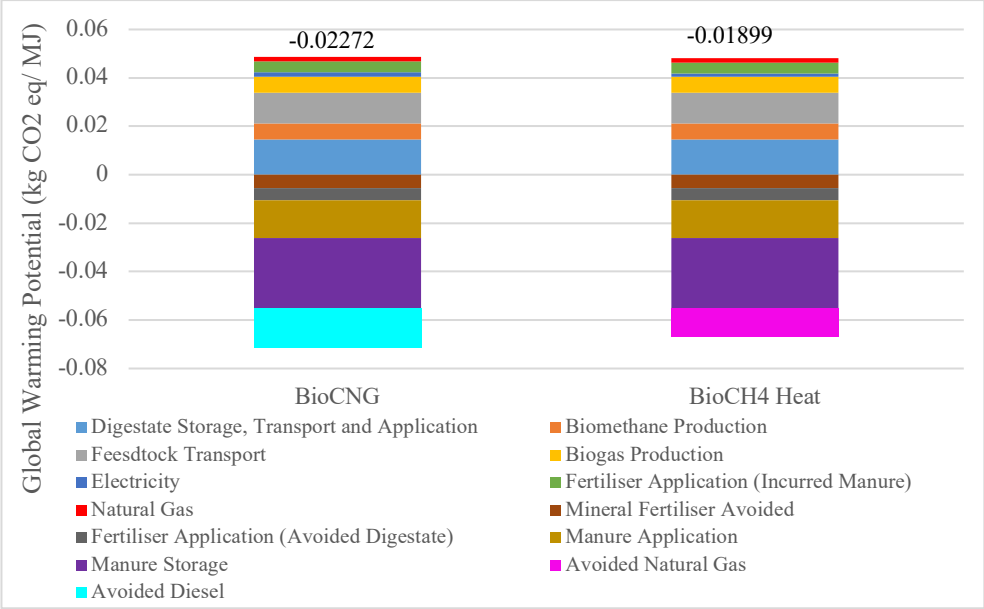

Figure 5-5: The well-to-tank environmental results of the consequential life cycle assessment of biomethane and bioCNG production for the of global warming potential impact factor.

Figure 5-6 shows the WTW GWP of bioCNG and biomethane. It is evident that the avoided tank – to – wheel (TTW) processes have the greatest impact in determining the overall emissions value. In the case of bioCNG, this is the offsetting of combustion of diesel fuel in a euro VI long haul truck, comparatively in the case of biomethane, the offset end use is combustion of natural gas in a residential condensing boiler for heat generation.

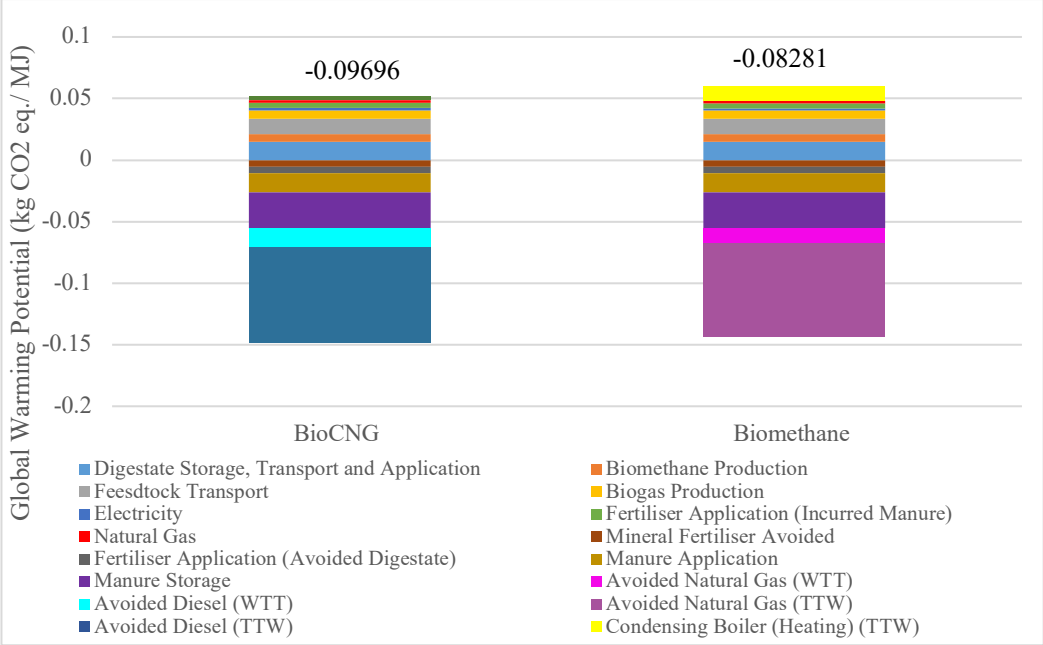

Figure 5-6: The well – to – wheel global warming potential results for the consequential life cycle assessment of biomethane and bioCNG.

5.4.1.2 *Freshwater Eutrophication*

The EP impact was determined to be -9.8 x 10^{-6} kg $P_{eq.}$ /MJ for bioCNG and 5.1 x 10^{-6} kg $P_{eq.}$ /MJ for biomethane. The feedstock transportation was the by far the most significant process to contributing to the incurred EP emissions of both bioCNG and biomethane, contributing 56% and 57% respectively. In the case of bioCNG, avoided diesel emissions accounted for 84% of the avoided emissions, and are the main factor in contributing to the net negative emissions value. Comparatively, the avoided natural gas emission are significantly smaller, only accounting for 13% of avoided emission and thus resulting in an overall net positive value for biomethane EP.

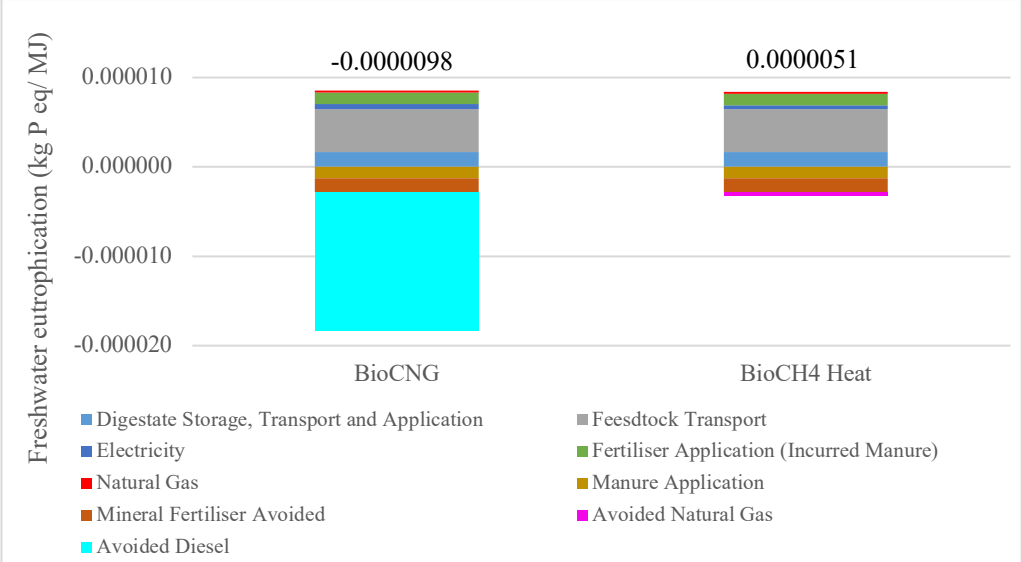

Figure 5-7: The well-to-tank environmental results of the consequential life cycle assessment of biomethane and bioCNG production for the of freshwater eutrophication impact factor.

5.4.1.3 *Fine Particulate Matter Formation*

The LCIA resulted in a net negative impact for PM with a value of -0.00011 kg $PM_{2.5\ eq.}$ /MJ for bioCNG and -0.00007 kg $PM_{2.5\ eq.}$ /MJ for biomethane. The process of avoided manure application is the largest contributor to the avoided emissions, accounting for 42% of bioCNG and 56% of biomethane avoided emissions. In the case of bioCNG, the offsetting of diesel fuel also contributes substantially, making up 30% of avoided emissions. For both bioCNG and biomethane, the feedstock transportation process resulted in the greatest share of incurred emissions at 57%.

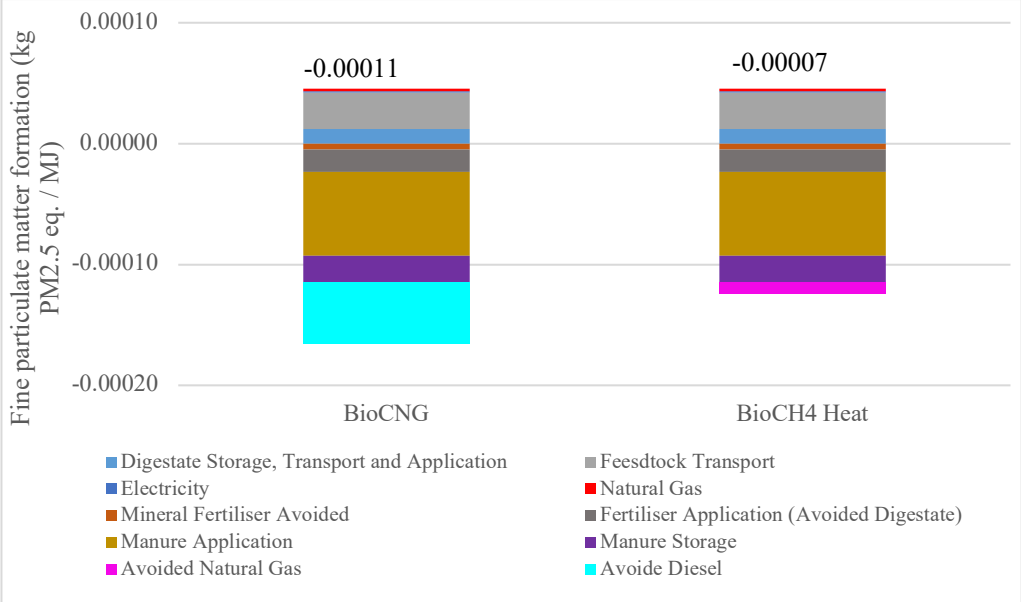

Figure 5-8: The well-to-tank environmental results of the consequential life cycle assessment of biomethane and bioCNG production for the fine articulate matter formation impact factor.

5.4.1.4 *Terrestrial Acidification*

In a similar trend to the other selected impact factors bioCNG is determined to have a greater AP saving in comparison to biomethane, with net values of -0.00083 kg $SO_{2\ eq.}$ /MJ and -0.00072 kg $SO_{2\ eq.}$ /MJ respectively. In this case, the avoided emissions can be primarily attributed to the avoided manure application, and avoided manure storage making up 57% and 18% of bioCNG avoided emissions and 64% and 20% of biomethane avoided emissions respectively. At 58% of incurred emission in both the cases of bioCNG and biomethane, the digestate storage, transportation and application was the largest contributing factor to the incurred emissions.

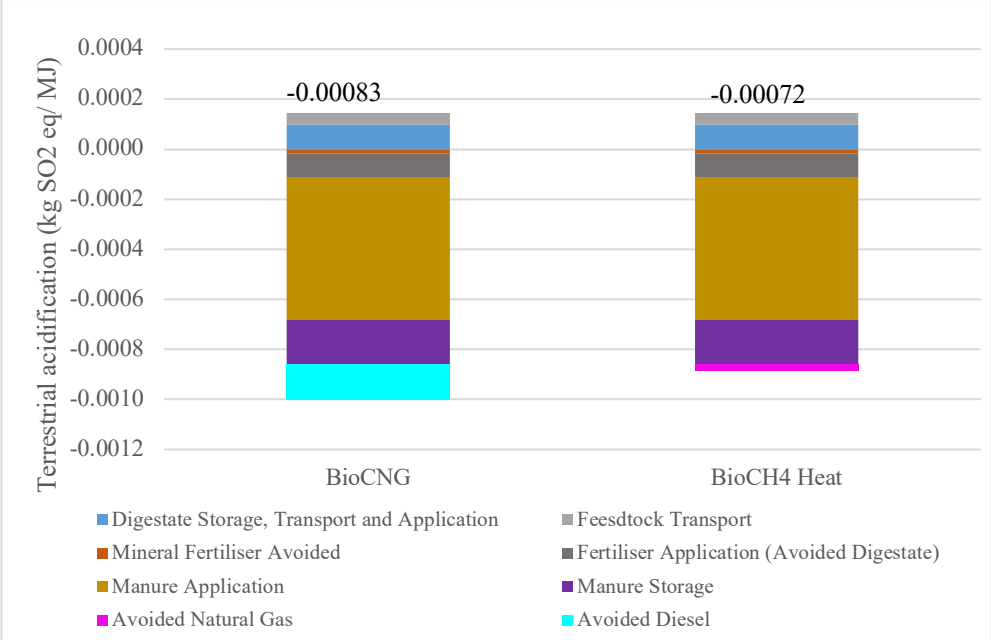

Figure 5-9: The well-to-tank environmental results of the consequential life cycle assessment of biomethane and bioCNG production for the terrestrial acidification impact factor.

The results show that in the impact categories of GWP, AP and PM, bioCNG and biomethane show environmental benefits over diesel and natural gas respectively. This is consistent with results from previous studies in the literature [127], [20], [19], [25]. The exception to this is the EP impact category, a net negative result is still observed for bioCNG, however, a net positive result is returned for biomethane. It is evident that across all impact categories that bioCNG results in greater environmental savings than biomethane.

5.4.2 Methane Sensitivity Analysis

Figure 5-10 depicts the results of the consequential WTT GWP for bioCNG, under different percentages of methane leakage from the anaerobic digester and upgrader. Two levels of methane leakage from the upgrader are investigated, the first is 1% leakage, represented by the blue bars, and the second is 1.5% leakage represented by the green bars. Both levels of methane leakage at the upgrader are examined with between 1% and 6% methane leakage at the AD. It is clear from the results that as the methane leakage percentage increases so too does the overall net environmental impact.

However, notably when the cumulative methane emissions exceed 5.5% the results are net positive, indicating that the process of producing bioCNG is more carbon intensive than the production of diesel.

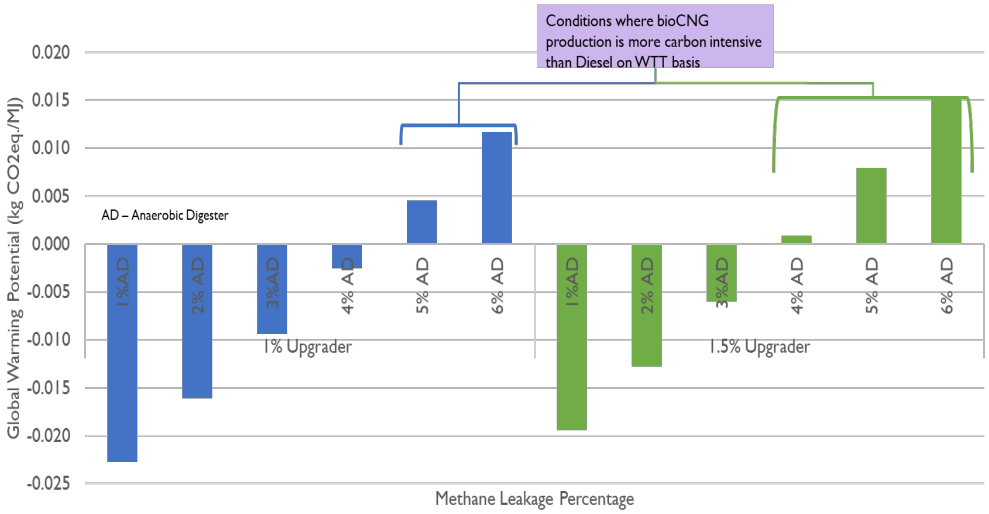

Figure 5-10: Methane leakage sensitivity analysis for the well- to wheel global warming potential of bio-CNG.

5.4.3 Total Cost of Carbon Abatement

Figure 5-11 shows the results of the TCA at each of the potential production and injection facility locations for the scenarios of maximum, minimum and no CNG demand at the grid connected CNG filling station. It is evident that across all injection locations and scenarios of CNG demand that the TCA is relatively steady before increasing dramatically. The point at which the TCA increases dramatically is the point at which increase in the size of the biomethane production plant has minimal impact on increasing the actual energy output, due to the injection capacity becoming significantly restricted by the limits imposed by the gas grid. For example, this is evident in Figure 5-11 (a) where the TCA increases from 84.41 €/tCO_2 at 94.50 GWh/a to 98.49 €/tCO_2 at 94.77 GWh/a for injection location 1 101.53 €/tCO_2 at 128.53 GWh/a to 118.82 €/tCO_2 at 128.77 GWh/a at injection location 2, and 133.85 €/tCO_2 at 121.29 GWh/a to 176.49 €/tCO_2 at 121.76 GWh/a. This clearly shows the necessity of considering the limitations imposed by the Dx network on the quantity of biomethane that can be injected.

Another trend that is evident across all three potential injection locations is that the greater the CNG demand the lower the TCA. This is can be attributed to two factors, firstly the increase in CNG demand, increases the overall network demand and thus grid capacity to accept biomethane. This means that the plant sizes being analysed are larger and the economies of scale implied by the power law relationship in the capex values in Equation 5-4 apply. Secondly, as can be seen in Figure 5-6, bioCNG results in larger environmental savings than biomethane. Thus, the increase in CNG demand increases the overall environmental savings. As the biomethane injected into the grid is first allocated to be used as bioCNG at the CNG filling station, with the remaining quantity offsetting residential heat, the results in the techno-econo-environmental optimum is realized at a smaller plant size than the techno-economic optimum plant size discussed in section 4.4. For example, in the scenario with maximum demand at the CNG filling station, the techno-economic optimum is achieved at a plant size of 115 GWh, while the techno-econo-environmental optimum is attained at a plant size of 98.7 GWh, both at injection location 2.

When comparing the results of the potential injection locations, it is evident that injection location 2 results in the lowest TCA, followed by injection location 1, with injection location 3 giving the largest TCA. This is primarily due to the difference in transportation distances of feedstocks to the biomethane production facilities. Injection location 3 is located on the outskirts of a large town centre, while injection locations 1 and 2 are located on more rural sections of the Dx network. As the feedstock in this case is grass silage and cattle slurry, injection locations 1 and 2 are substantially closer to the feedstock sources than injection location 3. Another factor that may contribute to injection location 3 being less profitable than injection location 1 or 2 is that in every CNG demand scenario, injection location 3 has a larger range between its minimum hourly flowrate and maximum hourly flowrate. This means that increasing the capacity of the plant does not have as great an impact on the annual energy output.

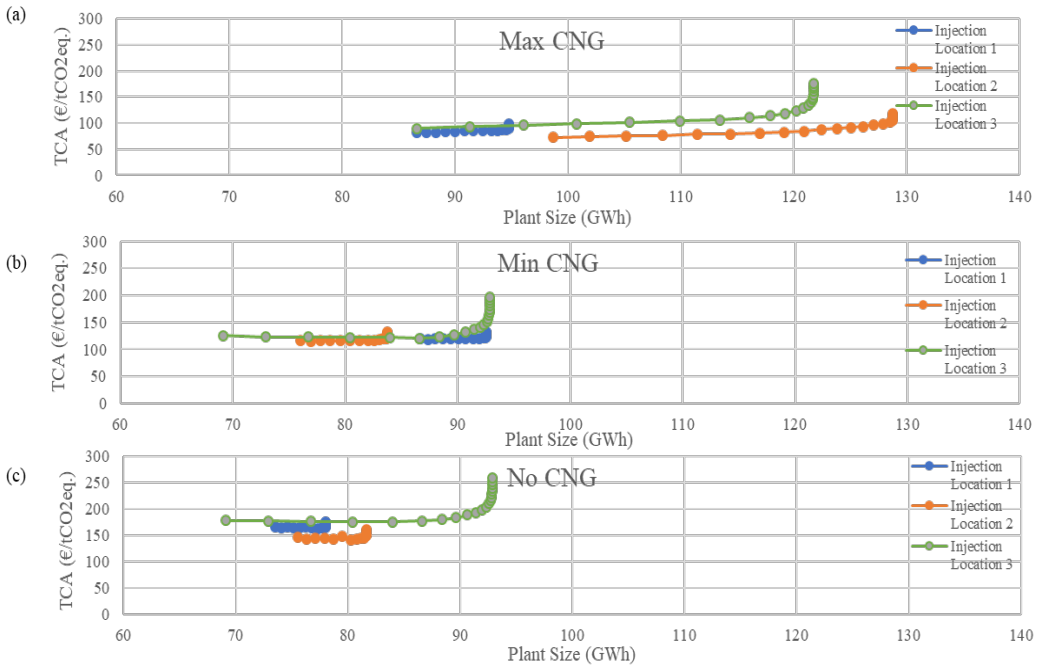

Figure 5-11: Results of the total cost of carbon abatement calculated for each potential injection location, with (a) maximum demand at the CNG filling station, (b) minimum demand at the CNG filling station and (c) no demand at the CNG filling station.

5.5 Conclusions

This chapter investigated the environmental cost and benefits of bioCNG as a vehicle fuel and biomethane as a source of residential heating, by conducting a consequential LCA. The results found that bioCNG offered significant environmental benefits across the selected impact categories of GWP, EP, PM and AP, as an alternative vehicle fuel to diesel. In the case of biomethane offsetting natural gas for residential heating, significant environmental savings were observed for the GWP, AP and PM. However, under the EP impact factor, biomethane was shown to have a greater environmental burden than the offset natural gas.

A sensitivity analysis was also undertaken to determine the impact methane leakage from the system has on the GWP of bioCNG. The study showed that methane leakage has a substantial impact on the WTT GWP of bioCNG, such that when the cumulative methane leakage exceeds 5.5%, the production of bioCNG is observed to be more carbon intensive than diesel.

Evaluation of the techno-econo-environmental impacts uses a novel method, incorporating the seasonal variation of gas demand. The gas Dx network simulation detailed in Chapter 3 was created to determine the grid capacity to accept biomethane at three potential injection locations, under the scenarios of maximum, minimum and no demand at CNG filling station. The results from this simulation were used to determine the range of biomethane plant sizes evaluated at each potential injection location and CNG scenario. This along with a spatial analysis of the feedstock data and various cost factors described in Chapter 4, was used to calculate the total cost of the plant. When combined, the total cost of the biomethane plant and an overall consequential LCA resulted in a TCA curve.

The results conveyed the importance of considering the technical limitations imposed by gas networks on the grid capacity to accept biomethane when considering the techno-econo-environmental impact of a biomethane plant size and location. In the maximum CNG demand scenario the TCA ranges from 72.49 €/tCO_2 at injection location 2 for an energy output of 98.69 GWh/a to 176.49 €/tCO_2 at injection location 3 for an energy output of 121.76 GWh/a. For this case study, injection location was determined to result in the lowest TCA for all scenarios of CNG demand. The optimum plant sizes resulted in an energy output of 98.69 GWh/a for the maximum CNG demand, 76.90 GWh/a for the minimum CNG demand and 80.24 GWh/a for no CNG demand. Considering the location, plant size and end use of the biomethane production, including the seasonal variation of demand and the technical limitations imposed by gas networks is of key importance in maximising the environmental savings in an economical way.

5.6 Chapter Summary

This chapter builds on the Dx network simulation detailed in Chapter 3 and the techno economic model described in Chapter 4 to evaluate the environmental impacts of biomethane production and usage as either a transport fuel for HGVs replacing diesel or offsetting natural gas for residential heating. The novelty of considering the seasonal variation in gas

demand and the technical limitations imposed by the gas grid is carried through into the consequential LCA. The results showed that both bioCNG and biomethane for heating can offer significant environmental savings over the fossil alternatives of diesel and natural gas respectively. Location 2 was determined to be the techno-econo-environmental optimum, at a TCA of 72.49 €/tCO_2, 114.86 €/tCO_2, 141.42 €/tCO_2 for the scenarios of maximum, minimum and no CNG demand at the grid connected filling station. The most competitive configuration produces 49.75 GWh/a bioCNG and 48.94 GWh/a of biomethane for heat, 24.85 GWh/a of bioCNG and 52.05 GWh/a of biomethane for heat and 80.24 GWh/a of biomethane for heating offsetting 33, 399 tCO_2/a, 25,423 tCO_2/a, and 25,322 tCO_2/a respectively.

Chapter 6 will summarise all the significant contributions and findings from the previous chapters and outline future work.

Chapter 6 Conclusions

6.1 Chapter Overview

This chapter summarises all the significant contributions and findings in the previous chapters. A summary of the outcomes, and contributions of this thesis are given in section 6.2. The overall conclusions are presented in section 6.3, and potential areas for future studies related to this work are identified and discussed in section 6.4.

6.2 Discussion

This thesis investigated the integration of CNG filling stations and biomethane production and injection facilities into gas networks, at a regional scale, applied to a case study of a representative Irish Dx network. A methodology is developed to assess the grid capacity to accept biomethane, design the supply chain, identify sites and sizes of biomethane production facilities, that allows evaluation of the economic and environmental impacts of biomethane production under various scenarios of demand at the grid connected CNG filling station.

Key contributions of this work include:

(i) A comprehensive review of technical and economic assessments of biogenic renewable gas injection into the gas grid and their inclusion of the technical limitations imposed by gas networks, production and supply chain modelling, the use of biomethane as a vehicle fuel, the impact of location of the biomethane production and injection facility, and incorporation of SCADA data.

(ii) A gas network simulation methodology to quantify the potential for biomethane injection, whilst ensuring technical constraints such as pressures and flowrates are within normal operating conditions.

(iii) An integrated model of biomethane supply chains that included feedstock sourcing, biomethane production, grid injection and consumption as either a fuel for residential heating or CNG HGVs.

(iv) A comprehensive modelling framework that includes technical, economic, and environmental aspects of the biomethane supply chain.
(v) Analysis of the modelling framework for a number of locations for the biomethane plant and demand scenarios at the CNG filling station.

In Chapter 2, technical and economic assessments of biomethane and bio-SNG injection into the gas grid are reviewed. 16 studies focused on biomethane, 3 on bio-SNG, and 4 on multiple gases. Prior studies can primarily be categorized into upstream models and downstream models. Upstream models focused on the optimisation of supply chains, locations and sizes for biogenic renewable gas production. Downstream models consider the dispersion of renewable gas after it has been injected into the gas network, analysing the impact on technical operation factors and gas quality, including pressure, WI, and HHV. The review, demonstrated the necessity for development of a comprehensive methodology that would take into account all identified elements of upstream and downstream modelling.

In Chapter 3, a framework for the dynamic modelling of a gas Dx network is developed to determine the maximum quantity of biomethane that can be injected, while considering the seasonal variation is gas demand, and the technical constraints imposed by gas network operation, quality and safety standards. The impact of location of the biomethane production and injection facility and the demand at the grid connected CNG station are also analysed. This framework was demonstrated for a case study of an existing by anonymised Dx network in the Irish gas network.

In Chapter 4, the results from the gas network simulation in Chapter 3 are used to determine a range of potential sizes for the biomethane production and injection plant, and formed the basis of the capital expenditure and operational expenditure calculations. A GIS model facilitated the calculation of the cost of transporting cattle slurry and grass silage to the plant. The feedstock transportation costs combined with the capital and operating costs of the biomethane production and injection plant, and the

CNG filling station allowed the calculation of LCOE and NPV of the gas and the possibility to select the most economically viable plant size and site.

In Chapter 5, the model built in Chapter 4 was integrated with a consequential LCA of the supply chain of biomethane production from cattle slurry and grass silage, for use as a fuel for residential heating or CNG HGVs. Environmental impacts for the collection, transport, and conversion of feedstocks into biomethane and its substitution of natural gas, diesel, the co-production of digestate, and the offsetting of mineral fertiliser was also considered. A sensitivity analysis of the percentage of methane leakage from both the AD and upgrader was conducted. The results of the LCA were combined with the overall costs of biomethane to calculate the TCA.

6.3 Conclusions

This research resulted in a number of key observations regarding the integration of biomethane production and injection facilities and CNG filling stations into gas networks:

From Chapter 2:

- Technical and economic studies that consider elements of both upstream and downstream modelling are limited, and there is no comprehensive study that gives consideration to all five of the identified key complementary elements (i) the technical constraints gas grids place on biogenic renewable gas injection, (ii) models for biogenic gas production and supply chains, (iii) the use of compressed natural gas (CNG) as a vehicle fuel, (iv) the optimisation of production and injection facility location, and (v) the incorporation of SCADA data.
- Models that aim to optimise the location of biomethane plants have been investigated from a number of supply chain stand points, including feedstock availability, and fluctuating seasonal gas demand,

but consideration has yet to be given to the ability of the natural gas grid to receive biomethane.

- Gas network SCADA data has been used in several of the reviewed studies to validate results or create accurate gas demand profiles, however incorporation of CNG demand profiles and their potential impacts have yet to be considered.

From Chapter 3:

- It is evident that the optimising the location and injection pipeline diameter of the biomethane production and injection facility can significantly impact the grid capacity to accept biomethane. In the case study analysed optimising the location could increase the grid capacity for biomethane by between 1.1% and 6%, and that optimising the injection pipeline diameter could increase the grid capacity for biomethane by between 5.5% and 18.3%.
- For the conditions in the case study examined it was determined there was the potential to inject up to 141GWh/a, 103 GWh/a and 102 GWh/a of biomethane in the scenario of maximum, minimum and no demand at the CNG filling station. Which corresponded to 49%, 42%, and 43% of the total annual demand for natural gas on the Dx network in the case study in 2018, respectively.

From Chapter 4:

- Technical limitation on the capacity of the grid to accept biomethane are shown to have a significant impact on the economic viability of the biomethane production and injection facility. In the case study examined for the scenario with maximum demand at the CNG filling station, the LCOE varies from 86.86 €/MWh for an energy output of 93.18 GWh/a to 90.71 €/MWh for an energy output of 94.77 GWh/a at injection location 1, from 81.61 €/MWh for an energy output of 114.4 GWh/a to 96.99 €/MWh for an energy output of 128.77 GWh/a at injection location 2, and from 88.19 €/MWh for an energy output of 109.88 GWh/a to 109.84 €/MWh for an energy output of 121.76 GWh/a at injection location 2.

- Plant profitability varied substantially with the location of the biomethane production and injection facility. Location 2 was determined to be the most profitable location for the case study examined. The NPV increased from 2.39 M€ at injection location 3 to 9.56 M€ at injection location 2 in the scenario of maximum CNG demand, -0.86 M€ at injection location 3 to 3.98 M€ at injection location 2 in the scenario of minimum CNG demand, and from -3.84 M€ at injection location 3 to 0.94 M€ at injection location 2.
- The incorporation of CNG filling stations into the gas grid had a significant impaction on the economic viability of the biomethane production and injection, due to the increase in incentives for using biomethane as a vehicle fuel compared to residential heating. Also the fact that the addition of the CNG demand increases the overall network demand, meaning that larger quantities of biomethane can be produced and injected, which benefit from economies of scale.

From Chapter 5:

- Biomethane production and use as a fuel for CNG HGVs showed environmental benefits in the categories of global warming potential, acidification, eutrophication and fine particulate matter formation. The alternate end use of biomethane as a fuel for residential heating also showed environmental saving in the categories of global warning potential, acidification and fine particulate matter formation. However, the resultant savings for residential heating are less that those observed in the ends use as a fuel for CNG HGVs. Also in the case of residential heating, it showed that eutrophication impacts are worsened.
- A sensitivity analysis of the methane leakage percentage from the anaerobic digester and upgrader showed that this parameter can have a considerable impact on the WTT global warming potential, such that when the cumulative methane leakage exceeds 5.5%, the production of bioCNG is observed to be more carbon intensive than diesel.

- When the environmental impact is coupled with the economic performance, smaller sizes of the biomethane plant are favoured to minimise the TCA. The most competitive configuration produces 49.75 GWh/a bioCNG and 48.94 GWh/a of biomethane for heat in the scenario of maximum CNG demand, 24.85 GWh/a of bioCNG and 52.05 GWh/a of biomethane for heat in the scenario of minimum CNG demand and 80.24 GWh/a of biomethane for heating in the scenario of no CNG demand, offsetting 33, 399 tCO_2/a, 25,423 tCO_2/a, and 25,322 tCO_2/a respectively.

6.4 Future work

A number of suggestion for the improvement, addition or extension of the work undertaken in this thesis are described.

In the case of the work presented in Chapter 3:

- The grid capacity to accept biomethane is dependent on the pressure of the AGI. Decreasing this pressure could allow for the grid capacity for biomethane to be increased at each injection location, however it could also result in large pressure drops on the network during periods of high demand. Investigating the maximum pressure reduction at the AGI without causing adverse effects on the network, should be evaluated for possible further decarbonisation of gas networks.
- The assessment of the grid capacity to accept biomethane is specific to the layout of the gas network, thus the methodology could be applied to other Dx networks and potentially Tx networks to determine impacts of different layouts and scale of the network.
- This methodology could also possible be adapted to investigate the ability of gas networks to accept hydrogen.

In the case of the work presented in Chapter 4:

- This work has been evaluated at a regional scale for a case study in rural Ireland, with an abundance of cattle slurry and grass silage available. Application to other regions may require consideration of alternative feedstocks. Further insight may also be gained by investigating the introduction of biomethane production and injection facilities to multiple Dx networks within reasonably close proximity to determine potential competition for the available resources.
- While incentives for biomethane and bioCNG have been included in this analysis, the impact of carbon taxes have not been investigated. This may improve the economic competitiveness in of biomethane and bioCNG in comparison to fossil alternatives.
- This work has assumed that all gas produced will be injected into the gas grid, however there is also the possibility of using biomethane for off- grid applications. Investigating possible synergies of the biomethane plant to supply both on-grid and off grid applications could improve the economics of producing biomethane at larger scales when it beings to become limited by the technical constraints of the gas network.

In the case of the work presented in Chapter 5:

- The potential capture and usage of the CO_2 removed from the biogas as part of the upgrading process should be explored to increase the circularity and sustainability of future economies.

Appendices

A.1 Initial Modelling Work (MATLAB)

A.1.1 Steady-State Model

Figure A.1-1 shows a schematic of the sample Dx network simulated in the steady-state MATLAB model. The model layout, along with the initial pressure, pipe diameters and lengths were soured from Abeysekera et al. [78]. Node one, highlighted in purple represents the original supply of gas to the distribution network, nodes 2 – 11, highlighted in blue represent demand points on the network and node 12, highlighted in green represents a biomethane production and injection facility supplying the network.

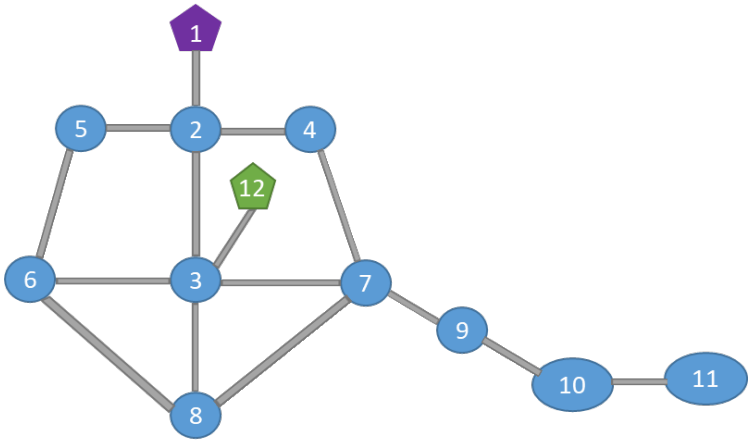

Figure A.1-1: Schematic of the sample dx network simulated in the steady-state MATLAB model.

Figure A.1-2 outlines the steps that the model follows to compute the pressure at each node and the flowrate of each pipe.

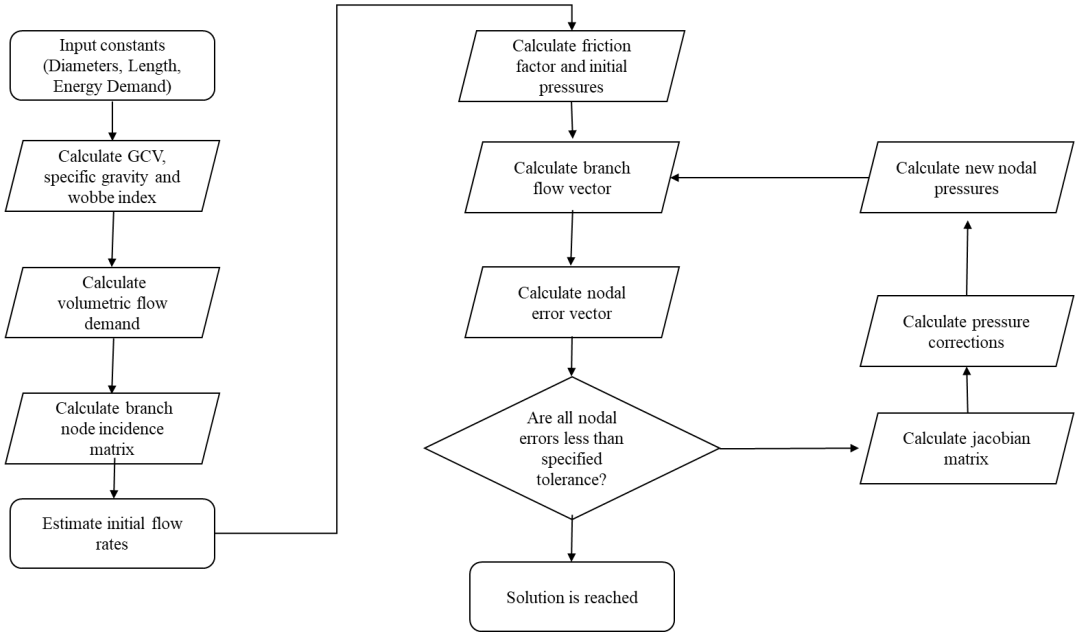

Figure A.1-2: Flowchart outlining the method for steady-state simulation of distribution network in MATLAB.

The proposed method consists of a set of algebraic equations equal in number to the set of variables to be calculated. The equations are formulated using Kirchhoff's laws and a version of the standard gas flow equation to each node, with the following assumptions:

- Steady flow.
- Isothermal flow due to heat transfer with the surroundings through the pipe wall.
- Negligible kinetic energy change in the pipe.
- Constant compressibility of the gas over the length of the pipe.
- Validity of Darcy friction loss relationship.
- Constant friction coefficient along the pipe length.

In the case of a low pressure network (< 0.75 barg) Lacey's Equation A-1 is used and in the case of a medium pressure network (0.75 – 7 barg) the Polyflo Equation A-2 is used [142].

Equation A-1: Lacey's equation

$$q_n = 5.72 \times 10^{-4} \sqrt{\frac{(P_1 - P_2)D^5}{fSL}}$$

$$f = 0.0044\left(1 + \frac{12}{0.276D}\right)$$

Equation A-2: Polyflo equation.

$$q_n = 7.57 \times 10^{-4} \times \frac{T_n}{P_n}\sqrt{\frac{(P_1 - P_2)D^5}{fSLT}}$$

$$\sqrt{\frac{1}{f}} = 5.338\ (Re)^{0.076}E$$

where, q is the flowrate, P is the nodal pressure, D is the pipe diameter, f is the friction factor, S is the specific gravity, L is the pipe length

The newton nodal formula Equation A-3 is then applied to assign the position of pipes in relation to each node and creating the nodal incident matrix Equation A-4.

Equation A-3: Newton nodal formula.

$$a_{ij} = \begin{cases} +1,\ if\ flow\ in\ branch\ j\ enters\ node\ i \\ -1,\ if\ flow\ in\ branch\ j\ leaves\ node\ i \\ 0,\ if\ branch\ j\ is\ not\ incident\ to\ node\ i \end{cases}$$

Equation A-4: Nodal Incident Matrix

$$A = [a_{ij}]_{(n \times m)}$$

From the standard gas equations above Equation A-1, Equation A-2, it is evident that the pipe flow is a function of the pressure drop and gas gravity and can thus the pipe flow vector can be expressed as :

Equation A-5: Pipe flow vector.

$$Q = \varphi(-A^T P, S)$$

Kirchhoff's first law states that the algebraic sum of the gas flow at any node is equal to zero. Kirchhoff's second law states that the pressure drop around any loop is equal to zero.

Equation A-6: Kirchhoff's Laws.

$$AQ = Q_{net\ demand}$$

$$\Delta P = -A^T P$$

An initial approximation of the pressures at each node are iteratively corrected using the Newton-Raphson method. The specific gravity, calorific value and flowrate in each pipelines calculated for each iteration. As the pressures initially are only approximations of their true values the left and right hand sides of Equation A-5 will not be balanced. The imbalance of each node is a function of all the unknown nodal pressure, and is calculated from Equation A-7.

Equation A-7: Nodal error matrix

$$F(P) = \varphi(-A^T P, S) - Q$$

The newton nodal method solves the nodal error matrix until all nodal errors are less than a specified tolerance. If nodal errors are outside the specified tolerance, a pressure correction is applied to the previously estimated pressures to calculate the pressure for the next iteration:

Equation A-8:Nodal pressure correction using Taylor series expansion.

$$P_{k+1} = P_k + \delta P_k$$

$$\delta P_k = -F(P_k) \times J^{-1}$$

where, δP is the pressure correction and J is the nodal jacobian matrix.

The results given in this simulation are for a low pressure distribution network with 1 natural gas source node, 1 bio-methane injection point and 10 demand nodes. The bar charts in Figure A.1-3 below show the model results for pressure and flowrate respectively. They are compared to the results obtained by Abeyskera et al. [78] to validate the model. It can be observed that there is relatively good agreement between the results. The slight variation can be attributed to a difference in the calculation of the gross calorific value GCV. As this is a thermal based model the GCV has a significant impact on calculating the flow rate which in turn has an impact on the pressure.

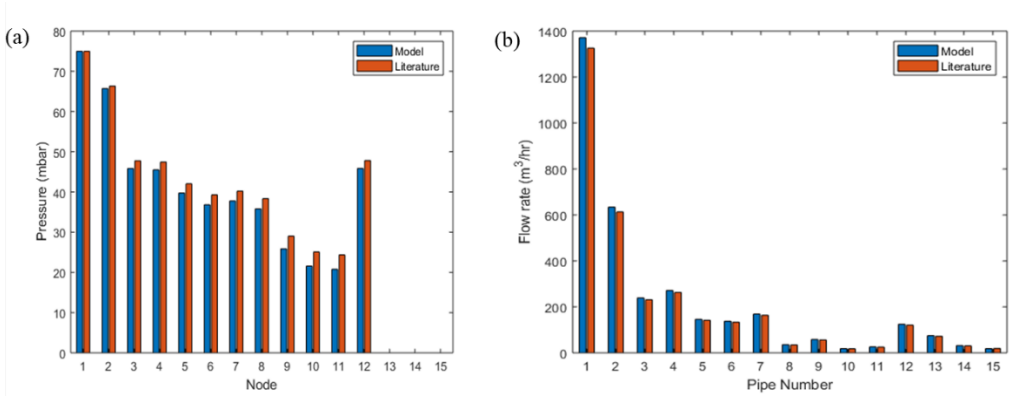

Figure A.1-3: Results of the steady-state MATLAB model validated against the literature.

A.1.2. Steady-State Gas Network Model Code

A.1.2.1 Main Script

```
clear all

clc
```

Gas Constants

```
D = [160; 160; 110; 110; 110; 110; 110; 80; 80; 80; 80; 80; 80; 80; 160]; %Pipe Diameters (mm)

L = [50; 500; 500; 500; 600; 600; 500; 600; 600; 780; 780; 200; 200; 200; 50]; % Pipe lengths (m)

H = [2500 2200 2000 2600 1800 500 2350 550 475 350 200];  %Energy Demand (kJ/s)

Hi = H*((60*60)/1000);

m = 2;

rho = 0.7;

vel= 10;

E = 0.9;

vis = 8*(10^-7);

Tn = 293.7;
```

```
Pn = 1.01;

T = 293.7;

tol = [1^-3;1^-3;1^-3];



methane = 39.9; %GCV methane (MJ/m^3)
methanem = 16.043; %Molecular weight methane

ethane = 69.9; %GCV ethane (MJ/m^3)

ethanem = 30.7; %Molecular weight ethane

propane = 101; %GCV propane (MJ/m^3)

propanem = 44.097; %Molecular weight propane

butane = 133; %GCV butane (MJ/m^3)

butanem = 58.123; %Molecular weight butane

carbond = 44.01; %Molecular weight CO2

hydrogenm = 2.016; %Molecular weight H2

hydrogen = 12.8; %GCV H2 (MJ/m^3)

nitrogen = 28.0134;%Molecular weight N2



GCVng=                                    41.04%0.9*(methane)+
0.06*(ethane)+0.01*(propane)+0.001*(butane);  %GCV  natural  gas
(MJ/m^3)
GCVhng                    =                    0.81*(methane)+
0.054*(ethane)+0.009*(propane)+0.0009*(butane)+0.1*(hydrogen);
%GCV high hydrogen ng (MJ/m^3)

GCVbiong   =   37.40   %0.94*(methane)+   0.05*(hydrogen);   %GCV
biomethane (MJ/m^3)

Sng              =                              (0.9*(methanem)+
0.06*(ethanem)+0.01*(propanem)+0.001*(butanem)+0.005*(carbond)+
0.02*(nitrogen))/29; %Specific gravity natural gas
```

```
Shng                    =                    (0.81*(methanem)+
0.054*(ethanem)+0.009*(propanem)+0.0009*(butanem)+0.1*(hydrogen
m)+0.0045*(carbond)+0.018*(nitrogen))/29; %Specific gravity high
hydrogen ng

Sbiong                          =          (0.94*(methanem)+
0.05*(hydrogenm)+0.025*(carbond)+0.025*(nitrogen))/29; %Specific
gravity biomethane



wobbeng = GCVng/sqrt(Sng); %Wobbe Index natural gas (MJ/m^3)
wobbehng = GCVhng/sqrt(Shng); %Wobbe Index high hydrogen natural
gas (MJ/m^3)

wobbebiong  =  GCVbiong/sqrt(Sbiong);%Wobbe  Index  biomethane
(MJ/m^3)

Qng = Hi/GCVng; %Load demand natural gas (m^3/h)

Qhng = Hi/GCVhng; %Load demand high hydrogen ng (m^3/h)

Qbiong  =  Hi/((GCVbiong+GCVng)/2)  ;  %Load  demand  biomethane
(m^3/h)
```

Initial Estimates

```
A = [-1 0 0 0 0 0 0 0 0 0 0 0 0 0; 1 -1 -1 -1 0 0 0 0 0 0 0 0 0
0; 0 1 0 0 -1 -1 -1 0 0 0 0 0 0; 0 0 1 0 0 0 0 0 -1 0 0 0 0 0;
0 0 0 1 0 0 0 -1 0 0 0 0 0 0; 0 0 0 0 1 0 0 1 0 -1 0 0 0 0; 0 0
0 0 0 1 0 0 1 0 -1 -1 0 0; 0 0 0 0 0 0 1 0 0 1 1 0 0 0; 0 0 0 0
0 0 0 0 0 0 0 1 -1 0; 0 0 0 0 0 0 0 0 0 0 0 0 1 -1; 0 0 0 0 0 0
0 0 0 0 0 0 0 1];

A1= A(2:end ,:);

A1in= pinv(A1);

AT = A.';
```

```
ATin= pinv(-AT);

Q = Qbiong.';

q0 =[1300 620 230 260 135 130 160 35 55 15 25 120 70 30 20];

q=q0;

for i=1:15

    Kl(i)                  =                  (Sng/(32.7184*(10^-
8)))*(0.0044+(0.1913/D(i)))*(L(i)/(D(i)^5));

    dp(i) = Kl(i)*q(i)^2; %change in pressure (delta P) mbar

    c(i) = 0.0044+(0.1913/D(i));

end
```

Solver

```
fi1     =     @(P1)     5.72*10^(-4)*sqrt((((75-P1))*(D(1)^5))/
(c(1)*Sng*L(1)));
fi2     =     @(P1,P2)     5.72*10^(-4)*sqrt((((P1-P2))*(D(2)^5))/
(c(2)*Sng*L(2)));

fi3     =     @(P1,P3)     5.72*10^(-4)*sqrt((((P1-P3))*(D(3)^5))/
(c(3)*Sng*L(3)));

fi4     =     @(P1,P4)     5.72*10^(-4)*sqrt((((P1-P4))*(D(4)^5))/
(c(4)*Sng*L(4)));

fi5     =     @(P2,P5)     5.72*10^(-4)*sqrt((((P2-P5))*(D(5)^5))/
(c(5)*Sng*L(5)));

fi6       =       @(P2,P6)5.72*10^(-4)*sqrt((((P2-P6))*(D(6)^5))/
(c(6)*Sng*L(6)));
```

```
fi7    =    @(P2,P7)    5.72*10^(-4)*sqrt((((P2-P7))*(D(7)^5))/
(c(7)*Sng*L(7)));

fi8      =      @(P4,P5)5.72*10^(-4)*sqrt((((P4-P5))*(D(8)^5))/
(c(8)*Sng*L(8)));

fi9      =      @(P3,P6)5.72*10^(-4)*sqrt((((P3-P6))*(D(9)^5))/
(c(9)*Sng*L(9)));

fi10     =     @(P5,P7)5.72*10^(-4)*sqrt((((P5-P7))*(D(10)^5))/
(c(10)*Sng*L(10)));

fi11     =     @(P6,P7)5.72*10^(-4)*sqrt((((P6-P7))*(D(11)^5))/
(c(11)*Sng*L(11)));

fi12     =     @(P6,P8)5.72*10^(-4)*sqrt((((P6-P8))*(D(12)^5))/
(c(12)*Sng*L(12)));

fi13     =     @(P8,P9)5.72*10^(-4)*sqrt((((P8-P9))*(D(13)^5))/
(c(13)*Sng*L(13)));

fi14    =    @(P9,P10)5.72*10^(-4)*sqrt((((P9-P10))*(D(14)^5))/
(c(14)*Sng*L(14)));

fi15    =    @(P11,P2)5.72*10^(-4)*sqrt((((P11-P2))*(D(15)^5))/
(c(15)*Sng*L(15)));




F1=   @(P1,P2,P3,P4)  fi1(P1)-fi2(P1,P2)-fi3(P1,P3)-fi4(P1,P4)  -
Q(1);
F2=    @(P1,P2,P5,P6,P7,P11)  fi2(P1,P2)-fi5(P2,P5)-fi6(P2,P6)-
fi7(P2,P7)+fi15(P11,P2) - Q(2);

F3=  @(P1,P3,P6) fi3(P1,P3)-fi9(P3,P6)-Q(3);

F4=  @(P1,P4,P5) fi4(P1,P4)-fi8(P4,P5)-Q(4);

F5=  @(P2,P4,P5,P7) fi5(P2,P5)+fi8(P4,P5)-fi10(P5,P7)-Q(5);

F6   =   @(P2,P3,P6,P7,P8)   fi6(P2,P6)+fi9(P3,P6)-fi11(P6,P7)-
fi12(P6,P8) -Q(6);

F7 = @(P2,P5,P6,P7) fi7(P2,P7)+fi10(P5,P7)+fi11(P6,P7)-Q(7);
```

```
F8 = @(P6,P8,P9) fi12(P6,P8)-fi13(P8,P9)-Q(8);

F9 = @(P8,P9,P10) fi13(P8,P9)-fi14(P9,P10) -Q(9);

F10 = @(P9,P10) fi14(P9,P10)-Q(10);

F11 = @(P11,P2) Q(11)-fi15(P11,P2);




fun       =       @(x)               [F1(x(1),x(2),x(3),x(4));
F2(x(1),x(2),x(5),x(6),x(7),x(11));          F3(x(1),x(3),x(6));
F4(x(1),x(4),x(5));                      F5(x(2),x(4),x(5),x(7));
F6(x(2),x(3),x(6),x(7),x(8));F7(x(2),x(5),x(6),x(7));
F8(x(6),x(8),x(9));                           F9(x(8),x(9),x(10));
F10(x(9),x(10));F11(x(11),x(2))]

%inital guess

p1 = 75;

p2 = p1-dp(1);

p3 = p2-dp(2);

p4 = p2-dp(3);

p5 = p2-dp(4);

p6 = p3-dp(5);

p7 = p3-dp(6);

p8 = p3-dp(7);

p9 = p7-dp(12);

p10 = p9-dp(13);

p11 = p10-dp(14);

p12 = p3 +dp(15);



x0 = [p2, p3, p4, p5, p6, p7,p8,p9,p10,p11,p12];
```

```
j= jacobiN(Sng, D, L, c, Q);

J10 = j(x0(1), x0(2), x0(3), x0(4), x0(5), x0(6), x0(7), x0(8),
x0(9), x0(10),x0(11));




options = optimset('TolX',1e-12); % set TolX
[x, resnorm, f, exitflag, output, jacob] = newtonraphson1(fun,
x0,options,j);

fprintf('\nexitflag:  %d,  %s\n',exitflag,  output.message)  %
display output message




xl=[75;(abs(x));0;0;0];
dp1=  [(75-x(1)),  (x(1)-x(2)),(x(1)-x(3)),(x(1)-x(4)),  (x(2)-
x(5)), (x(6)-x(2)), (x(2)-x(7)), (x(4)-x(5)), (x(3)-x(6)),(x(5)-
x(7)), (x(6)-x(7))];



ql(1)        =        5.72*10^(-4)*sqrt((((75-xl(2)))*(D(1)^5))/
(c(1)*Sng*L(1)));
ql(2)    =        5.72*10^(-4)*sqrt((((xl(2)-xl(3)))*(D(2)^5))/
(c(2)*Sng*L(2)));

ql(3)    =        5.72*10^(-4)*sqrt((((xl(2)-xl(4)))*(D(3)^5))/
(c(3)*Sng*L(3)));

ql(4)    =        5.72*10^(-4)*sqrt((((xl(2)-xl(5)))*(D(4)^5))/
(c(4)*Sng*L(4)));

ql(5)    =        5.72*10^(-4)*sqrt((((xl(3)-xl(6)))*(D(5)^5))/
(c(5)*Sng*L(5)));

ql(6)    =        5.72*10^(-4)*sqrt((((xl(3)-xl(7)))*(D(6)^5))/
(c(6)*Sng*L(6)));
```

```
ql(7)    =        5.72*10^(-4)*sqrt((((xl(3)-xl(8)))*(D(7)^5))/
(c(7)*Sng*L(7)));

ql(8)     =          5.72*10^(-4)*sqrt(((xl(5)-xl(6))*(D(8)^5))/
(c(8)*Sng*L(8)));

ql(9)    =        5.72*10^(-4)*sqrt((((xl(4)-xl(7)))*(D(9)^5))/
(c(9)*Sng*L(9)));

ql(10)     =     5.72*10^(-4)*sqrt((((xl(6)-xl(8)))*(D(10)^5))/
(c(10)*Sng*L(10)));

ql(11)     =     5.72*10^(-4)*sqrt((((xl(7)-xl(8)))*(D(11)^5))/
(c(11)*Sng*L(11)));

ql(12)     =     5.72*10^(-4)*sqrt((((xl(7)-xl(9)))*(D(12)^5))/
(c(12)*Sng*L(12)));

ql(13)     =     5.72*10^(-4)*sqrt((((xl(9)-xl(10)))*(D(13)^5))/
(c(13)*Sng*L(13)));

ql(14)    =    5.72*10^(-4)*sqrt((((xl(10)-xl(11)))*(D(14)^5))/
(c(14)*Sng*L(14)));

ql(15)     =     5.72*10^(-4)*sqrt((((xl(12)-xl(3)))*(D(15)^5))/
(c(15)*Sng*L(15)));


pp=[75  66.32  47.77  47.44  42.03  39.30  40.21  38.34  29.03  25.09
24.37 47.80 0 0 0]

qq = [1326 613.33 231.28 262.56 141.64 133.76 163.69 34.51 56.07
17.91 25.05 120.84 72.50 30.76 19.25]


figure (1)
b=[xl,pp.']

m = [ql.',qq.']

bar(b);      xlabel('Node');      ylabel('Pressure      (mbar)');
legend('Model', 'Literature')
```

```
figure (2)
bar(m);     xlabel('Pipe     Number');     ylabel('Flow     rate
(m^3/hr)');legend('Model', 'Literature')



for i=1:15
er (i,1)= (xl(i)-pp(i))/pp(i)*100;

er(i,2) = (ql(i)-qq(i))/qq(i)*100;

end
```

A.1.2.2 Jacobian Function

```
function [j] = jacobiN(Sng, D, L, c,Q,GCVng,GCVbiong)


    syms P1 P2 P3 P4 P5 P6 P7 P8 P9 P10 P11



fi1 =  5.72*10^(-4)*sqrt((((75-P1))*(D(1)^5))/ (c(1)*Sng*L(1)));
fi2 =  5.72*10^(-4)*sqrt((((P1-P2))*(D(2)^5))/ (c(2)*Sng*L(2)));
fi3 =  5.72*10^(-4)*sqrt((((P1-P3))*(D(3)^5))/ (c(3)*Sng*L(3)));
fi4 =  5.72*10^(-4)*sqrt((((P1-P4))*(D(4)^5))/ (c(4)*Sng*L(4)));
fi5 =  5.72*10^(-4)*sqrt((((P2-P5))*(D(5)^5))/ (c(5)*Sng*L(5)));
fi6 =  5.72*10^(-4)*sqrt((((P2-P6))*(D(6)^5))/ (c(6)*Sng*L(6)));
fi7 =  5.72*10^(-4)*sqrt((((P2-P7))*(D(7)^5))/ (c(7)*Sng*L(7)));
fi8 =  5.72*10^(-4)*sqrt((((P4-P5))*(D(8)^5))/ (c(8)*Sng*L(8)));
fi9 =  5.72*10^(-4)*sqrt((((P3-P6))*(D(9)^5))/ (c(9)*Sng*L(9)));
fi10 =  5.72*10^(-4)*sqrt((((P5-P7))*(D(10)^5))/ (c(10)*Sng*L(10)));
fi11 = 5.72*10^(-4)*sqrt((((P6-P7))*(D(11)^5))/ (c(11)*Sng*L(11)));
fi12 = 5.72*10^(-4)*sqrt((((P6-P8))*(D(12)^5))/ (c(12)*Sng*L(12)));
fi13 =  5.72*10^(-4)*sqrt((((P8-P9))*(D(13)^5))/ (c(13)*Sng*L(13)));
fi14          =          5.72*10^(-4)*sqrt((((P9-P10))*(D(14)^5))/
(c(14)*Sng*L(14)));
fi15       =             5.72*10^(-4)*sqrt((((P11-P2))*(D(14)^5))/
(c(14)*Sng*L(14)));



F1= (-fi1+fi2+fi3+fi4)+Q(1);
```

```
F2= (-fi2+fi5+fi6+fi7-fi15)+Q(2);
F3= (-fi3+fi9)+Q(3);
F4= (-fi4+fi8)+Q(4);
F5= (-fi5-fi8-fi10)+Q(5);
F6= (-fi6-fi9+fi11+fi12)+Q(6);
F7= (-fi7+fi10+fi11)+Q(7);
F8= (-fi12+fi13)+Q(8);
F9= (-fi13+fi14)+Q(9);
F10=(-fi14)+Q(10);
F11 = (-fi15+Q(11));



J                          =                          [diff(F1,P1),
diff(F1,P2),diff(F1,P3),diff(F1,P4),diff(F1,P5),diff(F1,P6),diff(F1
,P7),diff(F1,P8),diff(F1,P9),diff(F1,P10),diff(F1,P11);...
    diff(F2,P1),
diff(F2,P2),diff(F2,P3),diff(F2,P4),diff(F2,P5),diff(F2,P6),diff(F2
,P7),diff(F2,P8),diff(F2,P9),diff(F2,P10),diff(F2,P11);...
    diff(F3,P1),
diff(F3,P2),diff(F3,P3),diff(F3,P4),diff(F3,P5),diff(F3,P6),diff(F3
,P7),diff(F3,P8),diff(F3,P9),diff(F3,P10),diff(F3,P11);...
    diff(F4,P1),
diff(F4,P2),diff(F4,P3),diff(F4,P4),diff(F4,P5),diff(F4,P6),diff(F4
,P7),diff(F4,P8),diff(F4,P9),diff(F4,P10),diff(F4,P11);...
    diff(F5,P1),
diff(F5,P2),diff(F5,P3),diff(F5,P4),diff(F5,P5),diff(F5,P6),diff(F5
,P7),diff(F5,P8),diff(F5,P9),diff(F5,P10),diff(F5,P11);...
    diff(F6,P1),
diff(F6,P2),diff(F6,P3),diff(F6,P4),diff(F6,P5),diff(F6,P6),diff(F6
,P7),diff(F6,P8),diff(F6,P9),diff(F6,P10),diff(F6,P11);...
    diff(F7,P1),
diff(F7,P2),diff(F7,P3),diff(F7,P4),diff(F7,P5),diff(F7,P6),diff(F7
,P7),diff(F7,P8),diff(F7,P9),diff(F7,P10),diff(F7,P11);...
    diff(F8,P1),
diff(F8,P2),diff(F8,P3),diff(F8,P4),diff(F8,P5),diff(F8,P6),diff(F8
,P7),diff(F8,P8),diff(F8,P9),diff(F8,P10),diff(F8,P11);...
    diff(F9,P1),
diff(F9,P2),diff(F9,P3),diff(F9,P4),diff(F9,P5),diff(F9,P6),diff(F9
,P7),diff(F9,P8),diff(F9,P9),diff(F9,P10),diff(F9,P11);...
```

```
    diff(F10,P1),
diff(F10,P2),diff(F10,P3),diff(F10,P4),diff(F10,P5),diff(F10,P6),di
ff(F10,P7),diff(F10,P8),diff(F10,P9),diff(F10,P10),diff(F10,P11);..
.
    diff(F11,P1),
diff(F11,P2),diff(F11,P3),diff(F11,P4),diff(F11,P5),diff(F11,P6),di
ff(F11,P7),diff(F11,P8),diff(F11,P9),diff(F11,P10),diff(F11,P11)];

j = matlabFunction(J);
end
```

A.1.3 Dynamic Model

Figure A.1-4: Diagram of the sample dx network branch modelled in dynamic simulation. shows the diagram for the sample branch of a Dx network, which is modelled under dynamic conditions.

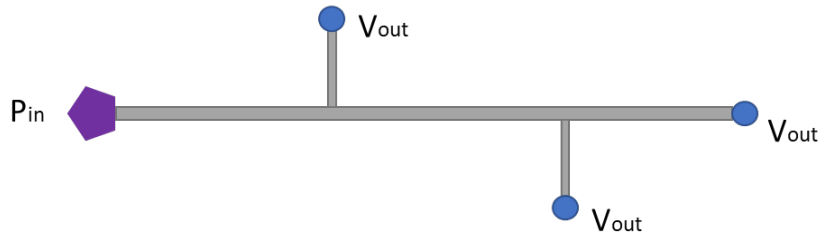

Figure A.1-4: Diagram of the sample dx network branch modelled in dynamic simulation.

Unsteady gas dynamics in a pipeline are governed by Euler equations or compressibility, which include the mass conservation Equation A-9, the momentum balance Equation A-10 and the energy conservation equation. However for this analysis it is assumed that that the gas flow is isothermal, which substitutes the energy conservation equation [82].

Equation A-9: Mass conservation equation.

$$\frac{\partial \rho}{\partial t} + \frac{\partial (\rho u)}{\partial x} = 0$$

Equation A-10: Momentum balance equation.

$$\frac{\partial (\rho u)}{\partial t} + \frac{\partial (\rho u^2)}{\partial x} + \frac{\partial p}{\partial x} + \lambda \rho \frac{u|u|}{2D} + \rho g \sin\theta = 0$$

where u is the gas velocity, ρ is the gas density, p is the pressure, g is the gravitational force, θ is the angle of pipe elevation, λ is the pipe friction factor and D is the internal pipeline diameter.

Assuming that the elevation of the pipe is zero and using Equation A-11, Equation A-12 and Equation A-13 the partial differential equations in Equation A-14 can be derived. [83].

Equation A-11: Equation of state for compressible gases.

$$P = \rho ZRT$$

Equation A-12: Gas velocity expressed in terms of the volumetric flowrate.

$$u = \frac{Q}{A}$$

Equation A-13: The Hofer formula for friction factor.

$$\lambda = \left[2\log_{10}\left(\frac{4.518}{Re}\log_{10}\frac{Re}{7} + \frac{\varepsilon}{3.71D}\right)\right]^{-2}$$

Equation A-14: Partial differential equations used in MATLAB model.

$$\frac{\partial P}{\partial t} = -\frac{P}{A}\left(\frac{\partial Q}{\partial x}\right)$$

$$\frac{\partial Q}{\partial t} = -\frac{\partial P}{\partial x}\left(\frac{ZRTA}{P}\right) - \frac{2\lambda Q|Q|}{ZRTDA}$$

where, Z is the gas compressibility factor, R is the gas constant, T is the temperature, Q is the volumetric flowrate, A is the cross-sectional area of the pipe, Re is the Reynolds number, and ε is the surface roughness.

The system is solved using the ode15s solver, which is a stiff ode solver function in MATLAB based on numerical differentiation formulas.

Figure A.1-5 shows the resultant pressure variation for the dx network branch simulated.

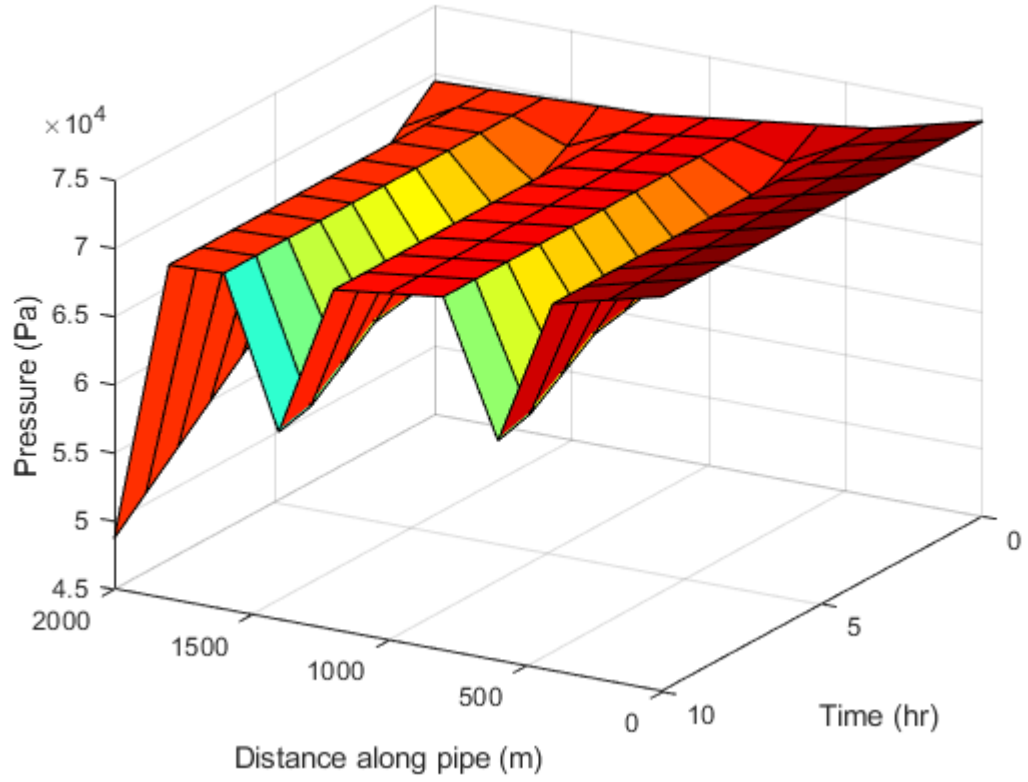

Figure A.1-5: Pressure results of the dynamic dx network model.

A.1.4 Dynamic Gas Network Model Code

A.1.4.1 Main Script

```
clc
clear all
R                          =                          (0.9*(518.28)+
0.06*(276.51)+0.01*(188.56)+0.001*(143.05)+0.005*(188.92)+0.02*(296
.8));  %specific mass gas constant (m^3 Pa K^-1 Kg^-1)
T = 294; %temperature (K)
D = 600*10^-3;  %pipe diameter (m)
rho0 = 1.225;    %air density (kg/m^3);
x= linspace(0,2000,11); %Distance (m)
tspan=[0 1 2 3 4 5 6 7 8 9 10]*60*60;%time (s)
ts =[0 1 2 3 4 5 6 7 8 9 10]*60*60 ;
Pmax = 75*10^6; %maximum pressure (Pa)

methane = 39.9; %GCV methane (MJ/m^3)
methanem = 16.043; %Molecular weight methane
ethane = 69.9; %GCV ethane (MJ/m^3)
ethanem = 30.7; %Molecular weight ethane
```

```
propane = 101; %GCV propane (MJ/m^3)
propanem = 44.097; %Molecular weight propane
butane = 133; %GCV butane (MJ/m^3)
butanem = 58.123; %Molecular weight butane
carbond = 44.01; %Molecular weight CO2
hydrogenm = 2.016; %Molecular weight H2
hydrogen = 12.8; %GCV H2 (MJ/m^3)
nitrogen = 28.0134;%Molecular weight N2

GCVngka=                                          0.904*(methane)+
0.0329*(ethane)+0.0093*(propane)+0.0049*(butane); %GCV natural gas
(MJ/m^3)
GCVngGa=                                        0.7908*(methane)+
0.0091*(ethane)+0.0036*(propane)+0.027*(butane); %GCV natural gas
(MJ/m^3)
GCVngkh=                                          0.986*(methane)+
0.0059*(ethane)+0.0009*(propane)+0.0006*(butane); %GCV natural gas
(MJ/m^3)
GCVngPa=                                           0.87*(methane)+
0.054*(ethane)+0.017*(propane)+0.0075*(butane); %GCV natural gas
(MJ/m^3)
GCVngBi=                                        0.8001*(methane)+
0.0138*(ethane)+0.00049*(propane)+0.0099*(butane); %GCV natural gas
(MJ/m^3)
GCVhng                        =                    0.81*(methane)+
0.054*(ethane)+0.009*(propane)+0.0009*(butane)+0.1*(hydrogen);
%Specific gravity high hydrogen ng
GCVbiong    =  0.94*(methane)+  0.05*(hydrogen); %Specific gravity
biomethane
a= [0.904 0.0329 0.0093 0.0049 0 0.0448 0;...
    0.7908 0.0091 0.0036 0.027 0.0708 0.0514 0;...
    0.986  0.0059 0.0009 0.0006 0 0.0055 0;...
    0.87 0.054 0.017 0.0075 0.0171 0.031 0; ...
    0.8001 0.0138 0.00049 0.0099 0.0841 0.0541 0;...
    0.81 0.054 0.009 0.0009 0.0045 0.018 0.1;...
    0.94 0 0 0 0.025 0.025 0.05];
```

```
gka                                                                =
(0.904*(methanem)+0.0329*(ethanem)+0.0093*(propanem)+0.0049*(butane
m)+0.0448*(nitrogen))/29; %Specific gravity natural gas
gGa=                                                (0.7908*(methanem)+
0.0091*(ethanem)+0.0036*(propanem)+0.027*(butanem)+0.0708*(carbond)
+0.0514*(nitrogen))/29;  %Specific gravity natural gas
gkh=                                                 (0.986*(methanem)+
0.0059*(ethanem)+0.0009*(propanem)+0.0006*(butanem)+0.00*(carbond)+
0.0055*(nitrogen))/29;  %Specific gravity natural gas
gPa=                                                  (0.87*(methanem)+
0.054*(ethanem)+0.017*(propanem)+0.0075*(butanem)+0.0171*(carbond)+
0.031*(nitrogen))/29;  %Specific gravity natural gas
gBi=                                                (0.8001*(methanem)+
0.0138*(ethanem)+0.00049*(propanem)+0.0099*(butanem)+0.0841*(carbon
d)+0.0541*(nitrogen))/29;  %Specific gravity natural gas
gGhng                        =                       (0.81*(methanem)+
0.054*(ethanem)+0.009*(propanem)+0.0009*(butanem)+0.1*(hydrogenm)+0
.0045*(carbond)+0.018*(nitrogen))/29;   %Specific   gravity   high
hydrogen ng
gGbiong                                =              (0.94*(methanem)+
0.05*(hydrogenm)+0.025*(carbond)+0.025*(nitrogen))/29;    %Specific
gravity biomethane

G=[gka,gGa,gkh,gPa,gBi,gGhng,gGbiong];

ka                                                                 =
0.904*(methane)+0.0329*(ethane)+0.0093*(propane)+0.0049*(butane);
Ga=                                                 0.7908*(methane)+
0.0091*(ethane)+0.0036*(propane)+0.027*(butane);
kh=                                                  0.986*(methane)+
0.0059*(ethane)+0.0009*(propane)+0.0006*(butane);
Pa= 0.87*(methane)+ 0.054*(ethane)+0.017*(propane)+0.0075*(butane);
Bi=                                                 0.8001*(methane)+
0.0138*(ethane)+0.00049*(propane)+0.0099*(butane);
Ghng                          =                       0.81*(methane)+
0.054*(ethane)+0.009*(propane)+0.0009*(butane)+0.1*(hydrogen);
Gbiong  = 0.94*(methane)+ 0.05*(hydrogen);

GC = [ka,Ga,kh,Pa,Bi,Ghng,Gbiong];
n(1) = 1;
```

```
k(1)=100;
    Gng(1)=G(1);
    HHV(1)=GC(1);
    rho(1) = Gng(1)*rho0;
   meu_cp(1)              =              (0.0107*0.9*sqrt(methanem)+
0.06*0.06*sqrt(ethanem)+0.0075*0.01*sqrt(propanem)+0.0073*0.001*sqr
t(butanem)+0.0147*0.005*sqrt(carbond)+0.0173*0.02*sqrt(nitrogen))/(
0.9*sqrt(methanem)+
0.06*sqrt(ethanem)+0.01*sqrt(propanem)+0.001*sqrt(butanem)+0.005*sq
rt(carbond)+0.02*sqrt(nitrogen)); %dynamic viscosity (cp)
 meu(1) = meu_cp(1)*10^-3; %dynamic viscosity (kg/m-s)

for i =2:11
    n(i) = randi([1 7],1,1);
    k(i) = randi([25 100],1,1);

    Ggng(i)=                 (a(n(i-1),1)*a(n(i),1)*methanem+a(n(i-
1),2)*a(n(i),2)*ethanem+a(n(i-1),3)*a(n(i),3)*propanem+a(n(i-
1),4)*a(n(i),4)*butanem+a(n(i-1),5)*a(n(i),5)*carbond+a(n(i-
1),6)*a(n(i),6)*nitrogen+a(n(i-1),7)*a(n(i),7)*hydrogenm)/29;
    GCng(i)=                   a(n(i-1),1)*a(n(i),1)*methane+a(n(i-
1),2)*a(n(i),2)*ethane+a(n(i-1),3)*a(n(i),3)*propane+a(n(i-
1),4)*a(n(i),4)*butane+a(n(i-1),7)*a(n(i),7)*hydrogen;

    Gng(i)=((100-k(i))/100)*(sqrt(G(n(i-
1))*G(n(i))))+(k(i)/100)*(sqrt(G(n(i-1))*G(n(i))));
    HHV(i)=((100-k(i))/100)*(sqrt(GC(n(i-
1))*GC(n(i))))+(k(i)/100)*(sqrt(GC(n(i-1))*GC(n(i))));
    rho(i) = Gng(i)*rho0;  %gas density (kg/m^3)

 meu_cp(i)              =              (0.0107*((a(n(i-1),1)*(100-
k(i))/100)+a(n(i),1)*(k(i)/100))*sqrt(methanem)+    0.0089*((a(n(i-
1),2)*(100-
k(i))/100)+a(n(i),2)*(k(i)/100))*sqrt(ethanem)+0.0075*((a(n(i-
1),3)*(100-
k(i))/100)+a(n(i),3)*(k(i)/100))*sqrt(propanem)+0.0073*((a(n(i-
1),4)*(100-
k(i))/100)+a(n(i),4)*(k(i)/100))*sqrt(butanem)+0.0147*((a(n(i-
1),5)*(100-
k(i))/100)+a(n(i),5)*(k(i)/100))*sqrt(carbond)+0.0173*((a(n(i-
```

```
1),6)*(100-
k(i))/100)+a(n(i),6)*(k(i)/100))*sqrt(nitrogen))/(((a(n(i-
1),1)*(100-k(i))/100)+a(n(i),1)*(k(i)/100))*sqrt(methanem)+
((a(n(i-1),2)*(100-
k(i))/100)+a(n(i),2)*(k(i)/100))*sqrt(ethanem)+((a(n(i-1),3)*(100-
k(i))/100)+a(n(i),3)*(k(i)/100))*sqrt(propanem)+((a(n(i-1),4)*(100-
k(i))/100)+a(n(i),4)*(k(i)/100))*sqrt(butanem)+((a(n(i-1),5)*(100-
k(i))/100)+a(n(i),5)*(k(i)/100))*sqrt(carbond)+((a(n(i-1),6)*(100-
k(i))/100)+a(n(i),6)*(k(i)/100))*sqrt(nitrogen));          %dynamic
viscosity (cp)
 meu(i) = meu_cp(i)*10^-3; %dynamic viscosity (kg/m-s)
end


 Q = [0,0,0,175,0,0,0,192,0,0,0]; %volumetric demand (m^3/hr)
 E = [0,0,0,-2000,0,0,0,-2200,0,0,-2500;...
     0,0,0,-1800,0,0,0,-2000,0,0,-2500;...
     0,0,0,-1500,0,0,0,-1700,0,0,-2500;...
     0,0,0,-1400,0,0,0,-1500,0,0,-2500;...
     0,0,0,-1000,0,0,0,-1200,0,0,-2500;...
     0,0,0,-800,0,0,0,-700,0,0,-2500;...
     0,0,0,-600,0,0,0,-700,0,0,-2500;...
     0,0,0,-600,0,0,0,-500,0,0,-2500;...
     0,0,0,-2000,0,0,0,-2200,0,0,-2500;...
     0,0,0,-2000,0,0,0,-2200,0,0,-2500;...
     0,0,0,-800,0,0,0,-700,0,0,-2500;...
     0,0,0,-600,0,0,0,-500,0,0,-2500;...
     0,0,0,-600,0,0,0,-500,0,0,-2500]; %Energy Demand (MJ/s)

 E = E/1000;
 S  = (pi()*(D)^2)/4; %pipe cross section (m^2)

 Qin = sum(Q)+219;
 pin = 0.75;%pressure (Pa)

Ein = 0.5-sum(E(1,:));

 for i=1:11
 Q0(i) = Qin-Q(i);
 Qin = Q0(i);
```

```
 E0(i) =Ein +E(1,i);
 Ein = E0(i);

 f= 0.0044*(1+(12/(0.0276*(D*10^3))));
 dp(i)                    =                    ((Q0(i)/(5.72*10^-
4)).^2).*(f*Ggng(2)*(x(2)))/((D*10^3)^5);
 p0(i) = pin-dp(i);
 pin=p0(i);
 Ql(i) = (sum(-E(i,:)+0.5)*10^3)/HHV(1);
 end
 P0 = p0*10^5

 J0 = [Q0,P0].';
 WI = HHV(1)/(sqrt(rho(1)/rho0)); %Wobbe Index (MJ/Sm^3)
 m=1;
 opts = odeset('RelTol',1e-3,'AbsTol',1e-3);
 [t,J,u]                    =                    ode15s(@(t,J)
odefcnn(t,J,D,R,T,S,HHV,rho,meu,Gng,x,Ggng,E,ts,Ql),tspan,J0,opts);
Presult = J(:,12:end);
Qresult =J(:,1:11);
t=t/3600
figure (1)
surf(x,t, Qresult); xlabel('Distance along pipe (m)');  ylabel('Time
(hr)');zlabel('Flow rate (KJ/s)');
colormap(jet);

figure (2)
surf(x,t,Presult); xlabel('Distance along pipe (m)'); ylabel('Time
(hr)'); zlabel('Pressure (Pa)');
colormap(jet)
```

A.1.4.2 ODE Function

```
function dydt = odefcnn(t,J,D,R,T,S,HHV,rho,meu,Gng,x,Ggng,E,ts,Ql)

if t<= ts(1)
    c=1;
elseif t<= ts(2)
```

```
    c=2;
elseif t<= ts(3)
    c=3;
elseif t<= ts(4)
    c=4;
elseif t<= ts(5)
    c=5;
elseif t<= ts(6)
    c=6;
elseif t<= ts(7)
    c=7;
elseif t<= ts(8)
    c=8;
elseif t<= ts(9)
    c=9;
elseif t<=ts(10)
    c=10;
elseif t<=ts(11)
    c=11;
else
    c=12

end
pc = (709.604-58.718*Gng(1))*6894.76;      %pseudo-critical reduced
pressure (Pa)
Tc = (170.491+307.344*Gng(1))*0.556;      %pseudo-critical reduced
temperature (K)

 pr=J(12:22)/pc;
 Tr=T/Tc;
 deltax = 200;     %change in distance (m)

h= (-3.52*pr).*(exp(1)^(-2.26*Tr));
a=((0.274.*(pr.^2)).*(exp(1)^(-1.87*Tr)));
z= 1+h+a;  %compressiblity factor

 dydt = zeros(2,1);

 deltaE = E(c,:); %[0;J(2)-J(1);J(3)-J(2);J(4)-J(3);J(5)-J(4);J(6)-
J(5); J(7)-J(6);J(8)-J(7);J(9)-J(8);J(10)-J(9);J(11)-J(10)];
```

```
 deltaQ= ((deltaE*10^3)/HHV(1)).';
 Pi= 0.75;
    Qin =Ql(1);
  for i=1:11
   Q(i)=Qin+deltaQ(i);
   Qin=Q(i);

 f= 0.0044*(1+(12/(0.0276*(D*10^3))));
 dp1(i)                  =                  (((deltaQ(i))/(5.72*10^-
4)).^2).*(f*Ggng(2)*(x(2)))/((D*10^3)^5);
 Pb(i)= Pi-dp1(i);
 dp=Pb(i);
  end
  Q=Q.'
   P=(Pb*10^5).';

 deltap = [dp1.'];

 e  = 0.045*10^-3; %surface roughness (m)
 u= ((Q/S)); %gas velocity (m^3/s)
 Re = (u.*D*rho(c))./meu(c);     %Reynolds number

 lambda = (2.*log10((4.518./Re).*log10(Re./7)+(e/(3.71*D)))).^(-2);
%friction factor

  v =  (deltaQ/deltax);
  b= ((z.*R*T*S)./(P)).*(deltap./deltax);
  h = (2*(lambda).*(Q.*abs(Q)))./(z.*R*T*S*D);
  m = P.*v;

 dydt(1:11) = b+(h);

 dydt(12:22) = (1./(z.*R*T*S)).*(m);

   g =isreal(J);
  if g==0
  disp(J)
  error('is complex')
 end
end
```

A.2 Additional results of Synergi Dx network simulation

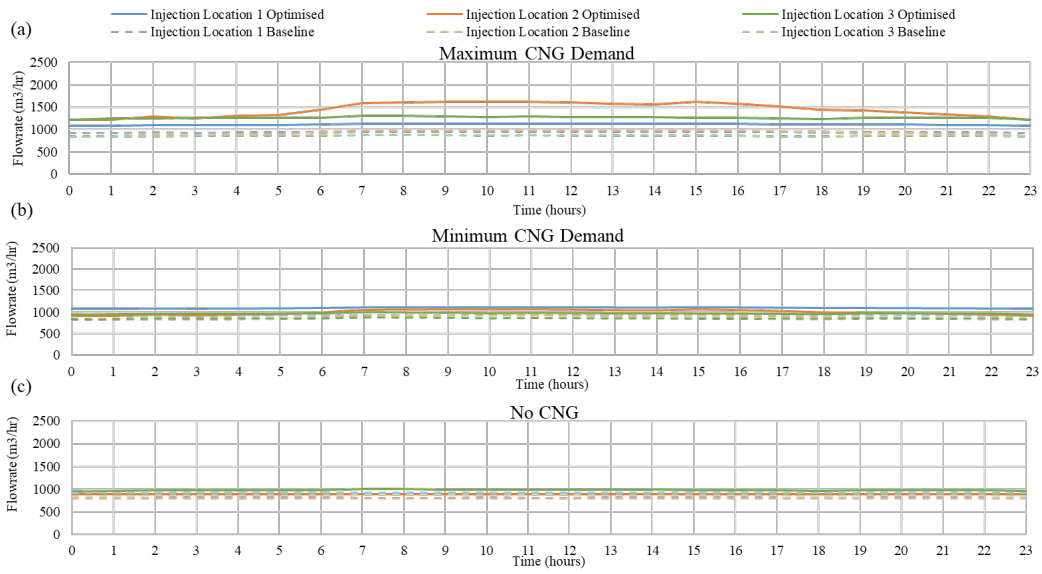

Figure A.2-1: Results for the minimum demand day scenario with (a) the minimum CNG demand, (b) maximum CNG demand, and (c) no CNG demand, for the candidate biomethane injection facility at Location 1 (blue), Location 2(orange) and Location 3(green).

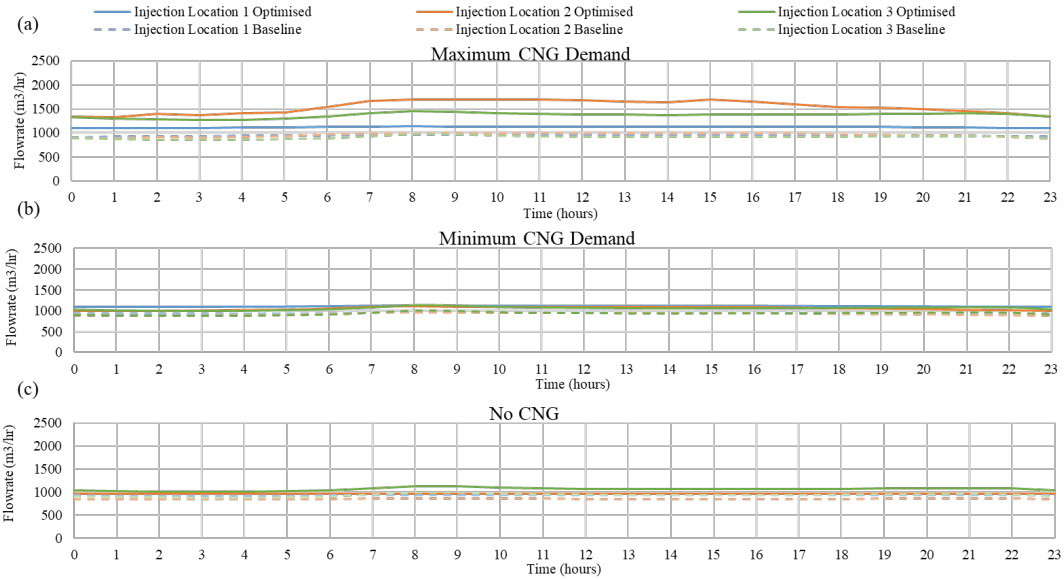

Figure A.2-2: Results for the average demand day scenario with (a) the minimum CNG demand, (b) maximum CNG demand, and (c) no CNG demand, for the candidate biomethane injection facility at Location 1 (blue), Location 2(orange) and Location 3(green).

References

[1] Untied Nations Framework Convention on Climate Change , “The Paris Agreement,” 2015. [Online]. Available: https://unfccc.int/process-and-meetings/the-paris-agreement/the-paris-agreement. [Accessed 04 05 2022].

[2] European Comission , “The European Green Deal,” 11 December 2019. [Online]. Available: https://eur-lex.europa.eu/resource.html?uri=cellar:b828d165-1c22-11ea-8c1f-01aa75ed71a1.0002.02/DOC_1&format=PDF. [Accessed 2022 April 11].

[3] Energy Transition Commission, “Making Mission Possible - Delivering a Net - Zero Economy,” September 2020. [Online]. Available: https://www.energy-transitions.org/wp-content/uploads/2020/09/Making-Mission-Possible-Executive-Summary-English.pdf.

[4] D. M. Wall, M. Dumont and J. D. Murphy, GREEN GAS Facilitating a future green gas grid through the production of renewable gas IEA Bioenergy Task 37 Green Gas Facilitating a future green gas grid through the production of renewable gas, 2018.

[5] International Energy Agency, “Key World Energy Statistics 2021,” 2021. [Online]. Available: https://www.iea.org/reports/key-world-energy-statistics-2021/supply.

[6] Speirs J., Jalil Vega F., Cooper J., Gerber Machado P., Giarola S., Brandon N. and Hawkes A., “The flexibility of gas: what is it worth?,” 2020.

[7] J. Speirs, P. Balcombe, E. Johnson, J. Martin, N. Brandon and A. Hawkes, “A greener gas grid: What are the options,” *Energy Policy,* vol. 118, pp. 291-297, 1 7 2018.

[8] Gas Initiative Green, “Gas and gas infrastructure – the green commitment,” 2016. [Online]. Available: https://www.greengasinitiative.eu/.

[9] European Comission , “REPowerEU: Joint European action for more affordable, secure and sustainable energy,” 2022. [Online]. Available: https://ec.europa.eu/commission/presscorner/detail/en/ip_22_1511.

[10] Sustainable Energy Authority of Ireland, “Energy in Ireland 2021,” 2021. [Online]. Available: https://www.seai.ie/publications/Energy-in-Ireland-2021_Final.pdf.

[11] D. Dineen, M. Howley and B. Ó Cléirigh, “ENERGY SECURITY IN IRELAND 2020 Report”.

[12] . Gas Networks Ireland, “Network Development Plan 2020,” 2020.

[13] R. O'Shea, I. Kilgallon, D. Wall and J. D. Murphy, “Quantification and location of a renewable gas industry based on digestion of wastes in Ireland,” *Applied Energy,* vol. 175, 2016.

[14] R. O'Shea, D. M. Wall, I. Kilgallon, J. D. Browne and J. D. Murphy, “Assessing the total theoretical, and financially viable, resource of biomethane for injection to a natural gas network in a region,” *Applied Energy,* vol. 188, pp. 237-256, 15 2 2017.

[15] Gas Networks Ireland, “GRAZE Gas Project,” [Online]. Available: https://www.teagasc.ie/media/website/publications/2021/Renewable-gas-and-the-Mitchelstown-Central-Grid-Injection-facility.pdf.

[16] NGV Journal, “Worldwide NGV Statistics,” [Online]. Available: http://www.ngvjournal.com/worldwide-ngv-statistics/. [Accessed 4 December 2020].

[17] NGVA Europe, [Online]. Available: https://www.ngva.eu/stations-map/. [Accessed 6th May 2020].

[18] D. Styles, E. M. Dominguez and D. Chadwick, “Environmental balance of the UK biogas sector: An evaluation by consequential life cycle assessment,” 2016.

[19] P. Börjesson, M. Lantz, J. Andersson, L. Björnsson, B. Fredriksson Möller, M. Fröberg, C. Hulteberg, E. Iverfeldt, J. Lundgren, A. Röj, H. Svensson and E. Zinn, “METHANE AS VEHICLE FUEL-A WELL-TO-WHEEL ANALYSIS (METDRIV),” 2016. [Online]. Available: www.f3centre.se.

[20] A. E. van den Oever, G. Cardellini, B. F. Sels and M. Messagie, *Life cycle environmental impacts of compressed biogas production through anaerobic digestion of manure and municipal organic waste,* vol. 306, Elsevier, 2021, p. 127156.

[21] I. D'Adamo, P. M. Falcone, D. Huisingh and P. Morone, *A circular economy model based on biomethane: What are the opportunities for the municipality of Rome and beyond?,* vol. 163, Pergamon, 2021, pp. 1660-1672.

[22] F. Ardolino, F. Parrillo and U. Arena, *Biowaste-to-biomethane or biowaste-to-energy? An LCA study on anaerobic digestion of organic waste,* vol. 174, Elsevier, 2018, pp. 462-476.

[23] P. Tratzi, M. Torre, V. Paolini, L. Tomassetti, C. Montiroli, E. Manzo and F. Petracchini, "Liquefied biomethane for heavy-duty transport in Italy: A well-to-wheels approach," Pergamon, 2022.

[24] D. A. Hagos and E. Ahlgren, "A state-of-the art review on the development of CNG/LNG infrastructure and natural gas vehicles (NGVs)," 2018.

[25] Ricardo Energy & Environment, "The role of natural gas and biomethane in the transport sector," 2016.

[26] M. Gustafsson and N. Svensson, "Cleaner heavy transports – Environmental and economic analysis of liquefied natural gas and biomethane," Elsevier, 2021.

[27] European Comission, "DIRECTIVES DIRECTIVE (EU) 2018/2001 OF THE EUROPEAN PARLIAMENT AND OF THE COUNCIL of 11 December 2018 on the promotion of the use of energy from renewable sources (recast) (Text with EEA relevance)".

[28] Gas Networks Ireland, "The Causeway Project," [Online]. Available: https://www.gasnetworks.ie/business/natural-gas-in-transport/the-causeway-project/. [Accessed 18 August 2020].

[29] European Comission, "Directive 2009/28/EC of the european parliament and of the council of 23 april 2009, vol. 140 (2009), 10.3000/17252555.L_2009.140.eng".

[30] European Commission, "REPORT FROM THE COMMISSION TO THE EUROPEAN PARLIAMENT, THE COUNCIL, THE EUROPEAN ECONOMIC AND SOCIAL COMMITTEE AND THE COMMITTEE OF THE REGIONS. Renewable Energy Progress Report," 14 October 2020. [Online]. Available: https://ec.europa.eu/energy/sites/ener/files/renewable_energy_progress_report_com_2020_952.pdf.

[31] B.-Ș. Zăbavă, G. Voicu and N. Ungureanu, "METHODS OF BIOGAS PURIFICATION-A REVIEW Incineration of municipal waste View project Conservative tillage technology View project".

[32] M. A. Voelklein, D. Rusmanis and J. D. Murphy, "Biological methanation: Strategies for in-situ and ex-situ upgrading in anaerobic digestion," 2 2019. [Online].

[33] J. D. Murphy, J. Browne, E. Allen and C. Gallagher, “The resource of biomethane, produced via biological, thermal and electrical routes, as a transport biofuel,” *Renewable Energy,* vol. 55, pp. 474-479, 2013.

[34] C. J. Quarton and S. Samsatli, “Power-to-gas for injection into the gas grid: What can we learn from real-life projects, economic assessments and systems modelling?,” *Renewable and Sustainable Energy Reviews,* vol. 98, pp. 302-316, 2018.

[35] A. Long and J. D. Murphy, “Can green gas certificates allow for the accurate quantification of the energy supply and sustainability of biomethane from a range of sources for renewable heat and or transport?,” *Renewable and Sustainable Energy Reviews,* vol. 115, p. 109347, 1 11 2019.

[36] IEA, Paris, “IEA (2019), World Energy Outlook 2019,” 2019. [Online]. Available: https://www.iea.org/reports/world-energy-outlook-2019.

[37] International Energy Agency, “Key World Energy Statistics 2019,” 2019. [Online]. Available: https://www.iea.org/reports/key-world-energy-statistics-2019.

[38] S. Folga, “Natural Gas Pipeline Technology Overview,” 2007.

[39] ENTSOG, “ENTSOG 2050 ROADMAP FOR GAS GRIDS,” 2019.

[40] Council of European Energy Regulators, “6 TH CEER BENCHMARKING REPORT ON THE QUALITY OF ELECTRICITY AND GAS SUPPLY-2016,” 2016.

[41] Gas Networks Ireland, “A look at the Irish Gas Market,” 2017.

[42] European Committee for Standardization, “CEN/TC 408-European Committee for Standardization (CEN), Natural Gas and Biomethane for Use in Transport and Biomethane for Injection in the Natural Gas Grid (2017),” [Online]. Available: https://standards.cen.eu/dyn/www/f?p=204:7:0::::FSP_ORG_ID:853454&cs=174897F88F3A6DE65FFC3CA2671DBF515.

[43] University of Miskolc; Hungarian Scientific Society of Energy Economics, “A register of all gas regulations and norms concerning the necessary gas quality for allowing the transport in the natural gas grid.,” 2008.

[44] ENTSOG, “Position Paper : A flexible approach for handling different and varying gas qualities,” 2018.

[45] K. Altfeld and D. Pinchbeck, “Admissible Hydrogen Concentrations in Natural Gas Systems”.

[46] . ENTSOG, “Technical paper on the injection of biogas into the natural gas networks,” 2011.

[47] J. Ohemeng-Ntiamoah and T. Datta, “Perspectives on variabilities in biomethane potential test parameters and outcomes: A review of studies published between 2007 and 2018,” *Science of The Total Environment,* vol. 664, pp. 1052-1062, 2019.

[48] M. Aghbashlo, Z. Khounani, H. Hosseinzadeh-Bandbafha, V. K. Gupta, H. Amiri, S. S. Lam, T. Morosuk and M. Tabatabaei, “Exergoenvironmental analysis of bioenergy systems: A comprehensive review,” 10 2021. [Online].

[49] M. Prussi, M. Padella, M. Conton, E. D. Postma and L. Lonza, “Review of technologies for biomethane production and assessment of Eu transport share in 2030,” *Journal of Cleaner Production,* vol. 222, pp. 565-572, 2019.

[50] T. Patterson, S. Esteves, R. Dinsdale and A. Guwy, “An evaluation of the policy and techno-economic factors affecting the potential for biogas upgrading for transport fuel use in the UK,” *Energy Policy,* vol. 39, no. 3, pp. 1806-1816, 2011.

[51] R. O’Shea, R. Lin, D. M. Wall, J. D. Browne and J. D. Murphy, “Distillery decarbonisation and anaerobic digestion: balancing benefits and drawbacks using a compromise programming approach,” 9 2021. [Online].

[52] A. Umar, D. Neagu and J. T. Irvine, “Alkaline modified A-site deficient perovskite catalyst surface with exsolved nanoparticles and functionality in biomass valorisation,” 2021. [Online].

[53] S. K. Sansaniwal, K. Pal, M. A. Rosen and S. K. Tyagi, “Recent advances in the development of biomass gasification technology: A comprehensive review,” 5 2017. [Online].

[54] C. Doczekal and R. Zweiler, “Project 'BIN2GRID' Turning unexploited food waste into biomethane supplied through local filling stations network Grant agreement No: 646560 Report on good practice of biomethane usage as a transportation fuel WP 6-Task 1 / D 6.1,” 2016.

[55] M. Tabatabaei, M. Aghbashlo, E. Valijanian, H. Kazemi Shariat Panahi, A. S. Nizami, H. Ghanavati, A. Sulaiman, S. Mirmohamadsadeghi and K. Karimi, “A comprehensive review on

recent biological innovations to improve biogas production, Part 1: Upstream strategies," 2 2020. [Online].

[56] M. Tabatabaei, M. Aghbashlo, E. Valijanian, H. Kazemi Shariat Panahi, A. S. Nizami, H. Ghanavati, A. Sulaiman, S. Mirmohamadsadeghi and K. Karimi, "A comprehensive review on recent biological innovations to improve biogas production, Part 2: Mainstream and downstream strategies," 2 2020. [Online].

[57] A. Singlitico, J. Goggins and R. F. D. Monaghan, "The role of life cycle assessment in the sustainable transition to a decarbonised gas network through green gas production," 2019. [Online]. Available: http://www.sciencedirect.com/science/article/pii/S1364032118306889.

[58] J. Bekkering, A. A. Broekhuis and W. J. T. van Gemert, "Optimisation of a green gas supply chain – A review," *Bioresource Technology,* vol. 101, no. 2, pp. 450-456, 2010.

[59] R. Ríos-Mercado and C. Boraz-Sánchez, "Optimization problems in natural gas transportation systems: A state-of-the-art review," *Applied Energy,* vol. 147, pp. 536-555, 2015.

[60] J. Bekkering, A. A. Broekhuis, W. J. T. van Gemert and E. J. Hengeveld, "Balancing gas supply and demand with a sustainable gas supply chain – A study based on field data," *Applied Energy,* vol. 111, pp. 842-852, 2013.

[61] J. Bekkering, E. J. Hengeveld, W. J. T. van Gemert and A. A. Broekhuis, "Designing a green gas supply to meet regional seasonal demand – An operations research case study," *Applied Energy,* vol. 143, pp. 348-358, 2015.

[62] J. Browne, A.-S. Nizami, T. Thamsiriroj and J. D. Murphy, "Assessing the cost of biofuel production with increasing penetration of the transport fuel market: A case study of gaseous biomethane in Ireland," *Renewable and Sustainable Energy Reviews,* vol. 15, no. 9, pp. 4537-4547, 1 12 2011.

[63] M. Cavana and P. Leone, "Biogas blending into the gas grid of a small municipality for the decarbonization of the heating sector," *Biomass and Bioenergy,* vol. 127, p. 105295, 1 8 2019.

[64] F. Cucchiella and I. D'Adamo, "Technical and economic analysis of biomethane: A focus on the role of subsidies," *Energy Conversion and Management,* vol. 119, pp. 338-351, 1 7 2016.

[65] F. Cucchiella, I. D'Adamo, M. Gastaldi and M. Miliacca, "A profitability analysis of small-scale plants for biomethane injection

into the gas grid," *Journal of Cleaner Production,* vol. 184, pp. 179-187, 20 5 2018.

[66] L. Gil-Carrera, J. D. Browne, I. Kilgallon and J. D. Murphy, "Feasibility study of an off-grid biomethane mobile solution for agri-waste," *Applied Energy,* vol. 239, pp. 471-481, 2019.

[67] E. Chan Gutiérrez, D. M. Wall, R. O'Shea, R. M. Novelo, M. M. Gómez and J. D. Murphy, "An economic and carbon analysis of biomethane production from food waste to be used as a transport fuel in Mexico," *Journal of Cleaner Production,* vol. 196, pp. 852-862, 20 9 2018.

[68] E. J. Hengeveld, W. J. T. van Gemert, J. Bekkering and A. A. Broekhuis, "When does decentralized production of biogas and centralized upgrading and injection into the natural gas grid make sense?," *Biomass and Bioenergy,* vol. 67, pp. 363-371, 2014.

[69] P. Y. Hoo, H. Hashim, W. S. Ho and N. A. Yunus, "Spatial-economic optimisation of biomethane injection into natural gas grid: The case at southern Malaysia," *Journal of Environmental Management,* vol. 241, pp. 603-611, 2019.

[70] P. Y. Hoo, H. Hashim and W. S. Ho, "Opportunities and challenges: Landfill gas to biomethane injection into natural gas distribution grid through pipeline," *Journal of Cleaner Production,* vol. 175, pp. 409-419, 2018.

[71] R. O'Shea, D. Wall, I. Kilgallon and J. D. Murphy, "Assessment of the impact of incentives and of scale on the build order and location of biomethane facilities and the feedstock they utilise," *Applied Energy,* vol. 182, pp. 394-408, 15 11 2016.

[72] N. Parker, R. Williams, R. Dominguez-Faus and D. Scheitrum, "Renewable natural gas in California: An assessment of the technical and economic potential," *Energy Policy,* vol. 111, pp. 235-245, 2017.

[73] P. Patrizio, S. Leduc, D. Chinese, E. Dotzauer and F. Kraxner, "Biomethane as transport fuel – A comparison with other biogas utilization pathways in northern Italy," *Applied Energy,* vol. 157, pp. 25-34, 2015.

[74] G. A. Von Wald, A. J. Stanion, D. Rajagopal and A. R. Brandt, "Biomethane addition to California transmission pipelines: Regional simulation of the impact of regulations," *Applied Energy,* vol. 250, pp. 292-301, 2019.

[75] C. Gallagher and J. D. Murphy, “What is the realistic potential for biomethane produced through gasification of indigenous Willow or imported wood chip to meet renewable energy heat targets?,” *Applied Energy,* vol. 108, pp. 158-167, 2013.

[76] A. Singlitico, I. Kilgallon, J. Goggins and R. F. Monaghan, “GIS-based techno-economic optimisation of a regional supply chain for large-scale deployment of bio-SNG in a natural gas network,” *Applied Energy,* vol. 250, pp. 1036-1052, 15 9 2019.

[77] E. Wetterlund, S. Leduc, E. Dotzauer and G. Kindermann, “Optimal localisation of biofuel production on a European scale,” *Energy,* vol. 41, no. 1, pp. 462-472, 2012.

[78] M. Abeysekera, J. Wu, N. Jenkins and M. Rees, “Steady state analysis of gas networks with distributed injection of alternative gas,” *Applied Energy,* vol. 164, pp. 991-1002, 15 2 2016.

[79] T. Fubara, F. Cecelja and A. Yang, “Techno-economic assessment of natural gas displacement potential of biomethane: A case study on domestic energy supply in the UK,” *Chemical Engineering Research and Design,* vol. 131, pp. 193-213, 2018.

[80] S. Pellegrino, A. Lanzini and P. Leone, “Greening the gas network – The need for modelling the distributed injection of alternative fuels,” *Renewable and Sustainable Energy Reviews,* vol. 70, pp. 266-286, 2017.

[81] A. Singlitico, K. Dussan, R. O’Shea, D. Wall, J. Goggins, J. D. Murphy and R. F. D. Monaghan, “Can thermal energy recovery from digestate make renewable gas from household waste more cost effective? A case study for the Republic of Ireland,” *Journal of Cleaner Production,* vol. 261, p. 121198, 2020.

[82] G. Guandalini, P. Colbertaldo and S. Campanari, “Dynamic modeling of natural gas quality within transport pipelines in presence of hydrogen injections,” *Applied Energy,* vol. 185, pp. 1712-1723, 2017.

[83] A. Herrán-González, J. M. De La Cruz, B. De Andrés-Toro and J. L. Risco-Martín, “Modeling and simulation of a gas distribution pipeline network,” *Applied Mathematical Modelling,* vol. 33, no. 3, pp. 1584-1600, 3 2009.

[84] A. J. Osiadacz and M. Chaczykowski, “Comparison of isothermal and non-isothermal pipeline gas flow models,” *Chemical Engineering Journal,* vol. 81, no. 1, pp. 41-51, 2001.

[85] A. Tursi, “A review on biomass: Importance, chemistry, classification, and conversion,” 2019. [Online].

[86] J. Sánchez, M. D. Curt, N. Robert and J. Fernández, “Chapter Two - Biomass Resources,” C. Lago, N. Caldés and Y. Lechón, Eds., Academic Press, 2019, pp. 25-111.

[87] P. Haro, F. Johnsson and H. Thunman, “Improved syngas processing for enhanced Bio-SNG production: A techno-economic assessment,” *Energy,* vol. 101, pp. 380-389, 2016.

[88] L. Maggioni and C. Pieroni, “Report on the biomethane injection into national gas grid.,” 2016. [Online]. Available: http://www.isaac-project.it/wp-content/uploads/2017/07/D5.2-Report-on-the-biomethane-injection-into-national-gas-grid.pdf.

[89] Office of Gas and Electricity Markets, “The City CNG Project,” 2015.

[90] G. Collantes and M. W. Melaina, “The co-evolution of alternative fuel infrastructure and vehicles: A study of the experience of Argentina with compressed natural gas,” *Energy Policy,* vol. 39, no. 2, pp. 664-675, 2 2011.

[91] H. Hahn, B. Krautkremer, K. Hartmann and M. Wachendorf, “Review of concepts for a demand-driven biogas supply for flexible power generation,” 1 2014. [Online].

[92] DNV, “Hydraulic modelling and simulation software - Synergi Gas,” DNV, [Online]. Available: https://www.dnv.com/services/hydraulic-modelling-and-simulation-software-synergi-gas-3894. [Accessed 25 03 2021].

[93] Department of Transport, “Trans-European Network for Transport (TEN-T) and Connecting Europe Facility (CEF),” 10 11 2021. [Online]. Available: https://www.gov.ie/en/publication/331b18-trans-european-network-for-transport-ten-t-and-connecting-europe-fac/. [Accessed 2021 12 08].

[94] Transport Infrastructure Ireland, “TII Traffic Data Site,” [Online]. Available: https://www.nratrafficdata.ie/c2/gmapbasic.asp?sgid=ZvyVmXU8jBt9PJE$c7UXt6.

[95] D. Dineen, M. Holland and M. Howley, “ENERGY IN IRELAND 2020 Report,” 2020.

[96] International Organization for Standardization, “Environmental management — Life cycle assessment — Principles and framework. (ISO Standard No. 14040),” 2006.

[97] International Organization for Standardization, “Environmental management — Life cycle assessment — Requirements and guidelines. (ISO Standard No. 14044),” 2006.

[98] N. Keogh, D. Corr and R. Monaghan, “Biogenic Renewable Gas Injection into Natural Gas Grids: A Review of Technical and Economic Modelling Studies. (Manuscript Number: RSER-D-21-01872R1),” *Renewable and Sustainable Energy Review,* Currently Under Review.

[99] N. Parker, R. Williams, R. Dominguez-Faus and D. Scheitrum, “Renewable natural gas in California: An assessment of the technical and economic potential,” *Energy Policy,* vol. 111, pp. 235-245, 2017.

[100] D. M. Wall, E. Allen, B. Straccialini, P. O'Kiely and J. D. Murphy, “Optimisation of digester performance with increasing organic loading rate for mono- and co-digestion of grass silage and dairy slurry,” 12 2014. [Online].

[101] D. M. Wall, P. O'Kiely and J. D. Murphy, “The potential for biomethane from grass and slurry to satisfy renewable energy targets,” 12 2013. [Online].

[102] . Sustainable Energy Authority of Ireland, “ELECTRICITY & GAS PRICES IN IRELAND,” 2020.

[103] DAFF animal by-products section., “Conditionsl for approval and operation of biogas plants treating animal by-products in Ireland.,” 2009.

[104] J. McEniry, P. O'Kiely, P. Crosson, E. Groom and J. D. Murphy, “The effect of feedstock cost on biofuel cost as exemplified by biomethane production from grass silage,” John Wiley & Sons, Ltd, 2011.

[105] F. Bauer, C. Hulteberg, T. Persson and D. Tamm, “Biogas upgrading-Review of commercial technologies (Biogasuppgradering-Granskning av kommersiella tekniker) SGC Rapport 2013:270 "Catalyzing energygas development for sustainable solutions"”.

[106] Irish Water, “Irish Water, Business Billing and Charges,” [Online]. Available: https://www.water.ie/business/billing/charges/. [Accessed 10 08 2021].

[107] Central Statistics Office, “Statistical Yearbook of Ireland 2020,” [Online]. Available: https://www.cso.ie/en/releasesandpublications/ep/p-syi/statisticalyearbookofireland2020/econ/prices/. [Accessed 10 07 2021].

[108] National Oil Reserves Agency (NORA), “Biofuels Obligation Scheme,” [Online]. Available: https://www.nora.ie/biofuels-obligation-scheme.141.html. [Accessed 20 06 2021].

[109] . Department of Agriculture Food and Marine and . Department of Housing Planning and Local Government, “NITRATES EXPLANATORY HANDBOOK for Good Agricultural Practice for the Protection of Waters Regulations 2018,” 2018.

[110] . Sustainable Energy Authority of Ireland, “Anaerobic Digestion for On-farm Uses-Overview,” 2020.

[111] N. Aryal, “Review of Biogas Upgrading,” 2017.

[112] K. Hoyer, C. Hulteberg, M. Svensson, J. J. And and Ø. Nørregård, Biogas upgrading-Technical Review, 2016.

[113] F. Ardolino, G. F. Cardamone, F. Parrillo and U. Arena, “Biogas-to-biomethane upgrading: A comparative review and assessment in a life cycle perspective,” 4 2021. [Online].

[114] J. Gonzales, “Costs Associated With Compressed Natural Gas Vehicle Fueling Infrastructure Factors to consider in the implementation of fueling stations and equipment Margaret Smith, New West Technologies (DOE HQ Technical Support),” 2014.

[115] Central Statistics Office, “CSO Statbank Database,” [Online]. Available: https://www.cso.ie/en/statistics/agriculture/livestocksurveydecember/. [Accessed 07 06 2020].

[116] ESRI, “ArcGIS Pro Release 2.7,” Environmental Systems Research Institute , Redlands CA, 2020.

[117] A. Comber, J. Dickie, C. Jarvis, M. Phillips and K. Tansey, “Locating bioenergy facilities using a modified GIS-based location–allocation-algorithm: Considering the spatial distribution of resource supply,” Elsevier, 2015.

[118] E. Hilsman, “The p-median structure as a unified linear model for location - allocation analysis,” *Environ Plan A,* vol. 16, pp. 305-318, 1984.

[119] M. Berglund and P. Börjesson, “Assessment of energy performance in the life-cycle of biogas production,” *Biomass and Bioenergy,* vol. 30, no. 3, pp. 254-266, 3 2006.

[120] M. Bojesen, M. Birkin and G. Clarke, “Spatial competition for biogas production using insights from retail location models,” *Energy,* vol. 68, pp. 617-628, 4 2014.

[121] S. Dagnall, “UK strategy for centralised anaerobic digestion,” *Bioresource Technology,* vol. 52, no. 3, pp. 275-280, 1 1995.

[122] D. Styles, J. Yesufu, M. Bowman, A. Prysor Williams, C. Duffy and K. Luyckx, *Climate mitigation efficacy of anaerobic digestion in a decarbonising economy,* vol. 338, Elsevier, 2022, p. 130441.

[123] M. Góralczyk, *Life-cycle assessment in the renewable energy sector,* vol. 75, Elsevier, 2003, pp. 205-211.

[124] B. P. Weidema, M. Pizzol, J. Schmidt and G. Thoma, *Attributional or consequential Life Cycle Assessment: A matter of social responsibility,* vol. 174, Elsevier, 2018, pp. 305-314.

[125] Sonnermann.G and Vigon.B, “Global Guidance Principles for Life Cyle Assessment Databases,” UNEP/SETAC Life Cycle Initative, Paris/Pensacola, 2011.

[126] O. Hijazi, S. Munro, B. Zerhusen and M. Effenberger, *Review of life cycle assessment for biogas production in Europe,* vol. 54, Pergamon, 2016, pp. 1291-1300.

[127] C. Beausang, K. McDonnell and F. Murphy, “Assessing the environmental sustainability of grass silage and cattle slurry for biogas production,” Elsevier Ltd, 2021.

[128] T. Rehl and J. Müller, “CO2 abatement costs of greenhouse gas (GHG) mitigation by different biogas conversion pathways,” Academic Press, 2013.

[129] European Commission, “Emissions in the automotive sector,” [Online]. Available: https://single-market-economy.ec.europa.eu/sectors/automotive-industry/environmental-protection/emissions-automotive-sector_en. [Accessed 10 08 2022].

[130] M. Williams and R. Minjares, “A technical summary of Euro 6/VI vehicle emission standards,” 2016.

[131] M. Stettler, M. Woo, D. Ainalis, P. Achurra-Gonzalez and J. Speirs, “Natural Gas as a Fuel for Heavy Goods Vehicles,” 2019.

[132] Cenex, “Dedicated to Gas Trial,” 2019.

[133] R. Vermeulen, R. Verbeek, S. Goethem and R. Smokers, “Emissions Testing of Two Euro VI LNG Heavy-Duty Vehicles in the Netherlands: Tank-to-Wheel Emissions,” Amsterdam: TNO, 2017.

[134] D. Peters-von Rosenstiel, “LNG in Germany: Liquefied Natural Gas and Renewable Methane in Heavy-Duty Road Transport.,” Dena, 2014.

[135] Smart Freight Centre, “Global Logistics Emissions Council Framework for Logistic Emissions Accounting and Reporting. Version 2.0,” 2019.

[136] European Comission , “Directive 2009/28/EC of the European Parliament and of the Council of 23 April 2009 on the promotion of the use of energy from renewable sources and amending and subsequently repealing Directives 2001/77/EC and 2003/30/EC. OJEU: L 140/16,” 2009.

[137] Green Delta, *openLCA,* [Window].Berlin: Version 1.10.3, 2019.

[138] M. Huijbregts, Z. Steinmann, P. Elshout, G. Stam, F. Verones, M. Vieira, A. Hollander, M. Zijp and R. van Zelm, “ReCiPe 2016 :A harmonized life cycle impact assessmentmethod at midpoint and endpoint level. Report I: Characterization,” 2016. [Online]. Available: https://www.rivm.nl/bibliotheek/rapporten/2016-0104.pdf. [Accessed 40 04 2022].

[139] Intergovernmental Panel on Climate Change, “2019 Refinement to the 2006 IPCC Guidelines for National Greenhouse Gas Inventories,” 2019. [Online]. Available: https://www.ipcc.ch/report/2019-refinement-to-the-2006-ipcc-guidelines-for-national-greenhouse-gas-inventories/. [Accessed 28 01 2022].

[140] J. Webb and T. H. Misselbrook, “A mass-flow model of ammonia emissions from UK livestock production,” 5 2004. [Online].

[141] Enviromental Protection Agency, “Ireland’s National Inventory Submissions. Common Reporting Format Table 3.B(a)s1,” 2019. [Online]. Available: https://www.epa.ie/pubs/reports/air/airemissions/ghg/nir2019/ . [Accessed 28 01 2022].

[142] Fuels for Ireland, “Pump Prices,” 16 09 2020. [Online]. Available: https://www.fuelsforireland.ie/news/pump-prices. [Accessed 07 01 2022].

[143] F. Cavalieri, “Steady-state flow computation in gas distribution networks with multiple pressure levels,” *Energy,* vol. 121, pp. 781-791, 2 2017.